LBL-28481
UC-406

# Lawrence Berkeley Laboratory
UNIVERSITY OF CALIFORNIA

## Physics Division

**Amorphous Silicon Detectors in Positron Emission Tomography**

M. Conti and V. Perez-Mendez

December 1989

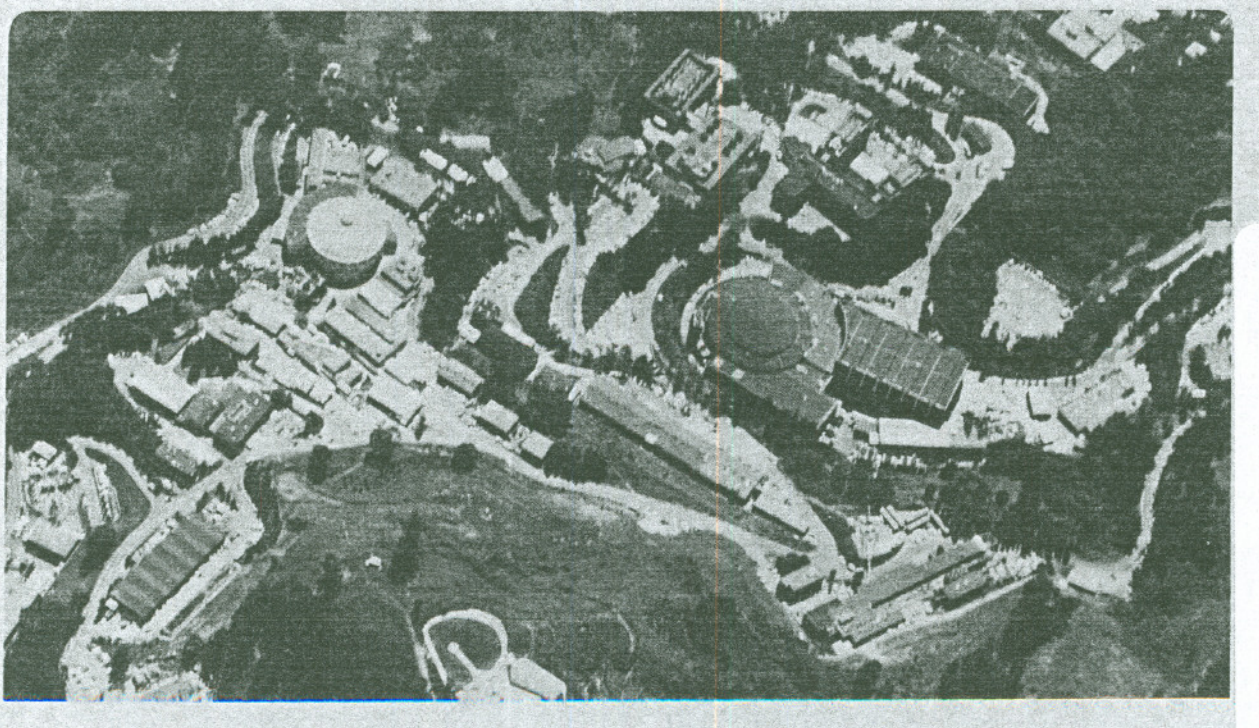



Prepared for the U.S. Department of Energy under Contract Number DE-AC03-76SF00098.

Available to DOE and DOE Contractors from the
Office of Scientific and Technical Information
P.O. Box 62, Oak Ridge, TN 37831
Prices available from (615) 576-8401, FTS 626-8401

Available to the public from
National Technical Information Service
U.S. Department of Commerce
5285 Port Royal Road, Springfield, VA 22161
Price: Printed Copy A06, Microfiche A01

# AMORPHOUS SILICON DETECTORS

# IN POSITRON EMISSION TOMOGRAPHY

Maurizio Conti

INFN Sezione di Pisa
Pisa, Italy
and
Lawrence Berkeley Laboratory
University of California
Berkeley, CA 94720

and

Victor Perez-Mendez

Lawrence Berkeley Laboratory
University of California
Berkeley, CA 94720

December 1989

# AMORPHOUS SILICON DETECTORS IN POSITRON EMISSION TOMOGRAPHY


1. Introduction 4

2. Amorphous Silicon Detectors 7
   - 2.1. Total Depletion and Bias 7
   - 2.2. Charge Transit Time 8
   - 2.3. References 8

3. Tantalum-Amorphous Silicon Multilayer Detectors for PET 9
   - 3.1. Tantalum/a-Si Detectors: a Monte Carlo Simulation 9
     - 3.1.1. Geometry 9
     - 3.1.2. Photon Interaction and Range of Electrons 10
     - 3.1.3. Electron Tracks in the Detector and Efficiency 11
     - 3.1.4. Spatial Resolution 14
   - 3.2. PET Architecture 14
     - 3.2.1. Total Efficiency 14
     - 3.2.2. Pixel Read-out Systems 15
   - 3.3. Conclusions 16
   - 3.4. References 17

4. CsI Scintillation Light & Amorphous Silicon Detectors for PET 18
   - 4.1. Thin CsI Layer : a Monte Carlo Simulation 18
     - 4.1.1. Geometry 18
     - 4.1.2. Incident Particle Properties 18
     - 4.1.3. Photon Interaction and Electrons 19
     - 4.1.4. Light Yield and Point Source 19
     - 4.1.5. Solid Angle Algorithm and Distribution of Light 20
     - 4.1.6. Efficiency 20
     - 4.1.7. Multilayer Structure Efficiency 25
   - 4.2. CsI Filled Glass tubes arrays: A Monte Carlo Simulation 26
     - 4.2.1. Geometry 26
     - 4.2.2. Incident Particle Parameters 26
     - 4.2.3. Photon Interaction and Produced Electrons 26
     - 4.2.4. Light Yield 27
     - 4.2.5. Light Detection in a-Si Pixels 27
     - 4.2.6. Efficiency 30
   - 4.3. Initial Test of CsI/Amorphous Silicon Detectors 32
     - 4.3.1. CsI Scintillation Light Yield 32
     - 4.3.2. First Experimental Data 33
   - 4.4. Conclusions 34
   - 4.5. Appendix to the Monte Carlo Calculation 35
     - 4.5.1. Distribution of Light on the Pixels: ANGALG 35
     - 4.5.2. Consideration on the Effects of the Glass Walls 36
     - 4.5.3. Total and Partial Reflection of Light in Tubes 37
     - 4.5.4. Parallax Considerations 37
   - 4.6. References 39

5. Xenon Scintillation Light & Amorphous Silicon Detectors for PET 40
5.1. Mechanism of Scintillation in Xenon 41
5.2. Light Yield and Drift Field 43
5.2.1. Experimental Background 43
5.2.2. Efficiency and Light Yield 44
5.3. Electron Drift and Drift Time 46
5.4. Conclusions 47
5.5. References 48

6. Timing and Electronics 49
6.1. Amorphous Silicon Electronics 49
6.2. Shaping Time 49
6.3. Noise 52
6.4. Detectors, Noise, Shaping Time: Applications 56
6.4.1. Shaping Time and Efficiency for Ta/a-Si PET 56
6.4.2. Shaping Time for CsI/a-Si and Xe/a-Si PETs 58
6.5. Conclusions 59
6.6. References 60

7. Conclusions : Evaluation of Merit Parameter $\varepsilon^2/\tau$ 61
7.1. A Comparison of $\varepsilon^2/\tau$ of each PET Project 62
7.2. References 63

8. Appendix 66
8.1. A Complete Reference List on Xenon Scintillation Light 67
8.1.1. Electrons in Gases 67
8.1.2. Electron Drift Velocity in Rare Gases 67
8.1.3. Mechanism of Scintillation in Rare Gases 67
8.1.4. Phenomenology of Scintillation in Rare Gases 68
8.1.5. Gas Scintillation Proportional Counters (Reviews) 68
8.1.6. Gas Scintillation Proportional Counters (Applications) 68
8.1.7. Electronic Excitation, Ionization, Elastic Scattering 69
8.1.8. Fluctuations and Statistics in GSPC 69
8.2. Monte Carlo Simulation: Inputs and Programs 70
8.2.1. CsI/Amorphous Silicon Detector 70
8.2.2. Tantalum/Amorphous Silicon Detector 70
8.3. Program Listing 70

## Acknowledgements

Thanks to Ichiro Fujieda for his collaboration in the CsI scintillation light yield measurements quoted in Chapter 4 and to Gyuseong Cho and Professor Selig Kaplan for their contribution in the part concerning amorphous silicon electronics and especially for the plots presented in Chapter 6: Figures 6.6.a and 6.6.b are the result of a computer simulation of charge signal development in detector and electronics run by Professor Kaplan, while Figures 6.7, 6.8, 6.9 are due to Gyuseong Cho.

This work has been financed by the National Science Foundation, the Istituto Nazionale di Fisica Nucleare, the Lawrence Berkeley Laboratory and supported by the Director, Office of the Energy Research, Office of the High Energy and Nuclear Physics, Division of the High Energy Physics of the US Department of Energy under contract #DE-AC03-76SF00098.

# 1. Introduction

Positron Emission Tomography at present has a wide use especially in medical research and physiology: movement of radioisotope-marked chemicals through organs can be monitored, in order to collect information about the physiology of the organs themselves, or localization of chemicals in different parts of the body can be studied.

In Positron Emission Tomography a radioisotope $\beta^+$ with appropriate half life is injected in the patient (or inhalated) ; commonly used $\beta^+$- emitters are $^{11}C$, $^{13}N$, $^{15}O$, $^{18}F$, with short lifetime (min) which are isotopes of those widely present in tissue, and $^{82}Rb$, $^{68}Ga$, technogically easier to produce and handle. The emitted positron after a short range of the order of a few mm due to the initial kinetic energy stops and annihilates with an electron in the matter (tissue) and emits two back-to-back 511 keV $\gamma$'s : from the time coincidence of the detection of the $\gamma$'s in two detectors placed at $2\pi$ we can select the annihilation events and determine the straight line (two $\gamma$'s are collinear within a few mrad) along which the annihilation occurred as the line joining the sites of interaction of a pair of annihilation $\gamma$'s. Reconstruction algorithms allow us to draw a map of the spatial distribution of radioactivity density from a set of lines traced as above. Positron range, $\gamma$'s non-collinearity, $\gamma$'s Compton scattering in the tissue, parallax error in thick detectors can result in degradation of spatial resolution and blurring of the image, that can be partially corrected via software..

The most commonly used detectors for PET are crystal scintillators such as NaI or BGO; their high density and Z ensure a good interaction efficiency for 511 keV $\gamma$'s. Due to the high cost of the crystals, the read-out technology and the associated electronics a limited number of single crystal detectors of a few millimeters in size are usually placed on a few rings around the body, covering only a small part of the solid angle.

The purpose of this work is to evaluate the feasibility of a PET system based on low cost amorphous silicon detectors and integrated electronics, capable of covering a large angle and with efficiency and spatial resolution comparable or competitive with crystal rings PET.

Amorphous silicon is widely used in solar cell technology, in which very thin layers ( $\leq 1$ $\mu$m ) are produced industrially in large areas to interact with visible light and in Thin Film Transistors (TFT) technology. In the field of high energy physics and medical physics amorphous silicon has been proposed as a detector alternative to crystal silicon detectors; although Signal to Noise ratio and charge mobility are smaller in amorphous silicon detectors, they provide the following advantages compared to the crystal silicon detectors:

- large area pixel detectors can be easily built;
- the cost is lower;
- the material is highly radiation resistant.

The basic structure of an amorphous silicon detector is a reverse biased p-i-n multilayer, with very thin p and n blocking contacts (much less than one micron) and a thick i-layer. Amorphous silicon detectors can be used to detect UV and visible photons (due to short absorption depth of light few $\mu$m of silicon are

enough) or charged particles (depleted thicknesses up to 50 μm are presently available): in our study we considered both applications.

Due to the low cross section for interaction for 511 keV γ's in silicon a high Z and high density "gamma/electron converter" is needed to have a reasonable interaction efficiency; the primary electron (photoelectric or Compton electron) can be directly detected by an amorphous silicon detector or produces light in a scintillator medium and the scintillation photons are detected by amorphous silicon photodiodes. Three structures are considered here as shown in Figure 1.1 :

- a thin Tantalum slab serves as γ-electron converter and amorphous silicon pixel detectors track electrons produced in the Tantalum;
- Cesium Iodade as a slab or within a honeycomb array of glass tubes is a γ-electron converter and a scintillator for electrons generated in the crystal itself. The amorphous silicon pixel photodiodes detect the scintillation photons.
- a honeycomb array of lead glass tubes is the γ-electron converter: primary electrons produced within the glass reach the interior of the tubes filled with Xenon gas; secondary electrons from the ionization track left in Xenon by a primary electron drift within the Xenon along the direction of an the electric field applied parallel to the axis of the tubes and create scintillation light while drifting; the scintillation photons are collected by amorphous silicon pixel photodiodes at the ends of the tubes.

The structural characteristics of each project are presented, the physics of the detection process is studied and the performances of different PET system are evaluated by theoretical calculation and/or Monte Carlo Simulation (using the EGS code) in this paper, whose table of contents can be summarized as follows:

- in Chapter 2 a brief introduction to amorphous silicon detectors and some useful equation is presented;
- in Chapter 3 a Tantalum/Amorphous Silicon PET project is studied and the efficiency of the system is studied by Monte Carlo Simulation;
- in Chapter 4 two similar CsI/Amorphous Silicon PET projects are presented and their efficiency and spatial resolution are studied by Monte Carlo Simulation, light yield and time characteristics of the scintillation light are discussed for different scintillators; some experimental result on light yield measurements are presented;
- in Chapter 5 a Xenon/Amorphous Silicon PET is presented, the physical mechanism of scintillation in Xenon is explained, a theoretical estimation of total light yield in Xenon and the resulting efficiency is discussed altogether with some consideration of the time resolution of the system;
- in Chapter 6 the amorphous silicon integrated electronics is presented, total noise and time resolution are evaluated in each of our applications;
- in Chapter 7 the merit parameters $\varepsilon^2/\tau$'s are evaluated and compared with other PET systems and conclusions are drawn.
- in Chapter 8 a complete reference list for Xenon scintillation light physics and its applications is presented altogether with the listing of the developed simulation programs.

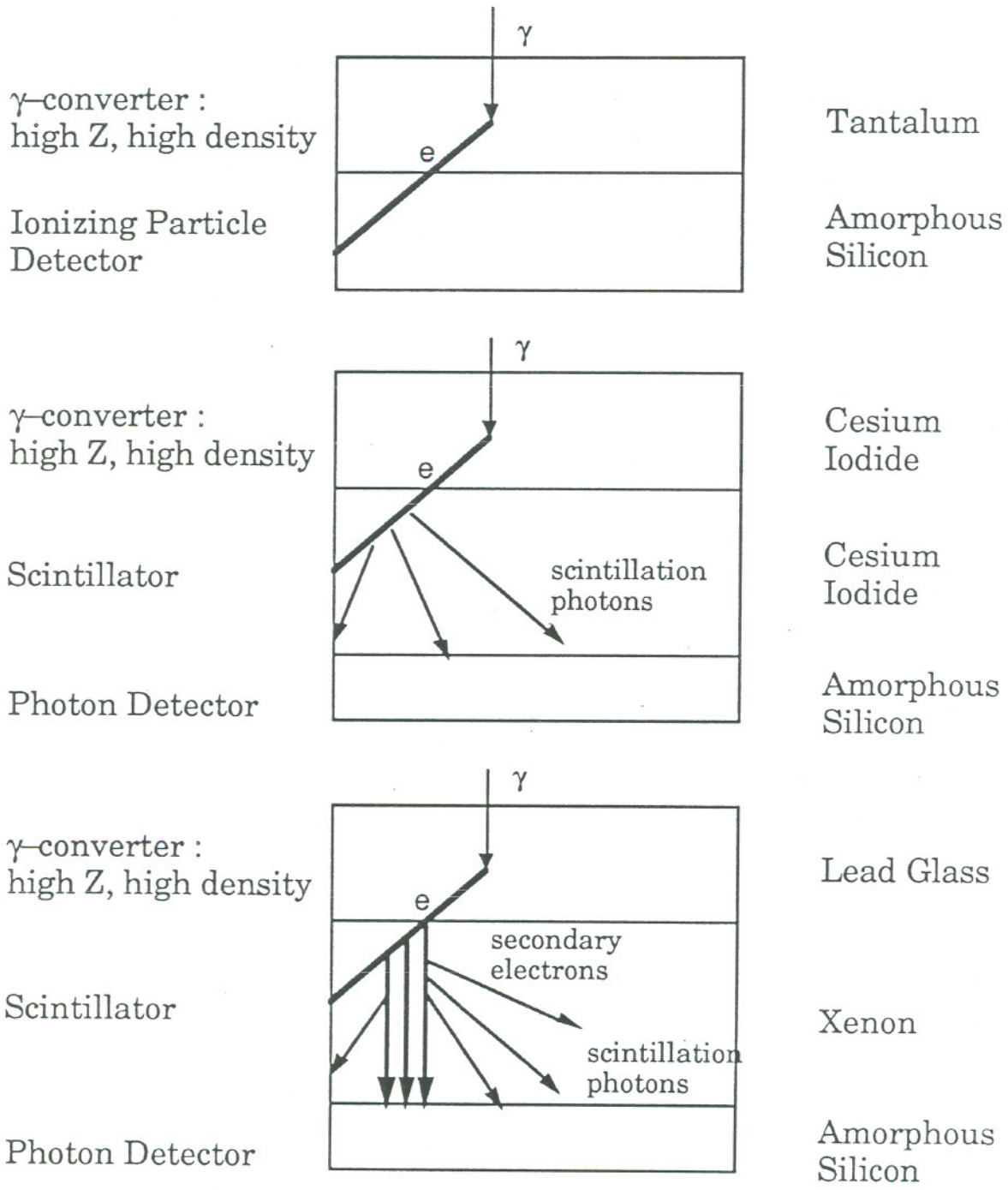


Figure 1.1 511 keV-γ rays interaction and detection model in three a-Si:H-based detectors proposed for PET.

## 2. Amorphous Silicon Detectors

Amorphous silicon detectors are presently being developed at LBL [1,2] for a wide range of applications, from medical physics to high energy physics, because of their ability to detect both visible and UV photons and ionizing particles. The basic structure of the devices is a reverse biased p-i-n multilayer, with thin (a few hundred nm) p and n layers used as blocking contacts and a thick (1-50 μm) i-layer . Dangling bonds in the material work as traps for the charges moving in the detector and hydrogenated amorphous silicon (a-Si:H) is used to reduce the density of dangling bonds; nevertheless dangling bonds are responsible for defect states in the conduction-valency gap (1.7-1.9 eV) that reduce the lifetime of charges.

In Figure 2.1 a simplified p-i-n device is shown.

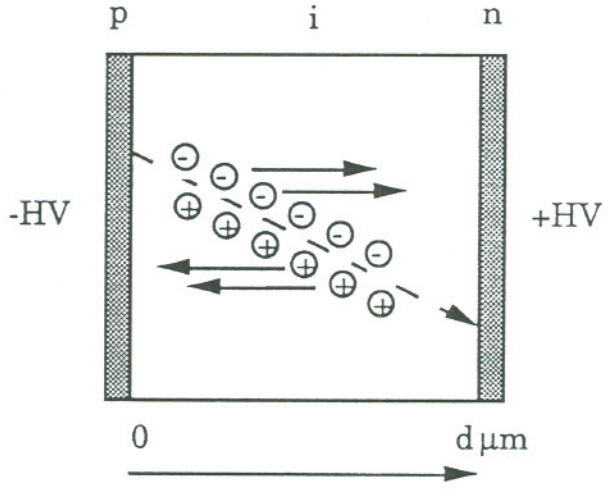


Figure 2.1 : Ionizing particle track within a p-i-n device of thickness d.

### 2.1. Total Depletion and Bias

Under the application of a reverse bias to the detector an electric field E is created within the silicon, ionizing part of the dangling bonds and generating a uniform positive charge density $N_d^*$ within the detector itself that affects the field.

Using $\frac{dE}{dx} = \frac{\rho}{\varepsilon_0 \varepsilon}$ and imposing the condition that the field is larger than zero everywhere in the i-layer we can estimate the minimum bias $V_{min}$ to be used in order to have complete depletion of the detector:

$$V_{min} = \frac{1}{2} \frac{\rho d^2}{\varepsilon_0 \varepsilon} = \frac{1}{2} \frac{N_d^* e d^2}{\varepsilon_0 \varepsilon}$$

$N_d^*$ was measured [2] to be about $7.\ 10^{14}$ cm$^{-3}$ in good quality hydrogenated amorphous silicon, and $\varepsilon$ is about 11.8. In Figure 2.2 the shape of the electric field E across the i-layer is shown, in cases of total and partial depletion. Since the i-layer is slightly n-type the depletion is developed from the p-i junction; in case of partial depletion the charges generated in the region close to the n-layer don't contribute to the current, and this results in loss of signal in the detector.

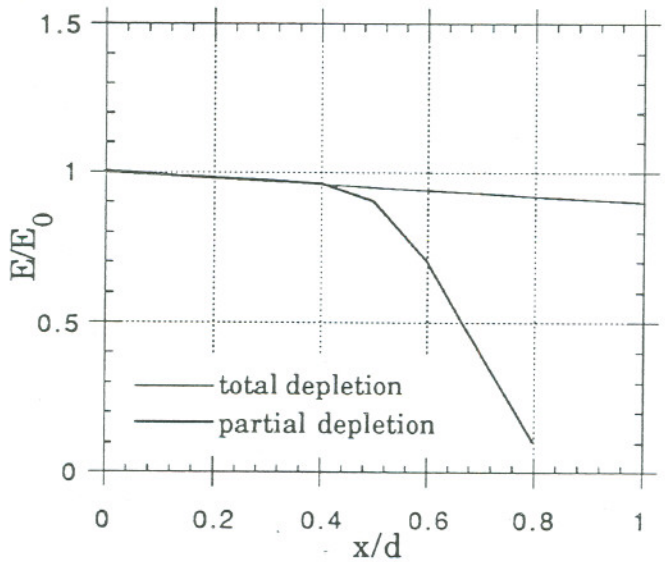


Figure 2.2 : Electric field shape across the i-layer in the detector as a function of the distance from the p-i junction.

## 2.2. Charge Transit Time

Mobility measurement of electrons and holes [2] in amorphous silicon sample diodes yield an electron mobility $\mu_e$ = 1.1-1.4 cm$^2$/Vs and a hole mobility $\mu_h$ = 0.003-0.004 cm$^2$/Vs. Different definitions of transit time or collection time can be presented for electrons and holes, but in our calculation we will use [3] $t_c = 0.53\frac{d^2}{\mu V}$, where d is the thickness in cm, V the applied bias in Volt, $\mu$ the mobility in cm$^2$/Vs.

## 2.3. References


[1] I. Fujeda et al., *Proc. Mater. Res. Soc. 118* , p.469 (1988).
[2] S. Qureshi et al., *IEEE Trans. Nucl. Sci NS-36* ,p.194 (1989).
[3] G. F. Knoll, *Radiation Detection and Measurement* , John Wiley & Sons, p.394 (1979).

## 3. Tantalum-Amorphous Silicon Multilayer Detectors for PET

A multilayer structure of Tantalum and Amorphous Silicon pixel detectors is considered here in order to detect 511 keV photons from positron annihilation for Positron Emission Tomography purposes. Thin Tantalum (about 100 μm) layers play the function of photon-electron converters and a-Si pixels (about 50 μm thick and 2 mm in size) detect the escaping electrons coming out from the Ta. A Monte Carlo Simulation is performed to calculate the expected efficiency of a single Ta-Si layer, and the total efficiency of a multilayer is extrapolated. Consideration of the amorphous silicon electronics are discussed to evaluate the opportunity of connecting in series or in parallel the a-Si detectors.

### 3.1. Tantalum/a-Si Detectors: a Monte Carlo Simulation

A Monte Carlo Simulation program BIGMAC (see Appendix) has been developed. Positron annihilation photons of 511 keV are considered incident on the detector; photons and electrons coming out from the interaction of photons in the material are followed and transported using the standard EGS4 code; 100000 events were processed in each run .

#### 3.1.1. Geometry

A simple geometry has been considered: a pixel 2 mm size square detector and a 2 mm size Tantalum converter on the front end. This structure is doubled (Ta-Si-Ta-Si) as shown in Figure 3.1 in order to consider the energy released in each detector from back scattered particles coming from the following Tantalum layer. The 511 keV photons hit the center of the 1st Tantalum converter, with direction parallel to the normal to the plane of the detector. The thickness of the a-Si detector is 50 μm (the maximum that presently we have been able to deplete), and the efficiency of a single detector is studied as a function of the thickness of the converter.

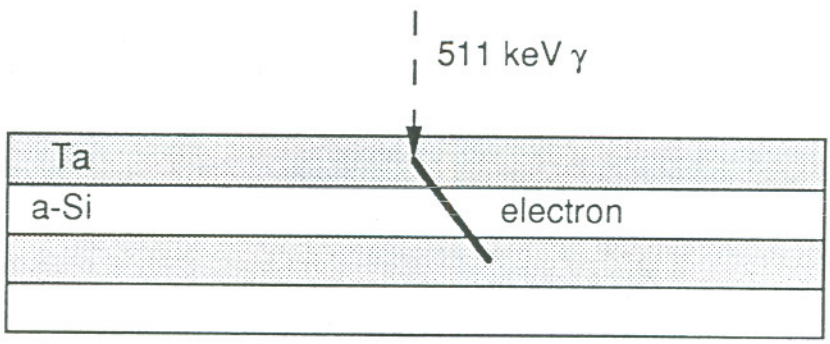


Figure 3.1 : Double deck Tantalum / a:Si sandwich.

### 3.1.2. Photon Interaction and Range of Electrons

The cross section of interaction for 511 keV photons in Tantalum [1] is about $\sigma=1.32\ 10^{-1}$ cm$^2$/g, with a ratio Compton:Photoelectric about 1:1. If t is the thickness of the Tantalum layer it is easy to figure out the expected interaction efficiency for $\rho$ = 16.6 g/cm$^3$, $1/\lambda = \sigma\rho$ = 2.19 cm$^{-1}$. If $I_0 e^{-x/\lambda}$ is the flux of photons after x cm in the Ta, n(x) is the number of photons that have interacted from 0 to x and t is the total thickness of the Ta, the total number of stopped photons n(t) is

$$n(t) = \int_0^t \frac{I_0}{\lambda} e^{-x/\lambda} dx$$

and the interaction probability $\varepsilon_{int} = n(t)/I_0$ is $(1 - e^{-t/\lambda})$.

In Table 3.1 values of $\varepsilon_{int}$(th) estimated in this way and $\varepsilon_{int}$(MC) from the Monte Carlo simulation are reported (in percent) for the considered t, with an excellent agreement and in Figure 2 they are plotted as a function of t.

Table 3.1

| t(μm) | $\varepsilon_{int}$(th) | $\varepsilon_{int}$(MC) |
|---|---|---|
| 25 | 0.6 | 0.6 ± 0.2 |
| 50 | 1.1 | 1.1 ± 0.3 |
| 100 | 2.2 | 2.2 ± 0.5 |
| 200 | 4.5 | 4.4 ± 0.7 |
| 300 | 6.8 | 6.3 ± 0.8 |

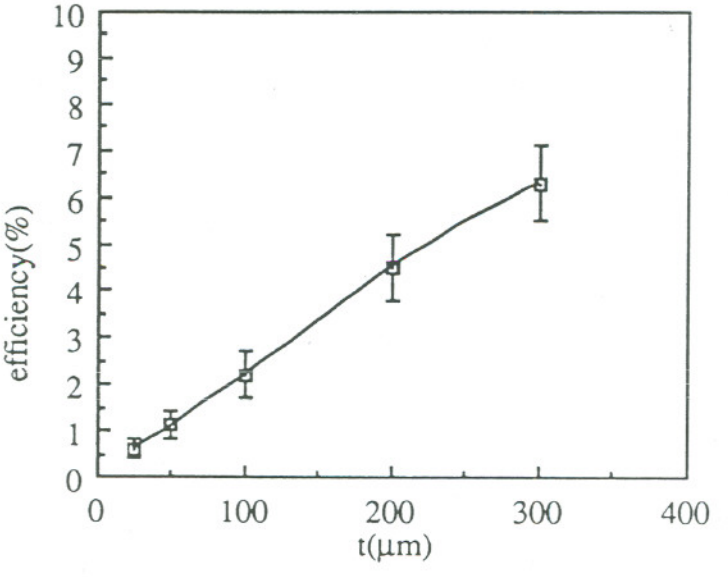


Figure 3.2 : Calculated interaction efficiency vs Tantalum thickness.

In view of an increasing interaction efficiency for thicker converter, the actual efficiency cannot increase in the same way, because of the short range of the electrons in Tantalum, that stops most of the electrons, preventing them from being detected . The range [3,4] of the 443 keV photoelectrons of Tantalum ( K edge at 67 keV) is about 170 μm , and is much less for the lower energy Compton electrons.

### 3.1.3. Electron Tracks in the Detector and Efficiency

In Figure 3.3 an energy spectrum of the electrons entering the a-Si detector (after 100μm Ta) is shown; the photoelectric peak is still visible, and the lack of electrons at low energy means that when electrons are slowed to very low energy, they lose memory of their original direction, and hardly get out of the Tantalum.

Figure 3.3:Energy spectrum of electrons entering a-Si

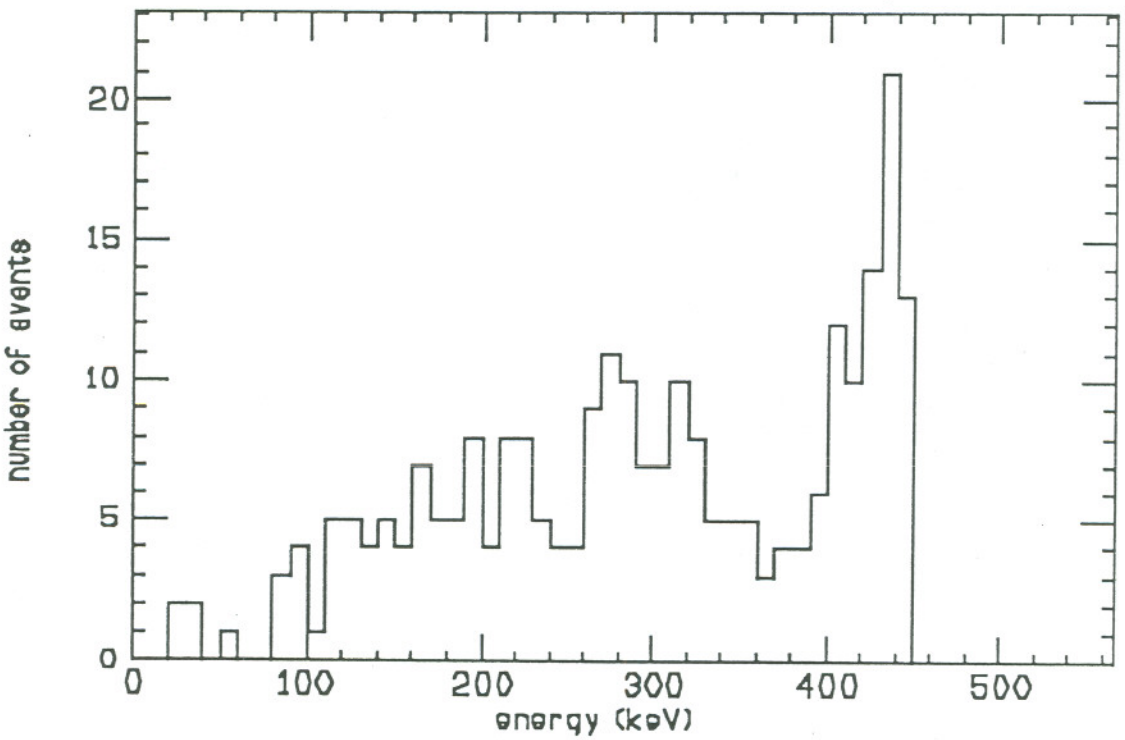


In Figure 3.4 a histogram of the energy deposited by electrons in the detector (for 100 μm Ta) is shown; since about 6 eV are needed to create an electron-hole pair in amorphous silicon [2] (a current measurements at LBL are lowering this number to about 4.8 eV) the charge signal histogram on the detector is easily obtained, and presented in Figure 3.5 .

Figure 3.4:Histogram of energy deposition in a-Si:H

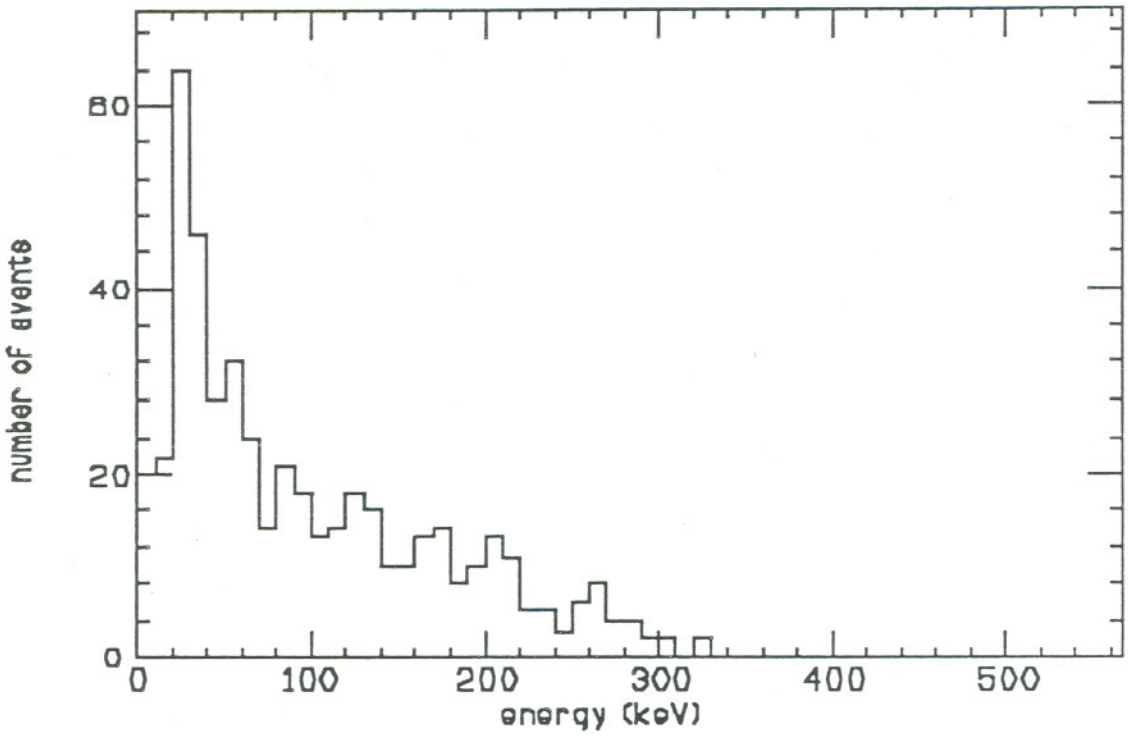


Figure 3.5: Histogram of e/h pairs in a-Si detector

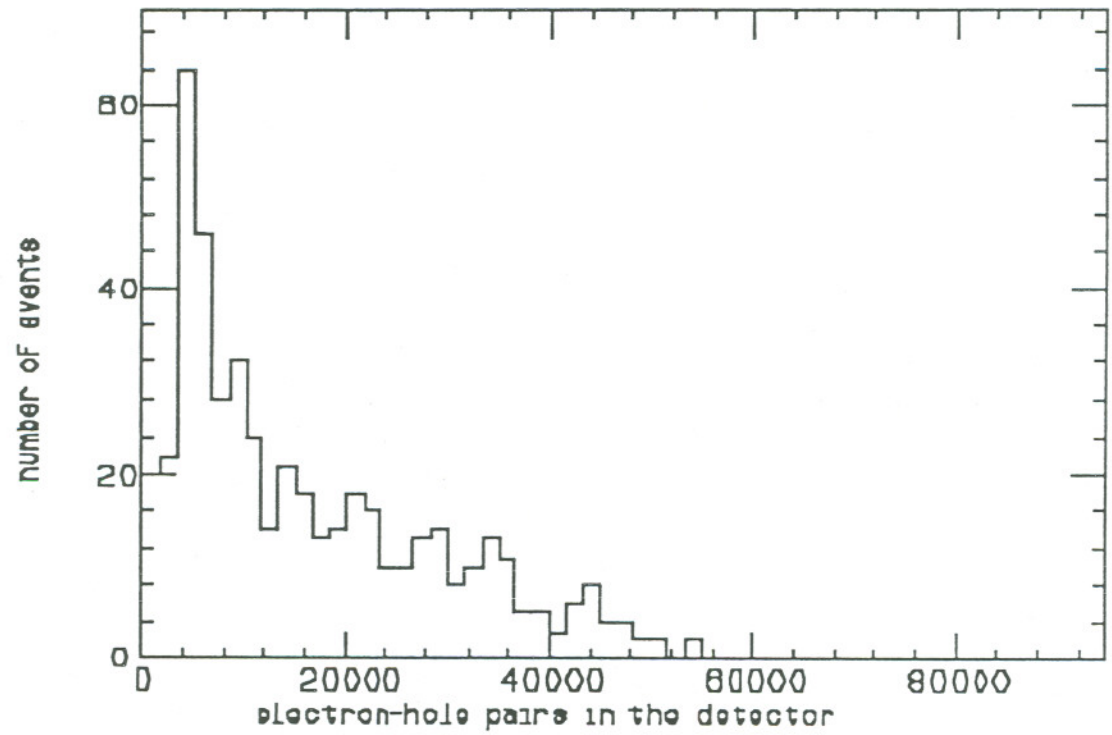

The actual efficiency ε is obtained as integral of the distribution N(n), where n is the number of electron-pair pairs produced, from the noise threshold of about 500 electrons to infinite, divided by 100000 total events. In our case we can approximate :

$$\varepsilon = \frac{\int_{500}^{\infty} N(n)\, dn}{100000} \approx \frac{\int_{0}^{\infty} N(n)\, dn}{100000}$$

In Table 3.2 the values of ε in percent are presented for different t of Tantalum, and are plotted in Figure 3.6 ; the efficiency initially increases with t, due to the increase of interaction efficiency in the Tantalum, then it saturates because of the limited probability for electrons to escape from the metal, finally slowly decreases for the attenuation of the thick Tantalum layer. A maximum value of about 0.5 % is obtained for t = 100 μm.

Table 3.2

| t(μm) | ε(%) | $\sigma_\varepsilon$ |
|---|---|---|
| 25 | 0.38 | 0.02 |
| 50 | 0.44 | 0.02 |
| 100 | 0.48 | 0.02 |
| 200 | 0.45 | 0.02 |
| 300 | 0.42 | 0.02 |

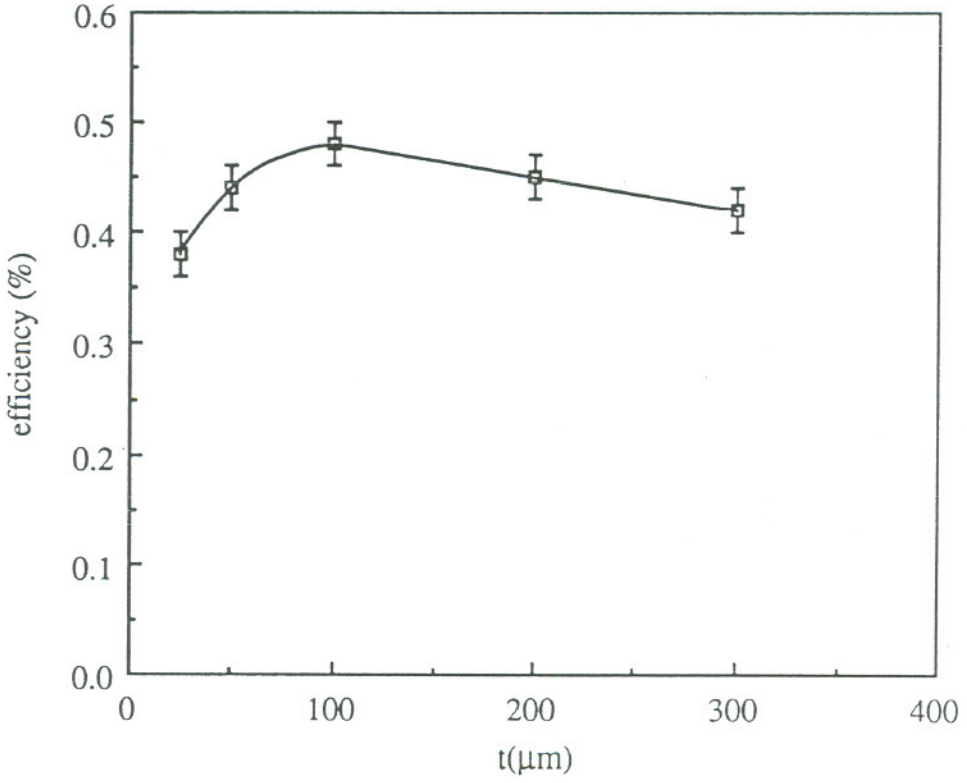


Figure 3.6 : Calculated detection efficiency vs Tantalum thickness.

Five runs were submitted to obtain a more accurate value of ε:

$$\bar{\varepsilon} = \sum_{i=1}^{5} \varepsilon_i \quad \sigma_{\bar{\varepsilon}} = \sigma_\varepsilon / \sqrt{4}$$

The numbers of detected particles in the 5 runs were : 480, 498, 445, 483, 482, from which we obtain a average $\varepsilon = (0.48 \pm 0.01)$ %.

### 3.1.4. Spatial Resolution

In order to estimate the spatial resolution of the system we evaluate the probability that an electron produced in a Tantalum 2x2 $cm^2$ pixel gets out of the corresponding detector (wide angle electrons); this probability is obviously very small, due to the very small ratio of the longitudinal dimension (50 μm) and lateral dimension (2000 μm) of the detector, and to the preferred forward direction of the electrons. A random simulation was performed to estimate this probability, generating electrons entering the detector with random direction, coming from a random point on the surface: $(8.6 \pm 0.9)$ % of the electrons came out of the detector, hitting neighbor detectors and deteriorating the spatial resolution; this number is anyway over estimated, since we didn't consider the forward directed angular distribution of the electrons. Therefore a spatial resolution of 2 mm FWHM (pixel size) can be assumed as a good approximation.

## 3.2. PET Architecture

### 3.2.1. Total Efficiency

In order to obtain a reasonable total efficiency of at least a few percent several layers of Tantalum/Silicon must be stacked; define n, the total number of double Ta/Si layers, ε the efficiency of a single layer, $I_i$ the number of photons that enter the i-th layer (less than $I_0$ due to absorption), $N_i$ the number of photons detected in the i-th detector ; define $\mu = \mu_{Ta} + 0.5\ \mu_{Si}$. Since $I(x) = I_0\ e^{-\mu x}$ , $I_i = I_0\ e^{-\mu t(i-1)}$. The total number N of detected photons is the sum of the product $\varepsilon\ I_i$ and the total efficiency $\varepsilon_{tot}$

$$\varepsilon_{tot} = \frac{N}{I_0} = \frac{1}{I_0} \sum_{i=1}^{n} N_i = \frac{1}{I_0} \sum_{i=1}^{n} \varepsilon I_{i-1} = \varepsilon \sum_{i=1}^{n} e^{-\mu t(i-1)}$$

where $\mu_{Ta} = \Sigma\rho = 2.19\ cm^{-1}$ ($\Sigma = 1.32\ 10^{-2}\ cm^2/g$ and $\rho = 16.6\ g/cm^3$ );
where $\mu_{Si} = \Sigma\rho = 0.20\ cm^{-1}$ ($\Sigma = 8.75\ 10^{-2}\ cm^2/g$ and $\rho = 2.33\ g/cm^3$ );
Therefore, since $\mu = 2.29\ cm^{-1}$ and $t = 100\ \mu m$, for $n = 20$ one can obtain:
$\varepsilon_{tot} = 16.22\ \varepsilon = (7.8 \pm 0.2)$ % .

### 3.2.2. Pixel Read-out Systems

Each detector can be coupled to its own amorphous silicon electronics, in a single pixel read-out; in order to reduce the number of channels few multi-pixel read-out architectures are presented. Since a multilayer detector structure is proposed and each layer is of the order of 100 μm, it is convenient to read as one pixel all detectors stacked with the same plane coordinates, or at least to group them in clusters. Each configuration we present has its pros and contras, but are possible, in any case .

The total number of channels, noise and power dissipation are the parameters to consider for each configuration: n is the number of layers, $N_{ch0}$ is the number of channels per layer, $P_0$ is the power dissipation per surface unit and $N_0$ is the number of noise electrons in a single detector of capacitance $C_D$ . As discussed in detail in Chapter 6, the minimum noise level $N_{noise}$ is proportional to the square root of the detector capacitance, in the case of good matching between total detector capacitance C and amplifier input capacitance ($C_{in} \approx C$).

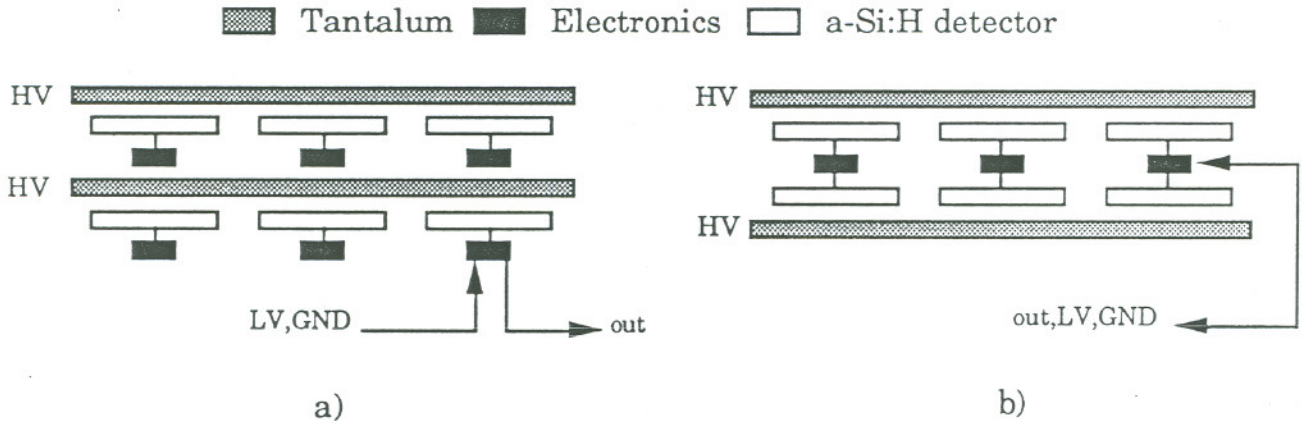


Figure 3.7 : a. Single pixel read-out, two basic elements of the stack, n=2; b. Double pixel read-out, one element, n=2.

A first solution is the simple single plane pixel read-out shown in Figure 3.7.a, in which the total structure is a stack of n basic elements consisting of a large Tantalum slab, a pixel detector plane, an amorphous silicon electronics plane (each amplifier coupled to one detector). The detector can be biased on one side by the high voltage detector bias ( ≈1000 V) on the Tantalum common slab and grounded on the other end through the electronics. A technological problem in this configuration and in some of the others is that from each electronics plane single outputs from each amplifier must be extracted from the sides. The total number of channel in this case is $N_{ch} = n\ N_{ch0}$ , the power per surface unit is $P = n\ P_0$ , the noise is $N_{noise} \approx \text{const.}\sqrt{C} = \text{const.}\sqrt{C_D} = N_0$ .

A second proposal in Figure 3.7.b connects two detector layers in parallel to the same amplifier, reducing the number of channels by a factor two and increasing the capacitance C by the same factor: $N_{ch} = n/2\ N_{ch0}$ , $P = n/2\ P_0$ , $N_{noise} \approx \text{const.}\ \sqrt{C} = \text{const.}\ \sqrt{2}\ \sqrt{C_D} = \sqrt{2}\ N_0$ .

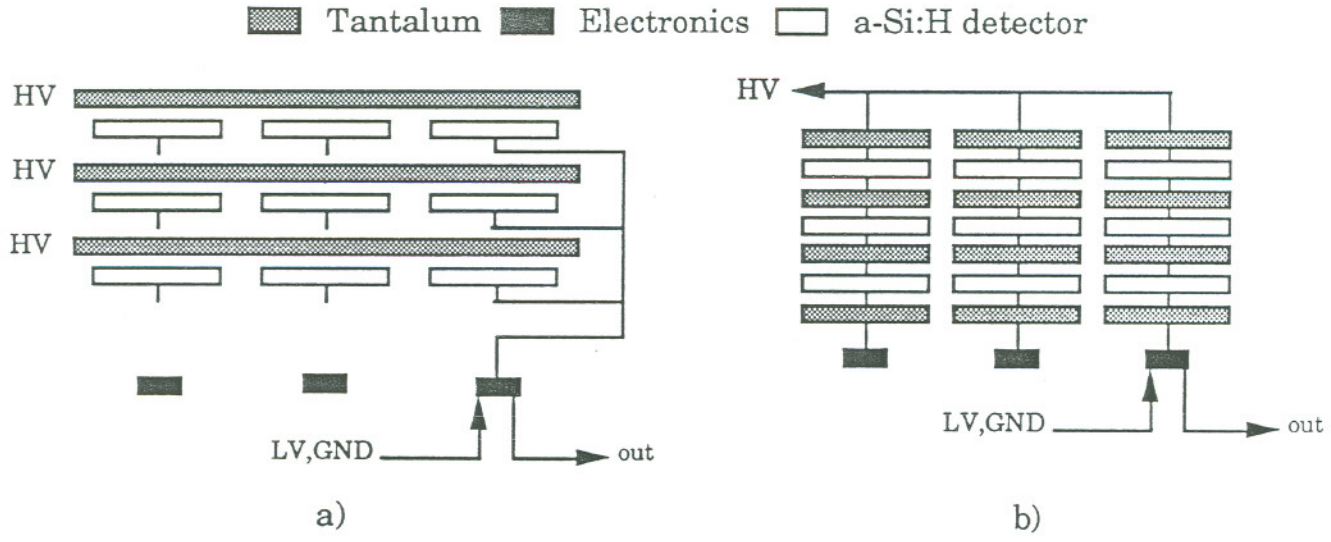


Figure 3.8 : a. Parallel read-out, three basic elements of the stack, n=3; b. Series read-out, three elements, n=3.

A third solution is shown in Figure 3.8.a , in which the same multilayer structure used in the single pixel read-out is used, but in this case all the detectors piled up with the same plane coordinates are connected in parallel to only one amplifier. Since the total capacitance is the sum of n $C_D$ the noise is very high in this case: $N_{ch} = N_{ch0}$ , $P = P_0$ , $N_{noise} \approx$ const. $\sqrt{C}$ = const. $\sqrt{n}\,\sqrt{C_D} = \sqrt{n}\,N_0$ .

The last proposal in Figure 3.8.b is a series connection for the detectors, with Tantalum pixels working also as metal electrodes for capacitors/detectors: in this case a stack of alternate Tantalum/silicon cells is piled up on each pixel; detector bias voltage is applied to one end of the stack, the signal is fed to one amplifier per stack on the other side. A considerable reduction of the electronics noise is expected in this case, but very high bias needed (n times 1000 V !) for each stack and difficulties to obtain a good electric isolation between the high voltage electrodes of neighboring stacks make this solution not reasonably feasible: $N_{ch} = N_{ch0}$ , $P = P_0$ , $N_{noise} \approx$ const. $\sqrt{C}$ = const. $\sqrt{C_D} / \sqrt{n} = N_0 / \sqrt{n}$.

### 3.3. Conclusions

As a result of Monte Carlo calculation an alternated structure of 100 μm Tantalum and 50 μm a-Si:H detector (2 mm pixel size) is proposed; 20 of these double deck layers are needed in order to reach a total efficiency of ( 7.8 ± 0.2 ) % .

Different solutions for pixel read-out are considered in order to reduce the large number of channels, as series or parallel connection of piled detectors to only one amplifier, but noise consideration or high voltage isolation problems make the single pixel read-out the less problematic solution.

## 3.4. References


[1] W. H. McMaster et al., *Compilation of X-Ray Cross Sections, UCRL Report 50174* (1970).

[2] S. N. Kaplan et al., *Nucl. Instr. Meth. A273* , p.611 (1988).

[3] Berger and Seltzer, *Stopping Power and Range Tables for Protons, Mesons and Electrons, NASA SP-3036* (1964).

[4] *Stopping Power and Range for Electrons, UCRL Report 2426* (1966).

# 4. CsI Scintillation Light & Amorphous Silicon Detectors for PET

The use of Cesium Iodide (crystalline or polycrystalline) together with amorphous silicon pixel photodiodes is considered for PET applications: the high Z and the high density of CsI guarantee a high interaction probability for 511 keV photons from positron annihilation. CsI(Tl) or CsI(Na) or pure CsI scintillators produce a large number of visible photons that can easily be detected by amorphous silicon pixel photodiodes ; an a-Si:H integrated electronics is deposited on the detector itself. The feasibility of two architectures is considered. A Monte Carlo simulation based on EGS4 code is used to study the performances of the systems.

## 4.1. Thin CsI Layer : a Monte Carlo Simulation

The Monte Carlo Simulation of the interaction of 511 keV photons in Cesium Iodide, and the tracking of the produced electrons is performed on the base of the EGS4 code; 10000 events were considered in the simulation.

A thin layer of CsI (1-2 mm) may be deposited directly on the silicon pixel array, avoiding any light coupling problem . A few percent (5-10 %) efficiency is expected, but simplicity and compactness of the mechanics make anyway worthwhile an attempt to evaluate the performances of the system. A Monte Carlo simulation program (CHESBUR, see Appendix ) was developed in order to study performance parameters of the detector (essentially efficiency and spatial resolution).

### 4.1.1. Geometry

The geometry shown in Figure 4.1 is very simple: a CsI infinite slab with variable thickness (1,2,3,5,10 mm), vacuum in the front end, and an array of squared pixels of 2 mm size and negligible thickness on the other end.

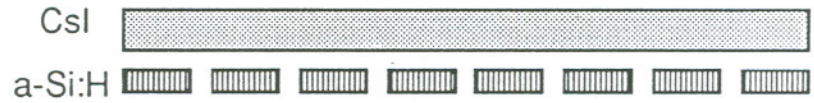


Figure 4.1 : CsI scintillation slab and a-Si pixel detectors.

### 4.1.2. Incident Particle Properties

Electron-positron annihilation photons of .511 MeV are considered hitting the detector in the same point (0,0), all of them with a null angle with the normal to the surface. 10000 events were considered in the simulation.

### 4.1.3. Photon Interaction and Electrons

For each charged particle (electrons from photoelectric interaction or Compton scattering) produced, the origin point, the end point and the released energy are recorded. For each event the program keeps track of the total energy released, the number (usually one, because of the thin detector), the energy and the position of the tracks in the CsI.

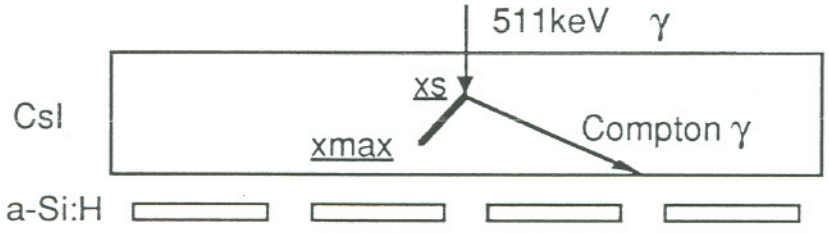


Figure 4.2 : Schematic drawing of the γ-interaction in CsI slab.

### 4.1.4. Light Yield and Point Source

For the sake of simplicity and faster calculation we assumed that all the light produced by each electron track (from the generation point through the point where the electron is discarded for under-energy-cutoff reason or for out-of-sensitive-region reason) is coming from a point source, located along the track (Figure 4.3) This location is determined by a weighted average of the position of the electron from the origin to the end of its history.

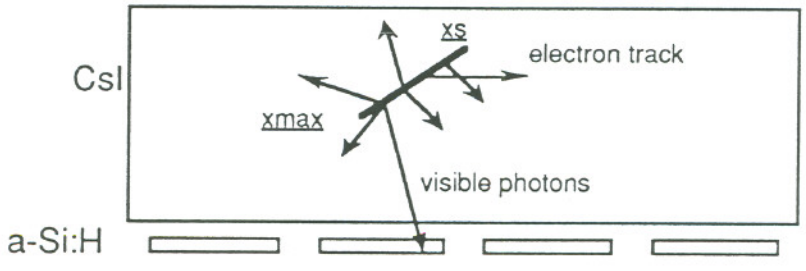


Figure 4.3 : Electron track and scintillation photons in CsI.

The point of light emission is determined by a weighted average of the position of the electron along the track , where the weight is given by the energy loss per centimeter dE/dx.

$$\langle \vec{X} \rangle = \frac{\int_{\vec{x}_s}^{\vec{x}_{max}} \vec{x} \frac{dE}{dx} dx}{\int_{\vec{x}_s}^{\vec{x}_{max}} \frac{dE}{dx} dx}$$

since $\frac{dE}{dx} \approx \frac{1}{v^2} \approx \frac{1}{E}$ then $dx = a\,E\,dE$, and $x = a\frac{E^2}{2}$, $E = \sqrt{2/a}\sqrt{x}$

and $\frac{dE}{dx} = \sqrt{2/a}\,\frac{1}{2}\frac{1}{\sqrt{x}}$ ; substituting in the previous formula this expression for the energy loss :

$$\langle \vec{x} \rangle = \frac{\int_{\vec{x}_s}^{\vec{x}_{max}} \vec{x}\,\frac{1}{\sqrt{x}}\,dx}{\int_{\vec{x}_s}^{\vec{x}_{max}} \frac{1}{\sqrt{x}}\,dx} = \frac{1}{3}(\vec{x}_s - \vec{x}_{max}) + \vec{x}_{max}$$

As a result, we consider for each track N, a point source in <x(N)>, generating a number of photons randomly directed equal to edep(N)(energy released along the track) times Y (light yield, in photons per MeV); the light yield value Y assumed is 50,000 photon per MeV, quoted for CsI(Tl) in Chapter 4.3.1.

### 4.1.5. Solid Angle Algorithm and Distribution of Light

For each point source of visible photons, the light is distributed on detectors of 2 mm size placed in an array 5 x 5 by a simple algorithm ANGALG based on the fraction of solid angle $\Omega$ covered by each of them, $\Omega = 2\,\pi\,(1 - \cos\theta)$ , where $\theta$ is related to the angle from which the point source sees the detector (cfr. Appendix to Monte Carlo Calculation) .

### 4.1.6. Efficiency

Several parameters are extracted from the simulation and considered:

a.Interaction efficiency $\varepsilon_{int}$, defined as the number of $\gamma$ interacting divided by the number of events considered; obviously increases with the thickness of CsI.

b.$E_{out}$ , percentage of light outside of the 5 x 5 array considered (1 x 1 $cm^2$), gives a rough idea of the light loss and of the degradation of spatial resolution. The thicker the CsI is, the larger is the light spread, from simple solid angle considerations.

c.The average number of photons in the central pixel $<N_{\#1}>$ and the average number in the neighbor one $<N_{\#2}>$; actually the histograms for the number of photons are far from having a peak, but the mean value is anyway a good parameter to compare. Values of CsI thickness can be accepted as long as the ratio $<N_{\#2}>/<N_{\#1}>$ remains reasonably small, i.e. the spatial resolution is not deteriorated too much.

d.The center-of-gravity spatial resolution R, defined as the mean value of the center of gravity of the light in the plane of the detectors array

$$\vec{R} = \frac{\sum_{i=1}^{25} N_i \vec{r}_i}{\sum_{i=1}^{25} N_i}$$

where $N_i$ is the no. of photons in i-detector

$\vec{r}_i$ is the position of the i-detector

The spatial resolution R calculated in this way has a surprising good value (few hundreds of microns).

All these results are listed in Table 4.1 .

Table 4.1 :

| Thick (mm) | εint (%) | $<N_{\#1}>$ | $<N_{\#2}>$ | Eout (%) | R (μm) |
|---|---|---|---|---|---|
| 1 | 4.2±.2 | 3818±2850 | 122±239 | 29±13 | 62±200 |
| 2 | 7.9±.3 | 2705±2550 | 202±297 | 39±15 | 99±260 |
| 3 | 12.0±.3 | 1993±2300 | 233±186 | 49±15 | 159±320 |
| 4 | 15.7±.4 | 1425±2000 | 229±255 | 42±15 | 226±375 |
| 5 | 18.7±.4 | 1444±1850 | 217±242 | 56±15 | 285±385 |
| 10 | 33.6±.6 | 612±1400 | 146±213 | 70±17 | 610±545 |

e.The actual efficiency ε presented in Table 4.2, calculated considering only the detected events with a number of photons over a threshold of 500 photons (number of electron hole pairs of the assumed electronic noise) in the 1st pixel:

$$\varepsilon = \frac{\int_{500}^{\infty} N(n)\, dn}{10000}$$ where n is no. of photons and N(n) is the distribution

In Figure 4.4 the histograms for the number of photons in the central pixel for 1 mm and 5 mm of CsI are presented; in Figure 4.5 the efficiency versus the CsI thickness is plotted.

Table 4.2 :

| Thick (mm) | ε (%) |
|---|---|
| 1 | 3.8±.2 |
| 2 | 6.6±.3 |
| 3 | 9.1±.3 |
| 4 | 9.5±.3 |
| 5 | 8.9±.3 |
| 10 | 7.6±.3 |

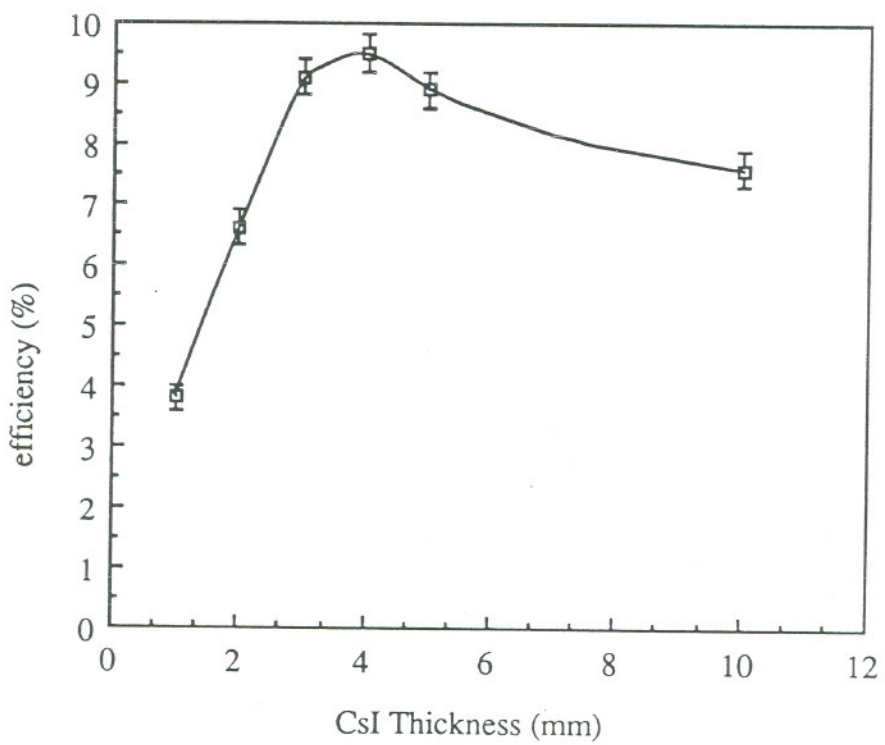


Figure 4.5 : Actual efficiency as a function of CsI thickness

Figure 4.4.a:photons per detected event(1 mm CsI)

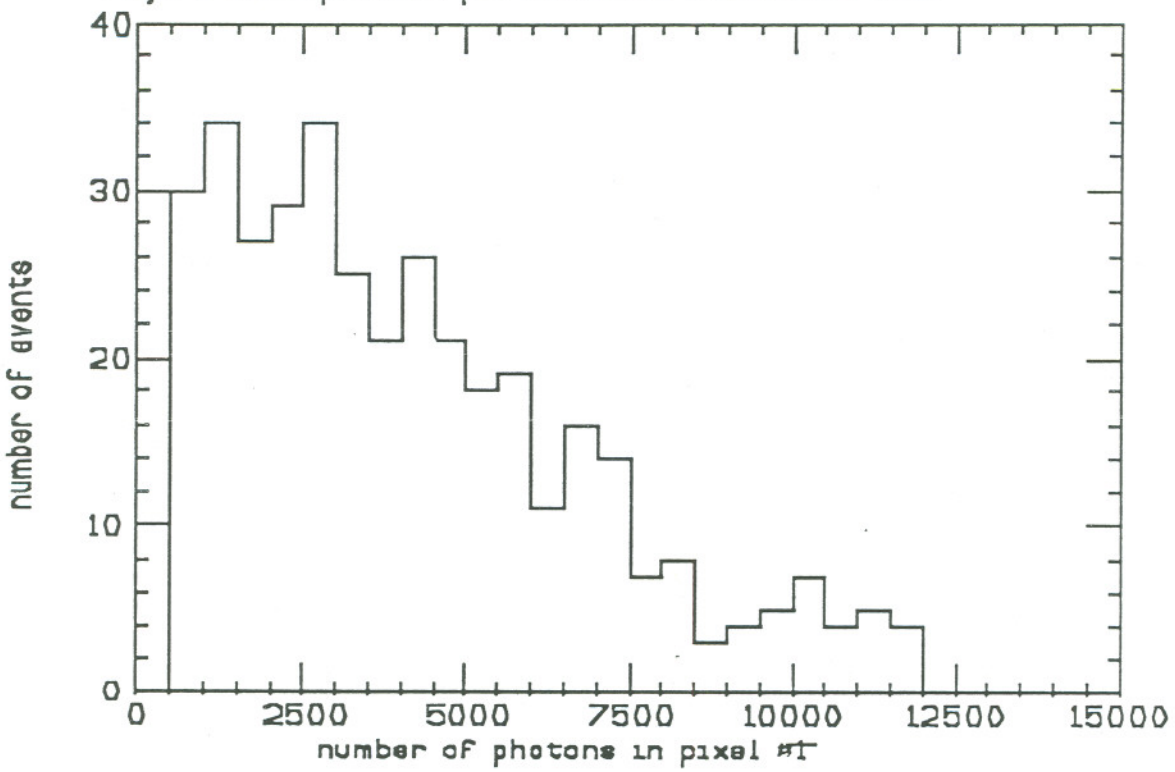


Figure 4.4.b:photons per detected event(5 mm CsI)

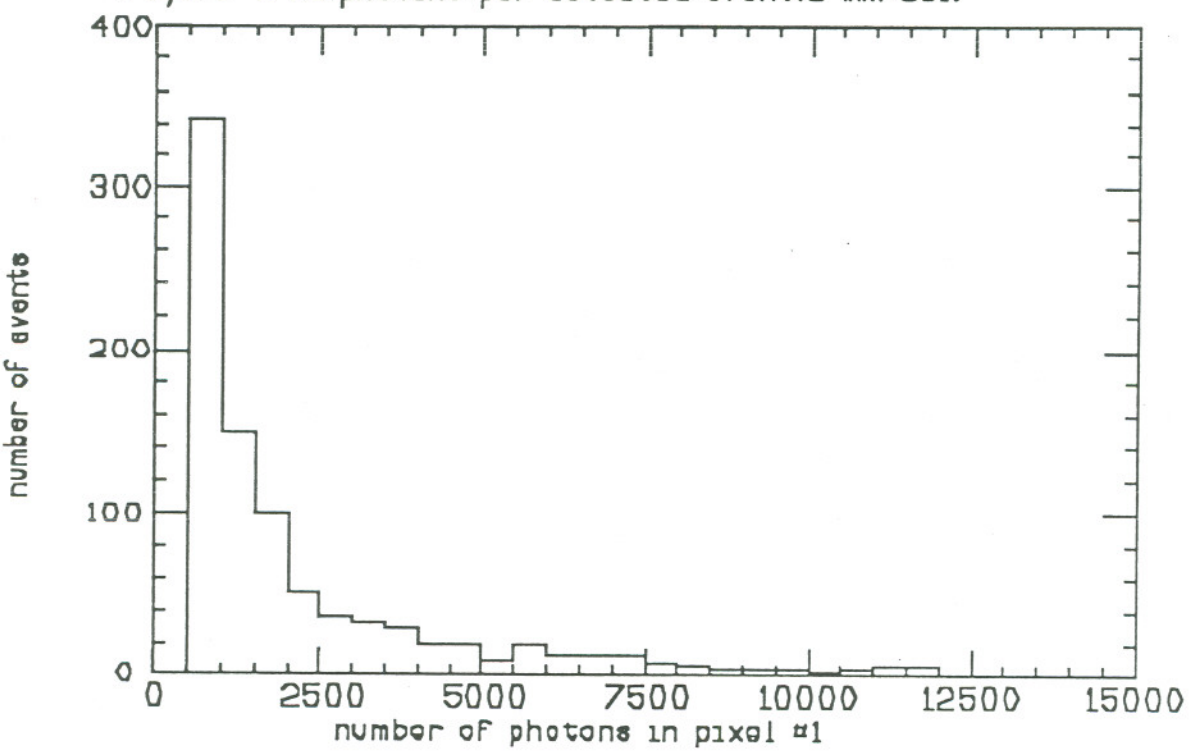

Increasing the thickness of the CsI for solid angle effect the light is not concentrated anymore on the detector pixel just facing the incoming photon, and the light tends to be more equally distributed in a bunch of detector pixels degrading the spatial resolution; in Figure 4.6 the total number of events above the threshold recorded in the central pixel #1 and the surrounding pixels is plotted as a function of the distance from the center of interaction, located above pixel #1; the events in pixel#2 are the sum of the events in 9 detectors around #1, events in pixel#3 are the sum of the 25 pixels all around. Data are presented in Table 4.3. The results are plotted only for CsI thickness of 1,2,5 mm. It is easy to see that the number of detected photons increases with the thickness of the CsI slab, but the spatial resolution is deteriorated. An intermediate solution must be chosen.

Table 4.3 :

| thick (mm) | event#1 | event#2 | event#3 |
|---|---|---|---|
| 1 | 378±20 | 54±22 | 0 |
| 2 | 664±30 | 639±75 | 25±25 |
| 3 | 913±30 | 909±90 | 100±50 |
| 4 | 948±30 | 954±92 | 25±25 |
| 5 | 891±30 | 1017±96 | 100±50 |
| 10 | 760±3= | 774±83 | 150±61 |

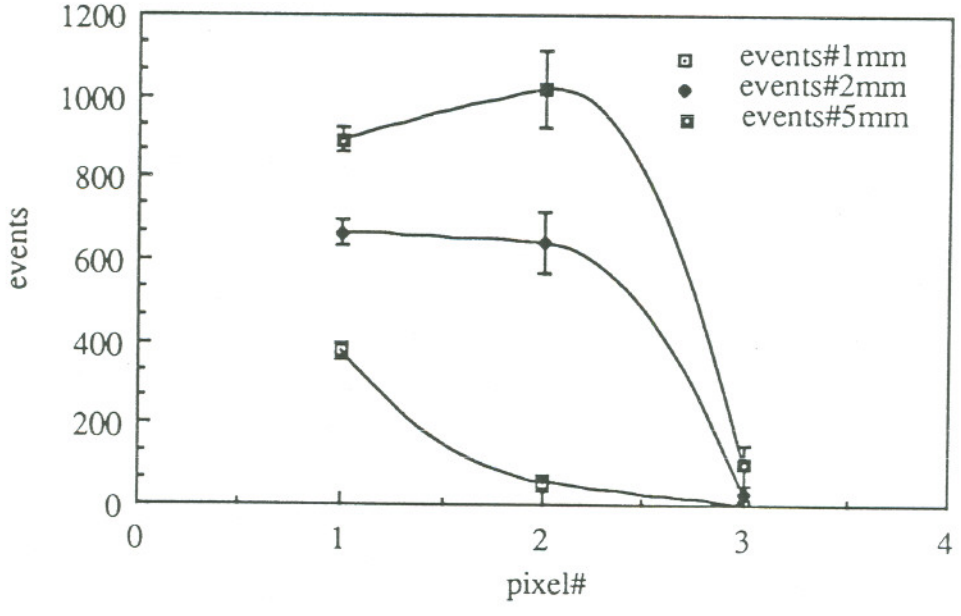


Figure 4.6 : Number of detected events per pixel for different CsI thicknesses

### 4.1.7. Multilayer Structure Efficiency

In order to obtain a better efficiency a multilayer structure can be proposed; two or more CsI/a-Si double deck layers can be considered, in analogy to the Tantalum/a-Si multilayer structure proposed in Chapter 3. Disadvantages in this case are multiplication of number of channels. The efficiency is evaluated here for variable number of layer for different scintillators (CsI Na-doped and Tl-doped) and different electron noise thresholds.

The efficiency of one layer is

$$\varepsilon = \frac{\int_{NoiseThr}^{\infty} N_{Sc}(n)\, dn}{10000}$$

where the number of photon distribution $N_{Sc}$ is the same for both scintillator, apart of a chance of scale (from 50000 photon/MeV to 40000 photon/MeV).

For a multilayer ( n layers) structure, in analogy to what we already calculated for Ta/a-Si, the total efficiency can be expressed :

$$\varepsilon_{tot} = \frac{N}{I_0} = \frac{1}{I_0}\sum_{i=1}^{n} N_i = \frac{1}{I_0}\sum_{i=1}^{n} \varepsilon I_{i-1} = \varepsilon \sum_{i=1}^{n} e^{-\mu t(i-1)}$$

where $\mu = \Sigma\rho = 0.44\ cm^{-1}$ for CsI and t = 1 mm.

One, two and ten layers are considered and the final efficiencies are presented in Table 4.4:

Table 4.4 :

| Scintillator | Noise (electrons) | 1 layer $\varepsilon_{tot}$ (%) | 2 layers $\varepsilon_{tot}$ (%) | 10 layers $\varepsilon_{tot}$ (%) |
|---|---|---|---|---|
| CsI(Na) | 400 | 3.7 ± 0.2 | 7.2 ± 0.4 | 31. ± 2. |
| CsI(Na) | 800 | 3.4 ± 0.2 | 6.7 ± 0.4 | 28. ± 2. |
| CsI(Na) | 1200 | 3.1 ± 0.2 | 6.1± 0.4 | 26. ± 2. |
| CsI(Tl) | 500 | 3.7 ± 0.2 | 7.2 ± 0.4 | 31. ± 2. |
| CsI(Tl) | 1000 | 3.4 ± 0.2 | 6.7 ± 0.4 | 28. ± 2. |

## 4.2. CsI Filled Glass tubes arrays: A Monte Carlo Simulation

In order to obtain a better position resolution an array of glass tubes (inner diameter of the order of 2 mm) filled with CsI is considered: the light produced by electrons (photoelectric or Compton electrons from $\gamma$ interaction) in the CsI is collimated within the tubes by total or partial reflection (Figure 4.7); total and partial reflection due to different indexes of reflection of CsI and glass we can obtain a collimation of the light on one end of the tubes of about 20% (simulation by REFLEX program, cfr. Appendix), using metal coated tubes we can achieve a theoretical collimation of 50%, adding a reflecting cap on one end of the tubes 100%; the light is eventually detected by an array of amorphous silicon pixel of about the same size than the diameter of the tubes (2 mm). A complete Monte Carlo simulation is performed by the WHOPPER Program listed in the Appendix.

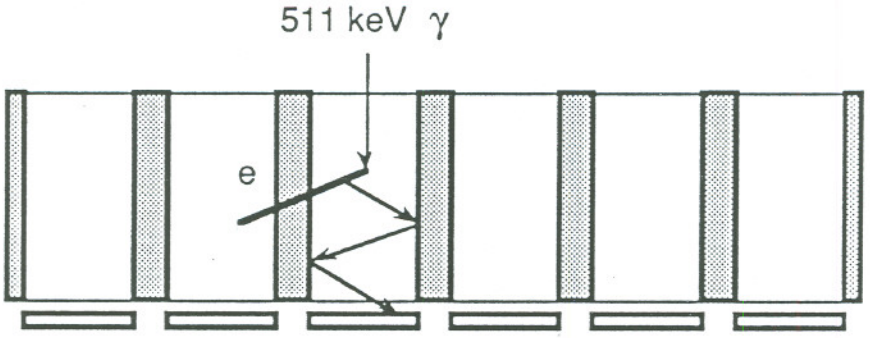


Figure 4.7 : $\gamma$ interaction and photon reflections within the tubes.

### 4.2.1. Geometry

In the first step of the simulation the geometry is very simple: a CsI infinite slab with variable thickness (0.5,1,1.5,2 cm), vacuum on the front end, and an array of square pixels of 2 mm size and negligible thickness on the other end; the effect of the glass is neglected as will be justified in the Appendix to the Monte Carlo Calculation in this Chapter.

### 4.2.2. Incident Particle Parameters

Electron-positron annihilation photons of .511 MeV are considered striking the detector at the same point (0,0), all of them with a null angle with the normal to the surface. 5000 events were considered in the simulation.

### 4.2.3. Photon Interaction and Produced Electrons

For each charged particle (electrons from photoelectric interaction or Compton scattering) produced, the origin point, the end point and the released energy are recorded. For each event the program keeps track of the total energy

released, the number (usually one, due to the thin detector), the energy and the position of the track in the CsI.

### 4.2.4. Light Yield

At this point the array structure of the CsI/glass converter is considered; a reasonable small array of tubes is considered ( 5 X 5 tubes of 2 mm diameter); for simplicity columns with a square base matching amorphous silicon detectors on one end are considered. Infinitely thin glass walls are assumed. For each track the location of the origin and end point are determined; if they are both in the same column, all the energy is released there, if they are located in two neighboring columns, 2/3 of the energy is assumed to be released in the end point column, 1/3 in the origin column. Energy loss in glass are neglected as will be justified in the Appendix to the Monte Carlo Calculation at the end of this Chapter. As a result, the total energy released in each region (or column) is converted to the number of photons generated within the same region (or column).

### 4.2.5. Light Detection in a-Si Pixels

At this point an algorithm (ALGPHO) takes care of the distribution of the light produced in each column on the detector that directly matches it and on the surrounding detectors. Three different cases are showed, depending on the type of system chosen in building the CsI tubes arrays:

1. metallic coating on the whole tube, but not on the end facing the detector: 100 % of the light is detected in the facing pixel, nothing outside;
2. metallic coating on the walls of the tubes: 50 % of the light on the facing pixel, nothing outside;
3. no coating: 20 % of the light on the facing pixel, negligible light outside.

From these parameters it is easy to foresee a good spatial resolution: in all the three cases only the facing pixel can receive enough light to detect the track.

In Figure 4.9 the histograms of the number of photons detected in the central pixel #1 are presented for different light collection efficiency (20 %, 50 %, 100 %), for tubes array 5 mm, 10 mm, 15 mm and 20 mm thick. It is interesting to stress that most of the events are concentrated in a peak with several thousands of photons, much higher than a reasonable noise level.

Figure 4.8.a:photons per detected event (5 mm CsI)

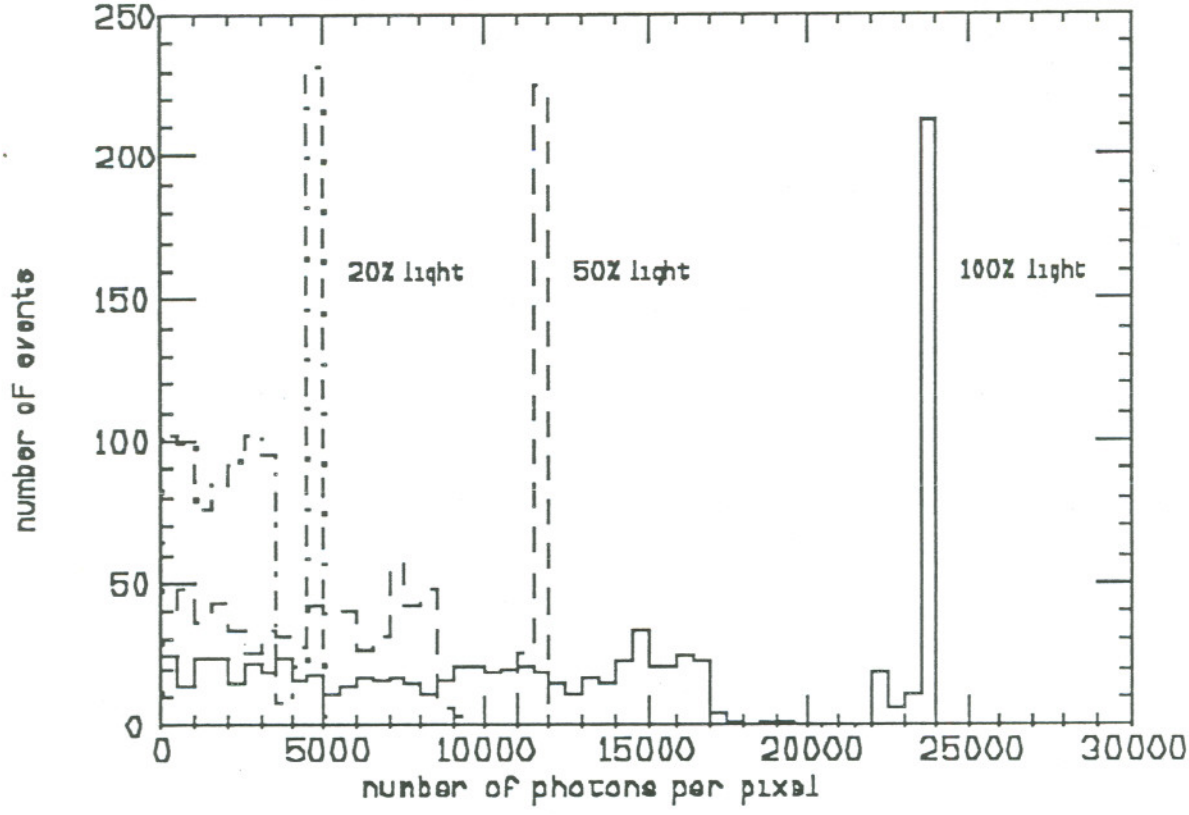


Figure 4.8.b:photons per detected event (10 mm CsI)

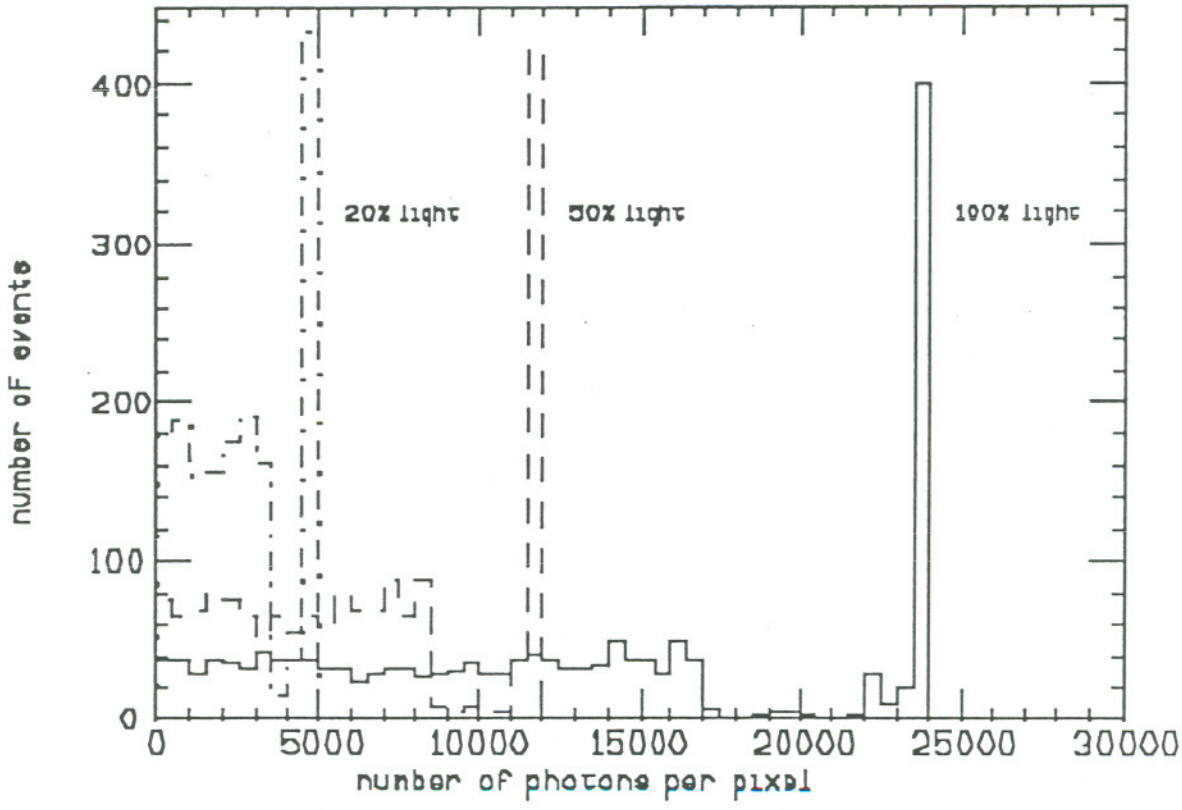

Figure 4.8.c:photons per detected event (15 mm CsI)

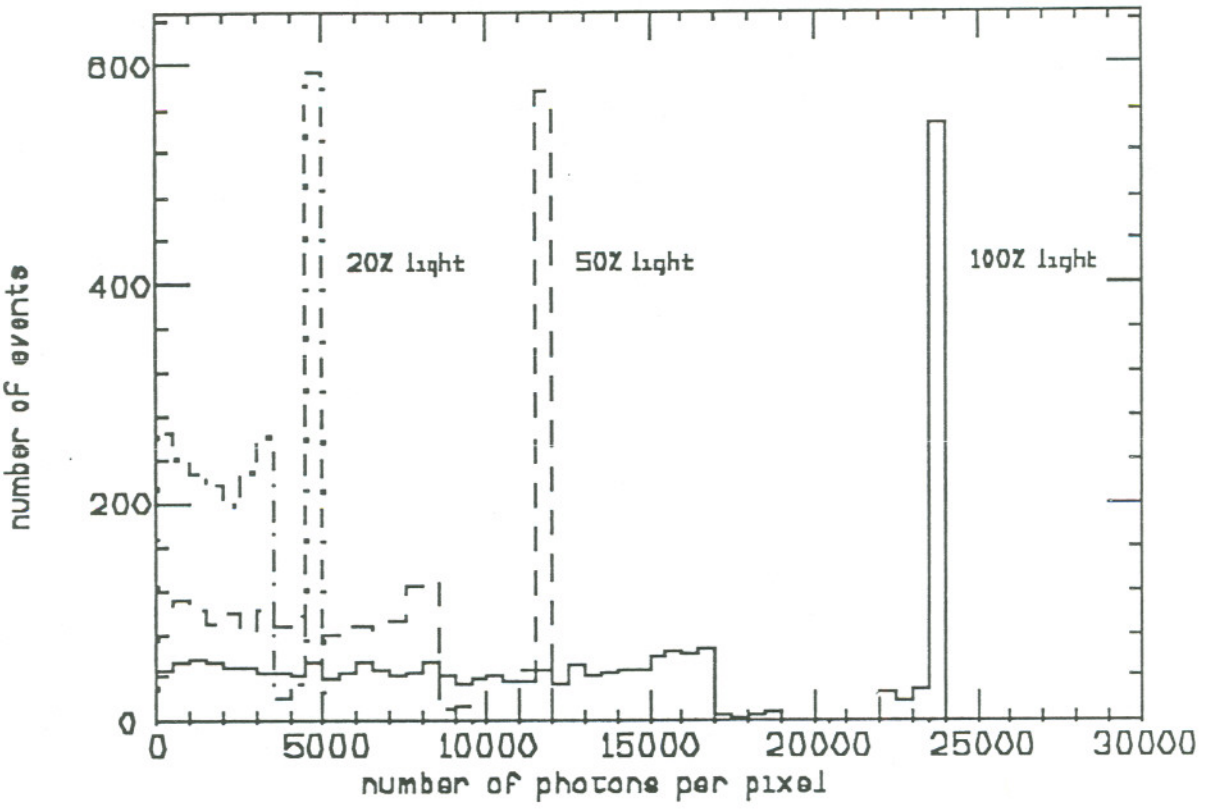


Figure 4.8.d:photons per detected event (20 mm CsI)

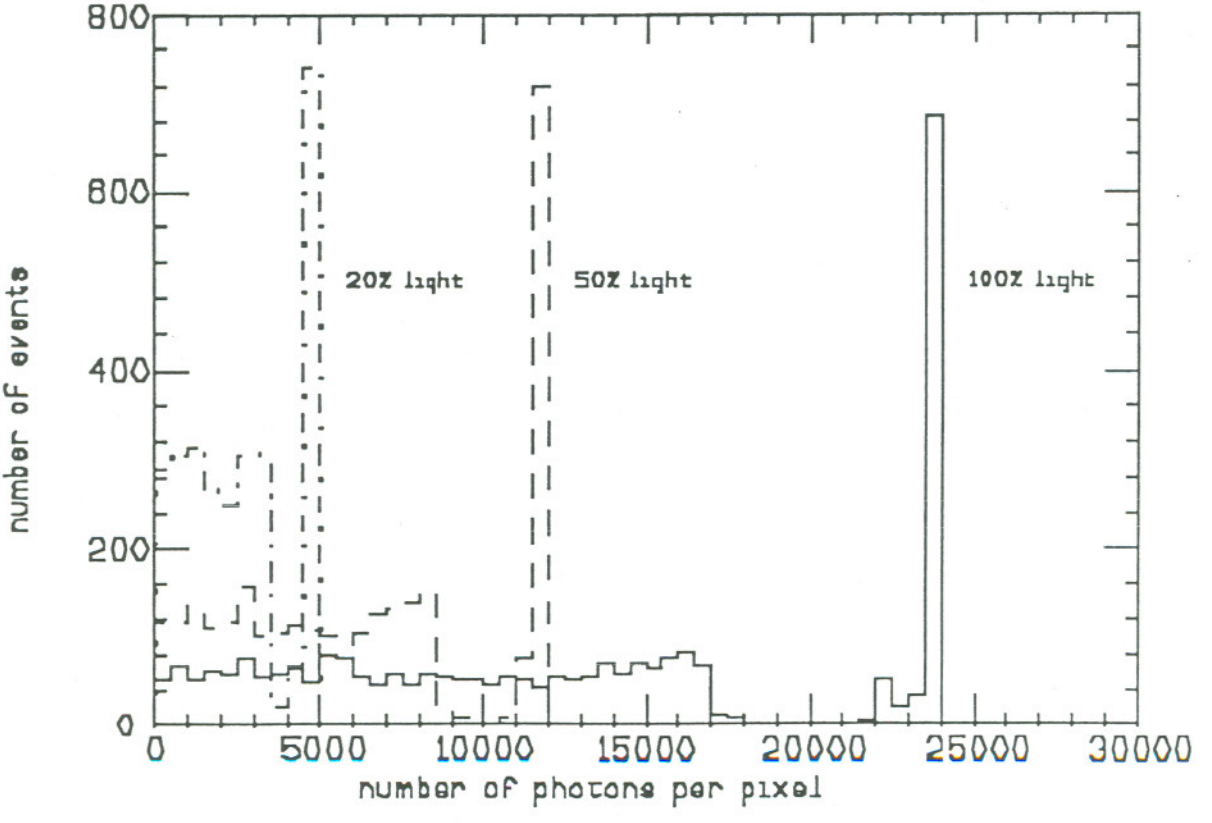

### 4.2.6. Efficiency

The interaction probability (number of 511 keV photons interacting in the CsI) is studied and presented in Table 4.5 as a function of the thickness of CsI; an increasing efficiency is obtained as the thickness increases, and the thicker detector increases also the percentage of total containment of the energy (total absorption in Compton scattering).

Table 4.5 :

| thick (cm) | peak (%) | $\varepsilon_{int}$ (%) |
|---|---|---|
| 0.5 | 38 | 18.2±.3 |
| 1.0 | 47 | 33.7±.4 |
| 1.5 | 53 | 45.7±.5 |
| 2.0 | 60 | 53.6±.5 |

The actual efficiency is obtained considering only the events above a threshold of 500 electrons (electronic noise of the amplifier):

$$\varepsilon = \frac{\int_{500}^{\infty} N(n)\, dn}{5000}$$

where n is no. of photons and N(n) is the distribution

In table 4.6 the value of the actual efficiency ε is presented as a function of the CsI thickness and the fraction of light detected at the end of the tubes(total and partial coating, no coating): the data are plotted in Figure 4.10.

Table 4.6 :

| light (%) / cm | 100 | 50 | 20 |
|---|---|---|---|
| 0.5 | 17.7±.3 | 17.5±.3 | 16.2±.3 |
| 1.0 | 33.0±.4 | 32.2±.4 | 30.2±.4 |
| 1.5 | 44.8±.5 | 43.7±.5 | 40.5±.5 |
| 2.0 | 56.2±.5 | 54.9±.5 | 51.4±.5 |

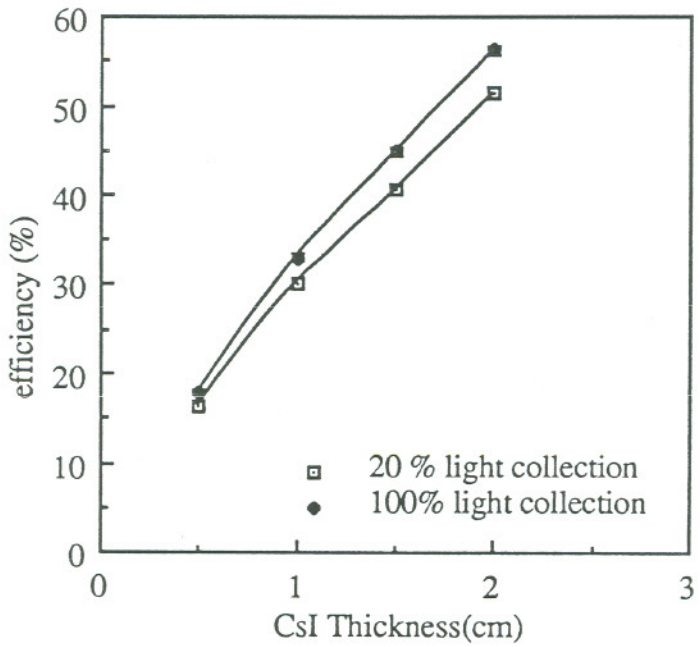


Figure 4.10 : Efficiency as a function of CsI Thickness for different optical coupling configurations

In the case of complete light collection (100 %) the efficiency is evaluated here for different light yield CsI, Na-doped and Tl-doped, for variable electron noise thresholds, for thin CsI arrays (0.5 and 1.0 cm).

The efficiency is

$$\varepsilon = \frac{\int_{NoiseThr}^{\infty} N_{Sc}(n)\, dn}{5000}$$

where the distribution $N_{Sc}$ of the number of photons is the same for both scintillators, apart from a change of scale (from 50000 photon/MeV to 40000 photon/MeV).

The final efficiencies are presented in Table 4.7 :

Table 4.7 :

| Scintillator | Noise (electrons) | ε (5 mm) (%) | ε (10 mm) (%) |
|---|---|---|---|
| CsI(Na) | 400 | 17.8 ± 0.6 | 33.0 ± 0.8 |
| CsI(Na) | 800 | 17.5 ± 0.6 | 32.2 ± 0.8 |
| CsI(Na) | 1200 | 17.0 ± 0.6 | 31.6 ± 0.8 |
| CsI(Tl) | 500 | 17.8 ± 0.6 | 33.0 ± 0.8 |
| CsI(Tl) | 1000 | 17.5 ± 0.6 | 32.2 ± 0.8 |

## 4.3. Initial Test of CsI/Amorphous Silicon Detectors

### 4.3.1. CsI Scintillation Light Yield

The photon yield per MeV of CsI is a critical parameter for the feasibility of this PET project. If we assume a Quantum Efficiency of a-Si:H photodiode as equal to 100 % for sake of simplicity (80 % could be more reasonable value in the range 300 nm - 700 nm considered, even if we have good optical coupling between CsI and a-Si) the number of photons per MeV is equal to the number of electron-hole pairs per MeV in the detector, therefore it is directly related to the signal on the detector. Because of the high noise of this large area (2 x 2 $mm^2$) detectors the Signal to Noise ratio is critically dependent on the light yield of the CsI. The light yield is strongly dependent on type of dopant in the CsI crystal, and literature is not consistent on the actual experimental value for the light yield. In general the light yield is slightly dependent on the dopant concentration above 1 % in weight [4,5]. Essentially CsI(Tl), CsI(Na), and pure CsI are considered.

In Table 4.8 the characteristics of the emission spectrum for each scintillator are presented [4,6] .

Table 4.8 :

| Crystal | Decay Time (ns) | Wavelength Peak (nm) | Wavelength Range* (nm) |
|---|---|---|---|
| CsI(Tl) | 900 | 550 | 420-700 |
| Cs(Na) | 500 | 420 | 350-550 |
| CsI(pure) fast | 10 | 310 | 280-350 |
| CsI(pure)slow | 500-3000 | | 480-600 |

* Emission intensity reduced to 10 % of the peak value.

In Table 4.9 some experimental values of scintillation light yield are presented; data were taken by the authors using Silicon PhotoDiodes (PD) or PhotoMultiplier Tubes (PMT), and are corrected by the Quantum Efficiency (QE) of the device at the emission wavelength of the scintillator.

Table 4.9 :

| Crystal | Holl et al.[7] PD | Sakai [8] PD* | Sakai [8] PMT | Grassmann et al. [4,9] PD | Kubota [6] & Bebek [10] PMT |
|---|---|---|---|---|---|
| CsI(Tl) | 51800 | 51300 | 56000 | 45000 | |
| CsI(Na) | 38500 | 41800 | 43000 | 12200 | |
| CsI(pure) | 16800 | | | | 2000** |

* The raw data published by the author are here corrected using the QE of the PD;
** Only fast component.

Due to the high light yield required by our high level of noise only CsI(Tl) and CsI(Na) can be considered suitable for our proposal; actually in the simulation we used the CsI(Tl) light yield of 50000 photons/MeV (a reasonable value from the literature).

For time resolution considerations the pure CsI fast component (about 10 ns) is very attractive, but the very low light yield and therefore the small efficiency of the detector make this choice unsuitable.

### 4.3.2. First Experimental Data

Tests of CsI(Na) deposition on glass substrates is presently in progress at LBL and the light yield of different samples is being measured as a first step toward deposition on the a-Si:H detector itself. Deposition is made by evaporation of CsI(Na) ( 1 % in weight of NaI) on glass substrate. In order to have a better collimation of the scintillation light within the CsI layer (avoiding the lateral spread of the light and the collimation on just on pixel detector)a microcolumnar structure [11,12,13] with column diameter of 50÷100 μm in the CsI layer is researched; for this purpose deposition rate, substrate temperature and cooling rate are varied. Our samples are 1 inch diameter circular CsI(Na) layers, 100-200 μm thick, on a 800 μm glass substrate, obtained at a deposition rate of 5-10 μm/min, substrate temperature ranging from 100 °C to 200 °C, cooling rate from 100 °C/h to 200 °C/h.

The light yield produced by a $^{249}Cf$ source (5.8 MeV α-particle) in the samples was measured by a Hamamatsu PIN Silicon Photodiode S 1723-04, operating at a reversed bias of 30 V, with a measured noise of about 1000 electrons. The range of the spectral response is 320÷1060 nm, with a peak wavelength of 900 nm; the Quantum Efficiency at 540 nm is 70 %. A pre-amplifier and a shaping amplifier with a 6.4 μs peaking time were used, and the output fed into a Pulse Height Analyzer. In Figure 4.13 a typical Pulse Height spectrum is presented.

The light yield Y of the sample was derived from the peak value $N_e$ in the spectrum according to

$$N_e = E_{dep} Y \ \Omega \ QE$$

where $E_{dep}$ is the deposited energy, $E_{dep}Y$ is the number of photons produced, Ω is the fraction of solid angle covered by the photodiode, QE is the photodiode Quantum Efficiency at 540 nm. Average $N_e$ about 25000 electrons was obtained in our samples, with a maximum value of 33000 electrons. For QE ≈ 0.70, Ω ≈ 0.5, $E_{dep}$ ≈ 5.8 MeV, we obtain an average light yield Y of 12300 photon/MeV and a maximum value of 16300 photon/MeV. The factor 2÷3 missing in our experimental results could be due to optical reasons: bad optical coupling between CsI and photodiode that can cause a large amount of backscattering on the surface and the often irregular polycrystalline structure of CsI layer that scatters light in all directions.

In order to improve the optical coupling between CsI layer and the a:Si pixels, deposition of CsI(Na) directly on an a:Si substrate is to be preferred, and a first test of deposition of CsI on an a:Si detector is in course.

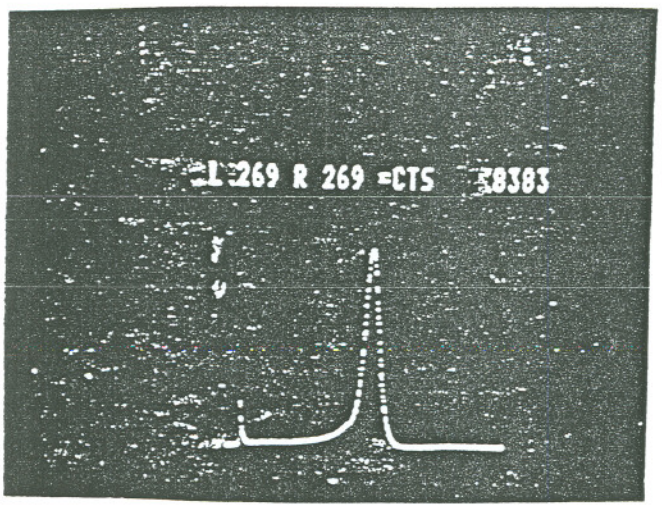


Figure 4.13: Photodiode electronic signal histogram for one of the CsI(Na) samples; the peak corresponds 2.4 $10^4$ photoelectrons.

## 4.4. Conclusions

Two structure have been studied : CsI/a-Si:H multilayers and CsI filled glass tubes. The tubes structure is technologically more feasible since only one detector layer is required and only one electronics plane and it has excellent spatial resolution due to the intrinsic collimation property of tubes. In order to reduce the spatial resolution degradation due to parallax error a CsI layer of about 10 mm is proposed, with a total efficiency of about 30 %.

## 4.5. Appendix to the Monte Carlo Calculation

### 4.5.1. Distribution of Light on the Pixels: ANGALG

The definitions of $\Omega$ and $\theta$ used in order to calculate the distribution of light on a pixel at a distance R from a light point source in the CsI layer is showed in Figure 4.11:

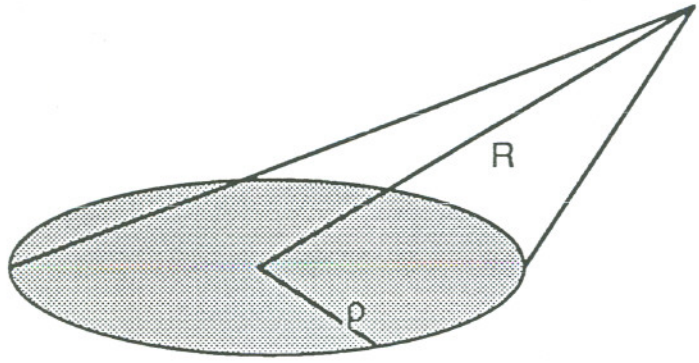


$$\psi = \text{arctg}\left(\frac{z}{r+\rho}\right)$$

$$\varphi = \text{arctg}\left(\frac{z}{r-\rho}\right)$$

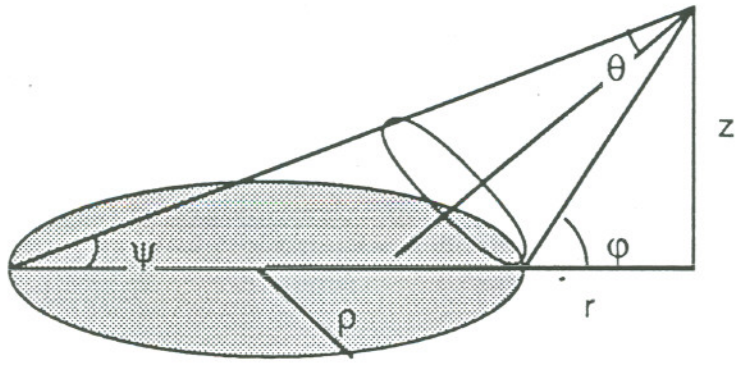


$$\theta = \frac{1}{2}(\varphi - \psi) \quad \text{if } \varphi > 0$$

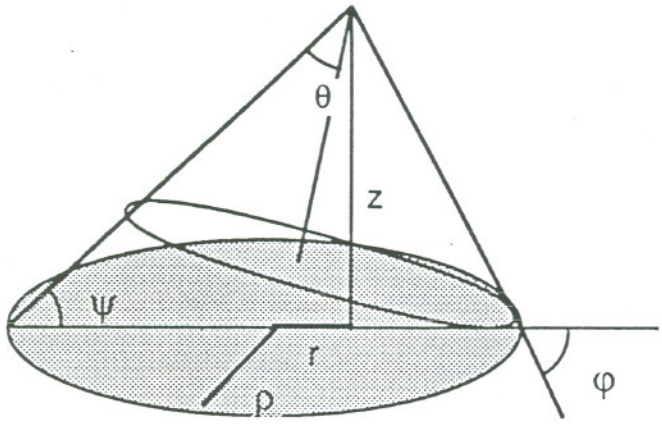


$$\theta = \frac{1}{2}(\varphi - \psi + \pi) \quad \text{if } \varphi < 0$$

$$\Omega = 2\pi(1 - \cos\theta)$$

Figure 4.11 : Solid angle $\Omega$ covered by a detector of radius $\rho$ for a point light source in R.

### 4.5.2. Consideration on the Effects of the Glass Walls

Since the CsI in contained in glass tubes of finite dimension one has to evaluate [1,2] the effect of the glass in the interaction of photons of 511 keV and its stopping power for electrons freed by photon interaction. We are considering a light glass (2.5 g/cm$^3$ density, essentially $SiO_2$), and thin wall (about 50 μm).

1.Photon interaction in glass [1] :

We can consider the effective mass absorbing coefficient $\mu\rho_{eff}$ obtained by adding the $\mu\rho$ of glass and CsI weighted by their volume ratios:

$$\mu\rho_{eff} = \frac{V_{glass}}{V_{tot}}\mu\rho_{glass} + \frac{V_{CsI}}{V_{tot}}\mu\rho_{CsI}$$

Estimating $\mu\rho_{glass}$ :

$\mu\rho_{glass} = N_{Si}\,\sigma_{Si} + N_O\,\sigma_O = N(\sigma_{Si} + 2\sigma_O)$ ,

where $N = \rho/Mol = \rho/(A_{Si}+2A_O)M_p$ and $M_p = 1.67\ 10^{-27}$ kg

where $\sigma_{Si}$ = 4.08 barn/atom

where $\sigma_O$ = 2.32 barn/atom

$\mu\rho_{glass} = 0.025\ cm^{-1}$ ( $\lambda = 1/\mu\rho_{glass} = 40.$ cm )

Estimating $\mu\rho_{CsI}$ :

$\mu\rho_{CsI} = N_{Cs}\,\sigma_{Cs} + N_I\,\sigma_I = N(\sigma_{Cs} + \sigma_I)$ ,

where $N = \rho/Mol = \rho/(A_{Cs}+A_I)M_p$

where $\sigma_{Cs}$ = 21.6 barn/atom

where $\sigma_I$ = 20.3 barn/atom

$\mu\rho_{CsI} = 0.44\ cm^{-1}$ ( $\lambda = 1/\mu\rho_{glass} = 2.27$ cm )

since $\mu\rho_{glass}/\mu\rho_{CsI} = .054$, we can approximate :

$$\mu\rho_{eff} \approx \frac{V_{CsI}}{V_{tot}}\mu\rho_{CsI}$$

In our simulation we just considered $\mu\rho_{eff} \approx \mu\rho_{CsI}$ ; in second approximation we could in any case correct the efficiency

$$\varepsilon_{eff} \approx \frac{V_{CsI}}{V_{tot}}\varepsilon_{CsI}$$

2.Range of electrons in glass [2,3] :

The electron produced by photoelectric interaction in CsI (about 50%) are 480 keV electrons (K-edges of Cs and I are about 35 keV), and the Compton electrons have a continuous spectrum. A rough estimation of the range R for the 480 keV electrons can be obtained weighing the range R in Si (.2 g/cm$^2$) and O (.19 g/cm$^2$) by the molar ratio w (1/3 and 2/3):

$$R(g/cm^2) = \sum_{i=1}^{2} w_i R_i = 0.2\ g/cm^2$$

$$R = \frac{R(g/cm^2)}{\rho} = 800\ \mu m$$

Therefore the glass walls (50μm) are almost transparent for most of the electrons.

### 4.5.3. Total and Partial Reflection of Light in Tubes

If n visible photons are generated within the tubes they have a probability P of being reflected depending on their angle ψ with the normal to the surface of the walls (Fresnel Law); part of the photons undergo total reflection ($\sin\psi\ n_{CsI} > n_{glass}$), part partial reflection.

In the first case:

$$\text{for } \sin\psi \le \frac{n_{glass}}{n_{CsI}} \qquad P = \frac{1}{2} R(\vartheta,\varphi,n)^{M(\vartheta,\varphi,r,z)}$$

In the second case:

$$\text{for } \sin\psi \ge \frac{n_{glass}}{n_{CsI}} \qquad P = \frac{1}{2}$$

where P is the probability for a photon generated in (r,z) with direction $(\vartheta,\varphi)$ to reach the detector on one end of the tube, R is the probability to be reflected within the tube, M is the number of reflections before emerging out of the tube, $n=n_{glass}/n_{CsI}$ (for a definition of R and M see program REFLEX, Appendix ). In our case $n_{glass} \approx 1.6$ (light glass, visible photons), $n_{CsI} \approx 1.8$ (for 560 nm), n = .89.

We calculated the average probability <P> generating 1000 photons randomly within a tube, and randomly directed: <P> ≈ .20, almost constant in the range of z ≈ 1÷2 cm, r ≈ .5÷1 mm; almost all these photons are due to total reflection. In the case of coating of the wall of the tubes <P> ≈ .50, with reflecting caps on the other side of the tubes <P> ≈ 1.

### 4.5.4. Parallax Considerations

In order to study the effects on spatial resolution due to a thick CsI converter (parallax error) was considered the case of 511 keV photons incident with a 10° angle with the axis of the tubes for a detector 10 mm thick. The program WHOPPER (cfr. Appendix) was run.

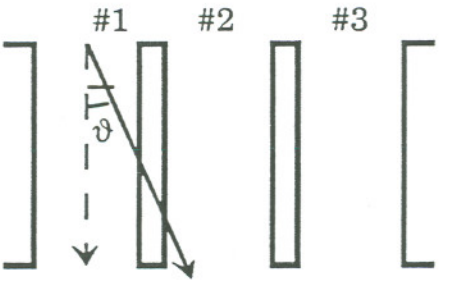


Figure 4.12 : $\gamma$ path through the tubes array in case of direction not parallel to the axis of the tubes.

The number of events detected in each tubes must be proportional to the attenuation of the photon beam $1 - e^{-\mu\rho x}$, where x is the track in each tube. For our values (tube length 10 mm, tube radius 1 mm, photon generated at one end of tube #1 on the axis of the tube with angle $\vartheta = 10°$),

$1 - e^{-\mu\rho x(\#1)} \approx .2239$ and $1 - e^{-\mu\rho x(\#2)} \approx .1366$ , and their expected ratio is .61 .

From the Monte Carlo Simulation (in the case of 100 % light collection) :

| pxl# | events (>500pho) |
|---|---|
| 1 | 1098 ±33 |
| 2 | 694 ± 26 |
| 3 | 19 ± 4 |

The ratio events#2/events#1 ≈ 0.63, is in agreement with what we were expecting. This number is still acceptable but in absence of any correction algorithm for parallax error the detector thickness should not exceed 10 mm in order not to deteriorate the spatial resolution.

For 5 mm of thickness and an opening of 10° almost all the events are detected in the pixel #1, as showed in the following table:

| pxl# | events (>500pho) |
|---|---|
| 1 | 983 ± 31 |
| 2 | 29 ± 5 |
| 3 | 10 ± 3 |

A ratio events#2/events#1 ≈ 0.03 was obtained for 5 mm thickness, which is a warranty of good spatial resolution.

## 4.6. References


[1] W. H. McMaster et al., *Compilation of X-Ray Cross Sections, UCRL Report 50174* (1970).
[2] Berger and Seltzer, *Stopping Power and Range Tables for Protons, Mesons and Electrons, NASA SP-3036* (1964).
[3] *Stopping Power and Range for Electrons, UCRL Report 2426* (1966).
[4] H. Grassmann et al., *Nucl. Instr. Meth. 228* , p.323 (1985).
[5] B. C. Grabmaier, *IEEE Trans. Nucl. Sci. NS-31* , p.372 (1984).
[6] S. Kubota et al., *Nucl. Instr. Meth. A268* , p.275 (1988).
[7] I. Holl et al., *IEEE Trans. Nucl. Sci. NS-35* , p.105 (1988).
[8] E. Sakai, *IEEE Trans. Nucl. Sci. NS-34* , p.418 (1987).
[9] H. Grassmann et al., *Nucl. Instr. Meth. A234* ,p.122 (1985).
[10] C.Bebek, *Nucl. Instr. Meth. A265* , p.258 (1988).
[11] C. W. Bates, *Adv. Electronics and Electron Physics 28A* , p.451 (1968).
[12] A.L.N. Stevels et al., *Philips Res. Reports 29* , p.340 (1974).
[13] A.L.N. Stevels et al., *Philips Res. Reports 29* , p.353 (1974).

# 5. Xenon Scintillation Light & Amorphous Silicon Detectors for PET

In this chapter the feasibility of a PET using Xe scintillation light is evaluated. Due to the low interaction probability for 511 keV-γ rays in Xe at pressures of few atmospheres, the gas is associated to a high Z and high density lead glass (70÷80 % PbO, 5÷6 g $cm^{-3}$ density), working as a converter for photons. The proposed geometry is a lead glass array of small tubes (1÷ 2 mm diameter, 1 cm long) immersed in a gas atmosphere; unlike the CsI-glass array project, in which CsI was both γ/electron converter and scintillator, and the tubes walls where just optical collimators for visible photons, in this case the lead glass tubes walls are γ/electron converters and optical collimators, while the gas is the scintillator.

γ-rays interact in the glass walls producing primary electrons (most of them photoelectric electrons); part of them reach the gas region within the tubes, leaving an ionization track of secondary electrons, that are drifted along the axis of the tubes by an electric field E due to a bias applied between the ends of the tubes. During their drift, electrons produces UV scintillation light in Xe, that is reflected by a coating on the walls of the tubes and collimated toward one end of the tube where amorphous silicon detectors are placed.

Detector pixel size of 2mm is assumed, small enough to allow a good spatial resolution, but large enough to avoid an excessive number of electronics channels. The detector thickness is chosen to be 25 μm, although a few microns are sufficient to detect all the UV photons, in order to reduce the capacity of the large detector.

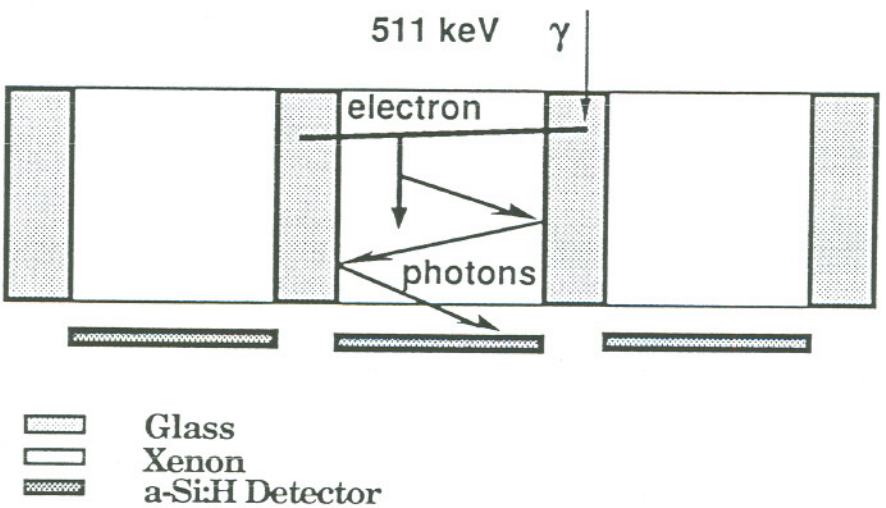


Figure 5.0 : Gamma interaction in Xenon filled lead glass tubes array.

## 5.1. Mechanism of Scintillation in Xenon

The scintillation light produced by electrons drifting in Xe (or rare gases in general) has been extensively studied both experimentally and theoretically (see Appendix for references): typical emission spectra present sharp atomic resonance lines (essentially transitions $^3P_1 \rightarrow {}^1S_0$ and $^1P_1 \rightarrow {}^1S_0$ in Xe atoms) and two broad bands named I continuum (peak at 1490 Å) and II continuum (peak at 1770 Å) that are due to decay of unstable $Xe_2$ molecules. It is known [1,2] that for reasonably high pressures (definitely [2] for pressures higher than 100 Torr) the atomic lines are suppressed.

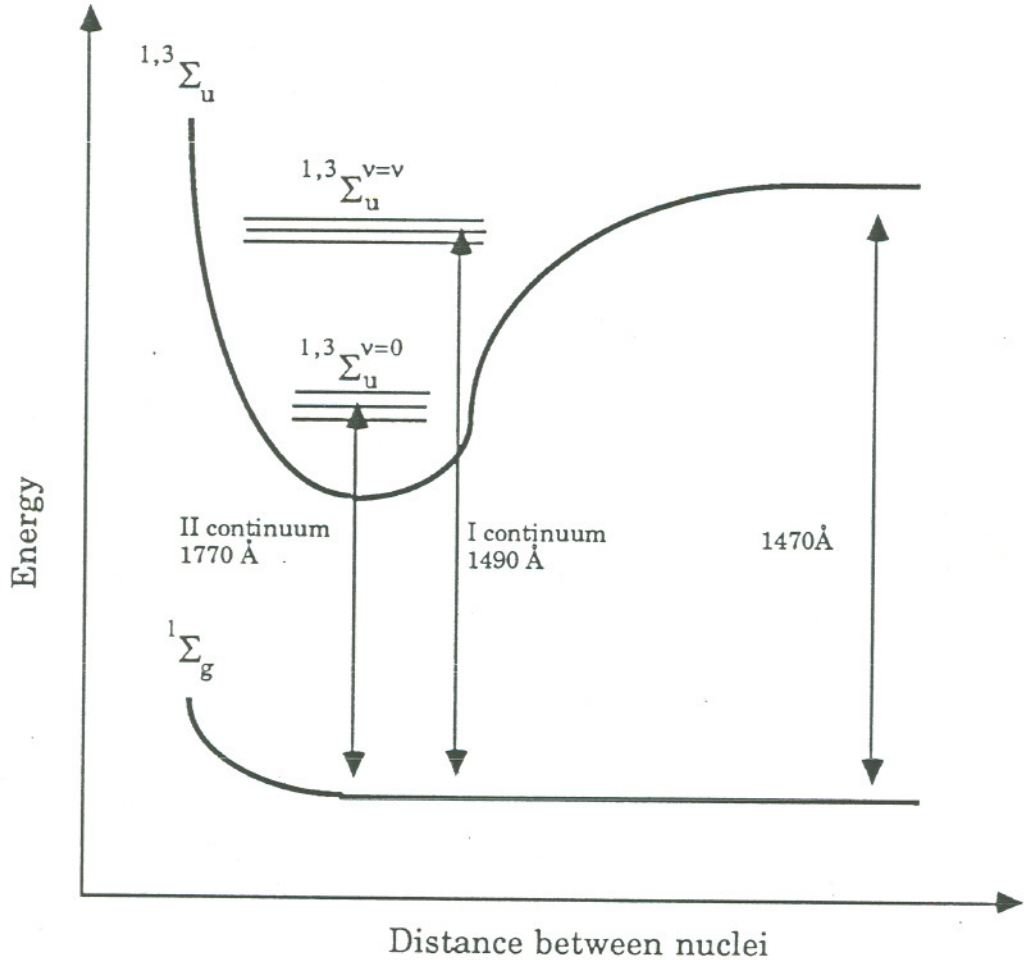


Figure 5.1 : Potential curves for lower excited states of Xenon molecule.

The two continua correspond to transitions from the excited states $^3\Sigma_u$ and $^1\Sigma_u$ (energetically hardly separated [3]) to the repulsive ground state $^1\Sigma_g$ of the $Xe_2$ molecule: the I continuum is attributed[1] to transition from the vibrationally excited states $^{3,1}\Sigma_u^{v}$ to the ground state $^1\Sigma_g$ and the II continuum to transition from the vibrationally relaxed levels $^{3,1}\Sigma_u^{v=0}$ to the same ground state $^1\Sigma_g$ . Since high pressures ease non-radiative collision decay of the vibrationally excited

states to vibrationally relaxed states $^{3,1}\Sigma_u^{v} \rightarrow {}^{3,1}\Sigma_u^{v=0}$, for pressures of the order of atmospheric pressure the I continuum is no longer visible [3].

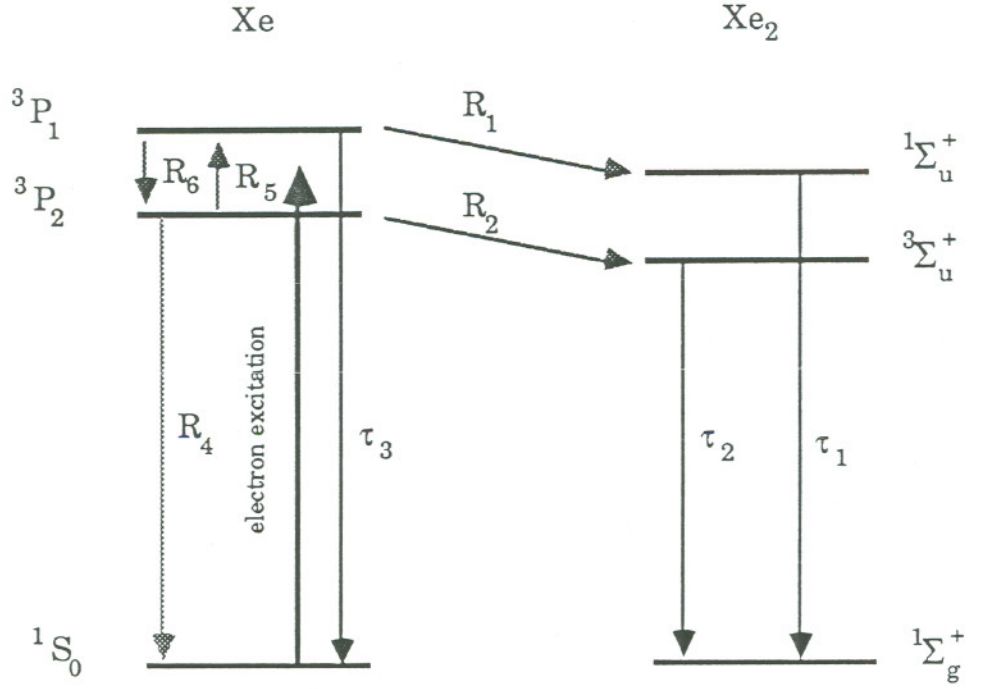


Figure 5.2 : Kinetic model for production of Xe scintillation light.

In Figure 5.2 is shown the kinetic model [4] for the production of Xe scintillation light (only the vibrationally relaxed $^{3,1}\Sigma_u^{v=0}$ states are considered here) :

excitation due to collision with drifting electrons populates at the same rate the two levels $^3P_1$ and $^3P_2$ ,

$\tau_1$ , $\tau_2$ are time constants for radiative decays of two $Xe_2$ excited levels $^{3,1}\Sigma_u$, energetically practically unresolved ($\tau_1 \approx 5$ ns, $\tau_2 \approx 100$ ns),

$\tau_3$ is a time constant for the radiative decay of Xe excited atom $^3P_1 \rightarrow {}^1S_0$ ($1/\tau_3 = 1.5\ 10^5$ sec$^{-1}$),

$R_4$ is the rate for a collision induced (otherwise forbidden) radiative decay of $^3P_2$ (two body process, $R_4 = 71$ sec$^{-1}$Torr$^{-1}$) ,

$R_5$ and $R_6$ are the rates for collision induced transition between the two excited states $^3P_2$ and $^3P_1$ of Xe atom (two body process, $R_5 = 9.1\ 10^3$ sec$^{-1}$Torr$^{-1}$, $R_6 = 49$ sec$^{-1}$Torr$^{-1}$),

$R_1$ is the rate for the formation of a $Xe_2(^1\Sigma_u)$ molecule from $^3P_1$ (three body process) : $Xe(^3P_1) + 2\ Xe(^1S_0) \rightarrow Xe_2(^1\Sigma_u) + Xe(^1S_0)$ , $R_1 = 46$ sec$^{-1}$Torr$^{-2}$ ,

$R_2$ is the rate for the formation of a $Xe_2(^3\Sigma_u)$ molecule from $^3P_2$ (three body process) : $Xe(^3P_2) + 2\ Xe(^1S_0) \rightarrow Xe_2(^3\Sigma_u) + Xe(^1S_0)$, $R_2 = 40$ sec$^{-1}$Torr$^{-2}$.

For pressures p of a few hundred Torr the three body processes are dominant; since $R_1p^2 \gg R_6p + 1/\tau_3$ and $R_2p^2 \gg R_5p + R_4p$ we can approximate the kinetic mechanism as in Figure 5.3 .

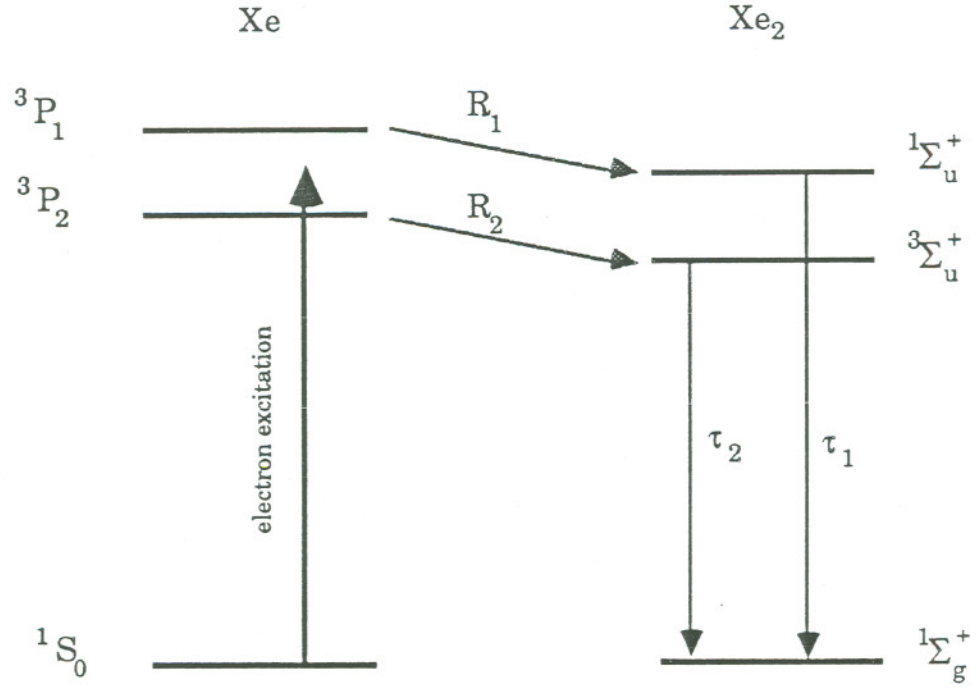


Figure 5.3 : Approximated kinetic model for production of Xe scintillation light.

As a result, the second continuum of Xe scintillation light has two components of about the same intensity, with decay times of 5 ns and 100 ns.

## 5.2. Light Yield and Drift Field

### 5.2.1. Experimental Background

Two complete experiments reported in the literature are the basis for the calculation. Conde [5] and Ngoc [6] both found a linear relationship between reduced light yield $\frac{1}{p}\frac{dn}{dx}\Big|_0$ (number of photons generated per unit of drift length - in this case it is a constant in x - and unit of pressure) and reduced electric field $\frac{E}{p}$ (electric field divided by pressure); both verified that at a high reduced field (about 5-6 $Vcm^{-1}Torr^{-1}$ for Ngoc, 6÷7$Vcm^{-1}$ $Torr^{-1}$) multiplication begins to occur and linearity fails. Conde' used 8.1 MeV α-particles, Ngoc different sources of γ-rays; both measured the total light yield and divided it by the number of primary electrons generated by ionization in Xenon (energy of the particle divided by 21 eV, the average ionization energy for Xenon). We present both, remarking that the slopes of the two straight lines differs for a factor 14. The units are V/cm for electric field E and Torr for pressure p.

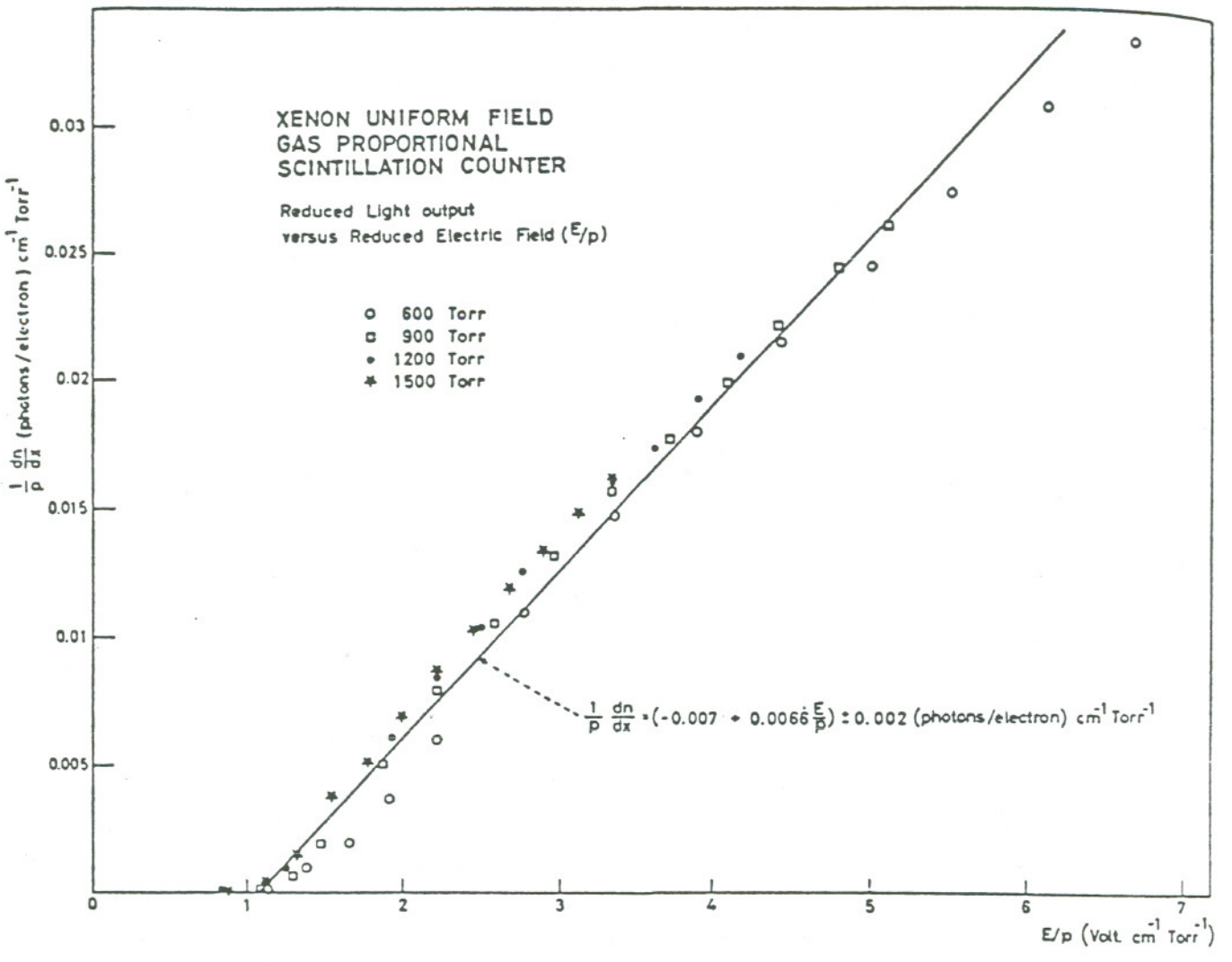


Figure 5.4 : Xenon scintillation light output from electrons drifting in uniform field as measured by Conde[5].

$$\frac{1}{p}\frac{dn}{dx} = 0.0066\frac{E}{p} - 0.007 \qquad \text{from Conde' et al.}$$

$$\frac{1}{p}\frac{dn}{dx} = 0.0840\frac{E}{p} - 0.148 \qquad \text{from Ngoc et al.}$$

In Figure 5.4 Conde's experimental data are presented.

### 5.2.2. Efficiency and Light Yield

Due to their short range in heavy lead glass, primary electrons have a limited probability for escaping the glass and reaching the gas within the tubes: this contributes to lower the efficiency of the system that is not simply the interaction efficiency of the glass itself. The resulting composite probability $\varepsilon_e$ has been evaluated by Monte Carlo Simulation Methods for similar PET [7], for 511 keV photons incident into a 1 cm thick array of heavy lead glass tubes. The efficiency decreases with the diameter of the tubes (for a fixed optimized outer diameter / inner diameter ratio of 1.2), as a power $\delta$ of the diameter D with $\delta < 1$. The total efficiency $\varepsilon_e$ to produce an electron that can reach the inside of the gas region is about 2.5 % for 2 mm diameter but if we cover the 2 mm size pixel area with a cluster of smaller tubes for instance of 0.6 mm diameter we can obtain a $\varepsilon_e$ of 7.5% . Note that smaller tubes are not technologically and cost convenient.

Electrons leave ionization tracks in the gas and stop on the walls of the tube because of the short range of electrons in heavy glass. The average track of electrons within the gas in a tube is about D, the diameter of the tube itself, and the number of secondary ionization electrons per track $n_{ept}$ is proportional to the pressure : $n_{ept} = 350\frac{p}{760}D$ (where D is in cm and p in Torr).

For smaller diameter tubes more $\gamma$-rays have tracks within the gas, but less UV photons for each event are available for the detector, since the scintillation light is produced by drifting secondary electrons and is then proportional to $n_{ept}$ , i.e. it can actually result in a lower total efficiency of the system, unless even a weak multiplication of the drifting electrons is obtained.

If a track is produced by a primary electron at a distance z from the end of the tube, the number of photons $N_{ph}(x_d)$ produced by drift of secondary electrons is

$$N_{ph}(x_d) = n_{ept}\int_0^{x_d}\left.\frac{dn}{dx}\right|_o dx \quad \text{where for} \quad \left.\frac{dn}{dx}\right|_0 \quad \text{we can use one of the experimental}$$

relationships by Ngoc or Conde.

Because of the low interaction efficiency for $\gamma$-rays the distribution of electrons entering the gas region (and leaving a track) is flat along the z axis of

the tube, and if $I_0$ is the intensity of γ-ray this distribution can be expressed as

$$\frac{dN_e}{dz}(z) = \frac{\varepsilon_e I_0}{z_0} .$$

An event is considered detected only if the number of photons $N_{ph}(x_d)$ that reach the a-Si detector is larger than the electron noise $N_{noise}$ ; we can define a minimum drift length $z_{min}$ below which the event is considered lost from $N_{ph}(z_{min})=N_{noise}$ .Therefore the number of detected events N is defined as

$$N = \int_{z_{min}}^{z_0} \frac{dN_e}{dz} dz$$

The value of $z_{min}$ is easy to find, since dn/dx is constant in x

$$N_{ph}(z_{min}) = n_{ept} \int_0^{z_{min}} \left.\frac{dn}{dx}\right|_0 dx = n_{ept} \left.\frac{dn}{dx}\right|_0 z_{min} = N_{noise}$$

$$\text{and } z_{min} = \frac{N_{noise}}{n_{ept} \left.\frac{dn}{dx}\right|_0} .$$

$$N = \int_{z_{min}}^{z_0} dN_e = \int_{z_{min}}^{z_0} \frac{\varepsilon_e I_0}{z_0} dz = \frac{\varepsilon_e I_0}{z_0}(z_0 - z_{min})$$

The resulting total efficiency $N/I_0$ is then

$$\varepsilon = \varepsilon_e(1 - \frac{z_{min}}{z_0}) = \varepsilon_e \left( 1 - \frac{N_{noise}}{z_0 350 \frac{D}{760} p \left.\frac{dn}{dx}\right|_0} \right) = \varepsilon_e(1 - \frac{N_{noise}}{N_1})$$

For $z_0$ = 1 cm, D = 2 mm, $N_1 = 0.0921 p \left.\frac{dn}{dx}\right|_0$ , where the reduced light yield depends on the experimental relationship we choose; we report the expected value according to both experiments of Conde' and Ngoc.

$N_1$ is the number of photons produced by an electron track per centimeter of drift.

$p \left.\frac{dn}{dx}\right|_0 = \left(a\frac{E}{p} - b\right)p^2 = \left(a\frac{E}{p} - b\right)\left(\frac{E}{p}\right)^{-2} E^2$ has a maximum for $\frac{E}{p} = 2\frac{b}{a}$ and chosen the reduced value according to this maximum we obtain the corresponding values for $N_1$ , plotted in Figure 5.5 :

$$N_1|_{Conde} = 0.0921 \cdot p \left.\frac{dn}{dx}\right|_{Conde} = 143 \cdot 10^{-6} \cdot E^2 \quad \text{for } \frac{E}{p} = 2.12 \text{Vcm}^{-1}\text{Torr}^{-1}$$

$$N_1|_{Ngoc} = 0.0921 \cdot p \left.\frac{dn}{dx}\right|_{Ngoc} = 1032 \cdot 10^{-6} \cdot E^2 \quad \text{for } \frac{E}{p} = 3.52 \text{Vcm}^{-1}\text{Torr}^{-1}$$

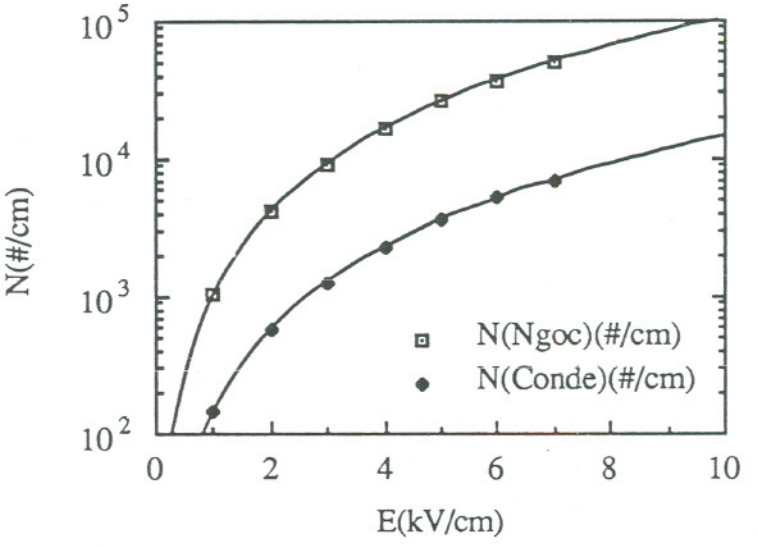


Figure 5.5 : Number of photons produced for each electronic track in Xenon after 1 cm of drift.

For a noise level of about 1000 electrons the plateau value (for a 2 mm diameter tube) of $\varepsilon \approx \varepsilon_e$ can be reached for $E/p \approx 8$ kV/cm in Conde's scheme, and $E/p \approx 3$ kV in Ngoc's.

In both Ngoc's and Conde's experiments the applied reduced field was small enough to avoid multiplication and long dead times that follow. In order to amplify the signal a small degree of multiplication can be considered, in the order of 10, easy to achieve at slightly higher fields. No complete experimental evidence has been found to support the possibility of a finely controlled multiplication for electrons in Xenon, but it can be the subject of a possible experimental research.

### 5.3. Electron Drift and Drift Time

A complete study of electron drift velocity in pure Xe in our range of reduced field (1÷15 V/cmTorr) is not available in the literature, but $v_d$ should be [8] in the range 0.1÷1. cm/μs ; most of the author [8,9] measured 0.15 cm/μs below 1 V/cmTorr, Charpak [10] measured 0.73 cm/μs at 13 V/cmTorr. Slight additions of quenching gas ($N_2$ , $CO_2$) can improve the drift velocity but generally reduce the light yield; a compromise should be found in order to optimize the product drift velocity - light yield. In Table 5.1 a brief summary of experiments are presented, showing the quantity of added gas, the factor of gain in drift velocity, the percentage of light lost and the range of drift field.

Table 5.1 :

| Quenching gas | drift velocity gain factor | light loss (%) | field range V/cmTorr | Author |
|---|---|---|---|---|
| 1.0 % $N_2$ | ? | 50 | ≤ 2 | Takahoshi [14] |
| 1.5 % $N_2$ | 3.5 | 10 | ? | Iqbal [11] |
| 1.5 % $N_2$ | 2 | 50 | 0.2÷0.5 | Alichanian[13] |
| 1.5 % $N_2$ | 3.5 | ? | 0.5÷1.3 | Alichanian[13] |
| 10.0 % $N_2$ | 2 | ? | 0÷13 | Charpak [10] |
| 1.0 % $CO_2$ | 10 | 20 | ≥ 0.4 | Sadoulet [12] |
| 1.0 % $CO_2$ | ? | 50 | ? | Iqbal [11] |
| 1.2 % $CO_2$ | 10 | ? | ≤ 1 | English [9] |
| 4.0 % $CO_2$ | 16 | ? | ≤ 1 | English [9] |

As a conclusion, we can assume in the best case a $v_d$ of about 1 cm/μs with no light loss, that for 1 cm of drift length corresponds to a drift time of 1 μs.

### 5.4. Conclusions

Although a general agreement is achieved on the theoretical explanation of the scintillation mechanism of Xenon in presence of drifting electrons and the experimental references agree on the general linear trend of the light yield as a function of the reduced drift field, the numerical values of the light yield obtained from the experiments can be different by an order of magnitude, leaving a wide indetermination for an accurate calculation of the performances of our proposed system. Nonetheless, since the efficiency upper limit for the system is determined by geometrical and material parameters of the glass structure, this plateau limit can be reached tuning the light yield by varying the reduced field E/p in the range of 1÷ 15 V/cmTorr, even using a weak electron multiplication if needed.

On the other hand the drift velocity of electrons in pure Xenon is very low (about 0.1 cm/μs), but small percentages of quenching gas can increase the velocity of 1 order of magnitude (about 1.0 cm/μs); also in this case the literature is convergent in the general trend but in disagreement on the numbers.

As a result we can reasonably assume that an optimal efficiency of 7.5 % and a maximum drift time of 1 μs could be obtained (for 1 cm long, 0.6 mm diameter, tubes).

## 5.5. References


[1] A. Policarpo, *Physica Scripta 23* , p.539 (1981).
[2] R. Brodmann et al., *J. Phys. B: Atom. Molec. Phys. 10* , p.3395 (1977).
[3] R.S.Mulliken, *J. Chem. Phys. 52* , p.5170 (1970).
[4] P. Leichner et al., *Phys. Rev. 13A* , p.1787 (1976).
[5] C. Conde et al., *IEEE Trans. Nucl. Sci. NS-24* , p.221 (1977).
[6] H. Nguyen Ngoc, *Nucl. Instr. Meth. 172* , p.603 (1980).
[7] A. Del Guerra et al., *Proc. VII Intl. Conf. on Positron Annihilation,* New Delhi, World Scientific, p.810 (1985).
[8] Brown, *Basic Data of Plasma Physics* .
[9] English, *Canad. J. Phys. 31* , p.768 (1953).
[10] G. Charpak, *Nucl. Instr. Meth 126* , p.381 (1975).
[11] Ibqal et al., *Xe-TPC, Cal. Inst. Tech.* (1986).
[12] B. Sadoulet et al., *IEEE Trans. Nucl. Sci. NS-34* , p.52 (1987).
[13] A. Alichanian et al., *Nucl. Instr. Meth.* (1979).
[14] Takahoshi et al., *Nucl. Instr. Meth. 205* , p.591 (1983).

# 6. Timing and Electronics

## 6.1. Amorphous Silicon Electronics

Amorphous silicon can be used to build an integrated electronics array on the detector itself, reducing stray capacity and noise; compared to crystal silicon electronics, amorphous silicon electronics presents some disadvantages such as lower frequency limit, larger noise and lower amplification, and advantages such as better radiation resistance and low cost.

A simple amorphous silicon electronics array has been projected for amorphous silicon detectors application and prototypes are presently under study at LBL and Xerox; in Figure 6.1 the electronics scheme is shown as proposed; different proposals are considered in order to reduce the power dissipation (of the order of 1 mW) and noise [1,2].

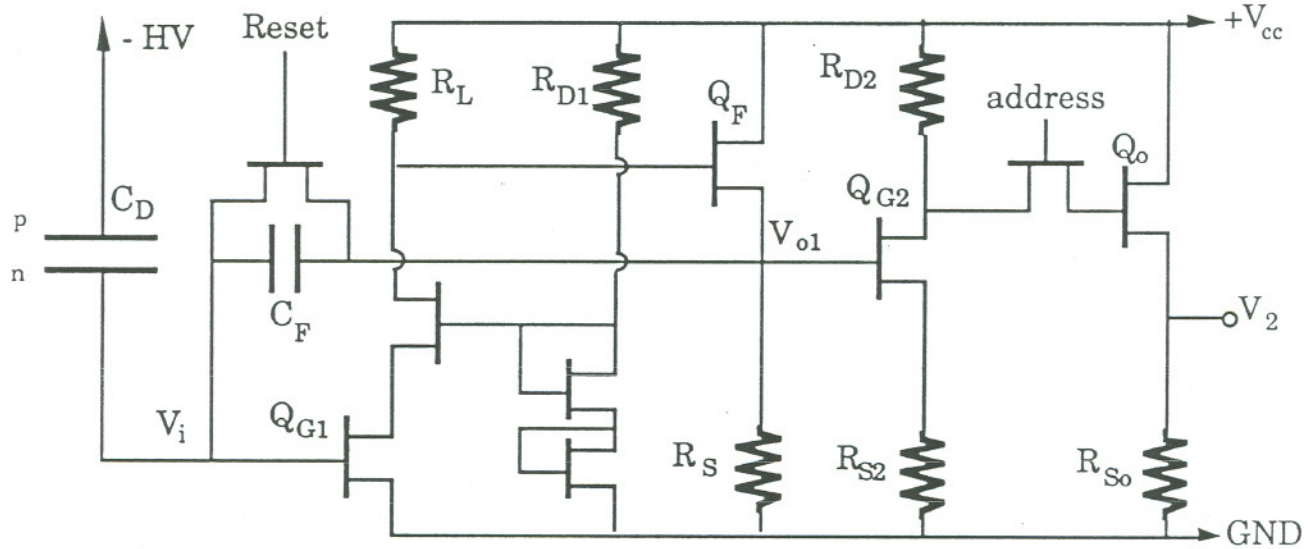


Figure 6.1 : Amorphous silicon integrated electronics scheme.

The $Q_{G1}$ and $Q_{G2}$ FETs are the actual amplification stages with gain $G_1$ and $G_2$, while $Q_o$ is a bare output stage and $Q_F$ is a source follower configuration meant to work as a buffer between the two stage.

## 6.2. Shaping Time

The charge signal from the amorphous silicon detector is processed through several stages that are schematically shown in Figure 6.2 : from the charge signal Q(t) whose characteristic time $\tau_0$ is due to the dominant slower physical phenomenon (transit time of charge in thick silicon detectors, scintillation decay time in scintillation detector system, electron drift time in Xenon), to an input stage that collects the charge in the capacitor $C_{tot} \approx C_D + G\,C_F + C_{in}$ ($C_{in}$ is the

total input capacitance if TFT $Q_{G1}$ ), to a charge preamplifier with gain G, to a RC-CR shaper amplifier whose time constant is $\tau_{RC} = RC$.

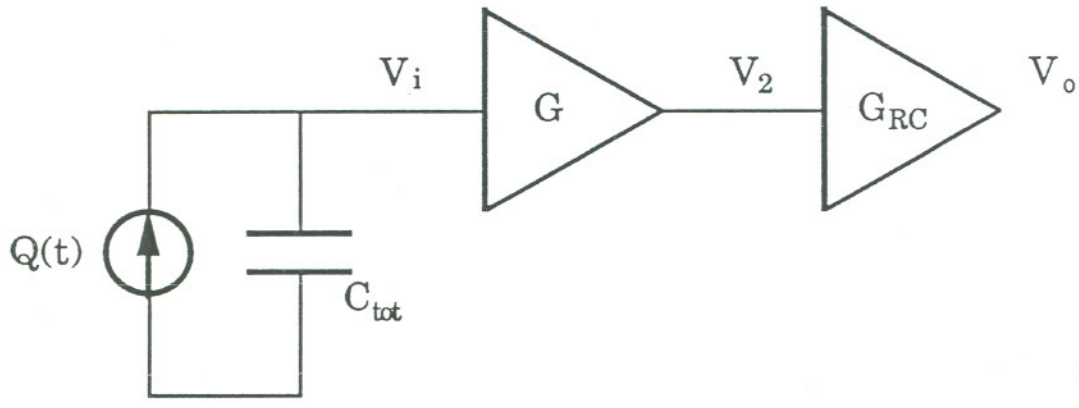


Figure 6.2 : Analog electronics scheme.

Q(t) can be expressed as $Q_0 e^{-t/\tau_0}$,

In order to study the output signal we move into the Laplace space: the current coming in the detector is $\hat{I}(s) = \frac{Q_0}{1+s\tau_0}$; we can express the voltage signal at different stages as:

$$\hat{V}_i(s) = \frac{Q_0}{1+s\tau_0}\frac{1}{sC_{tot}}$$

$$\hat{V}_2(s) = \hat{G}(s)\hat{V}_i \cong G_0\hat{V}_i$$

$$\hat{V}_0(s) = \hat{G}_{RC}(s)G_0\hat{V}_i$$

In the time domain, $V_{in}$ is a quasi-step pulse of height $\frac{Q_0}{C_{tot}}$ and a rise time $\tau_0$ as shown in Figure 6.3.

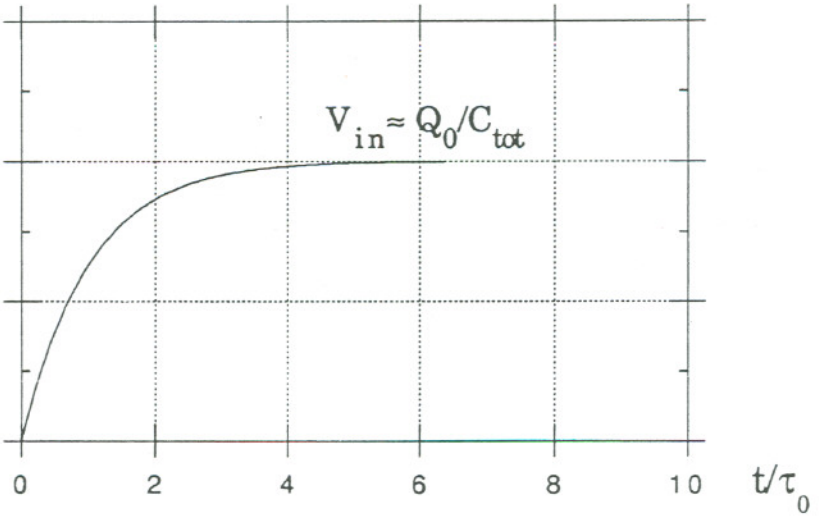


Figure 6.3 : Input Voltage as a function of time.

G(s) is in general a function of s with some pole in $1/\tau_G$, but if the amplifier is fast enough , i.e. $\tau_G \leq \tau_0$ and $\tau_G \ll \tau_{RC}$ , the transfer function can be approximated to a constant $G_0$, and the output of G has the same step pulse amplified by a factor $G_0$.

In the Laplace space the transfer function for the amplifier $G_{RC}$ (one stage of integration and one stage of differentiation) is:

$$\hat{G}_{RC}(s) = \frac{s\tau_{RC}}{(1+s\tau_{RC})^2}$$

Therefore the output voltage signal is :

$$\hat{V}_o(s) = G_0 \frac{Q_0}{C_{tot}} \frac{1}{1+s\tau_0} \frac{1}{s} \frac{s\tau_{RC}}{(1+s\tau_{RC})^2}$$

The choice of $\tau_{RC}$ is critical in our system: since it is directly related to the time resolution of the tomograph, a short $\tau_{RC}$ would be better, but if $\tau_{RC}$ is chosen too small compared to $\tau_0$ part of the charge is not collected and we lose signal amplitude: in fact, if $\tau_{RC} \ll \tau_0$ then the output is

$$\hat{V}_o(s) \equiv G_0 \frac{Q_0}{C_{tot}} \frac{\tau_{RC}}{1+s\tau_0}$$

In the time domain this is a decreasing exponential depressed by a factor $\tau_{RC}/\tau_0$; in other words the signal is differentiated before a complete collection of charge.

The condition that must be chosen is $\tau_0 \leq \tau_{RC}$ : in this case the output signal is:

$$\hat{V}_o(s) \equiv \hat{G} \frac{Q_0}{C_D} \frac{\tau_{RC}}{(1+s\tau_{RC})^2}$$

Going back to the time domain :

$$V_o(t) = \mathcal{L}^{-1}(\hat{V}_o) = G\frac{Q_0}{C_D}\frac{t}{\tau_{RC}}e^{-t/\tau_{RC}}$$

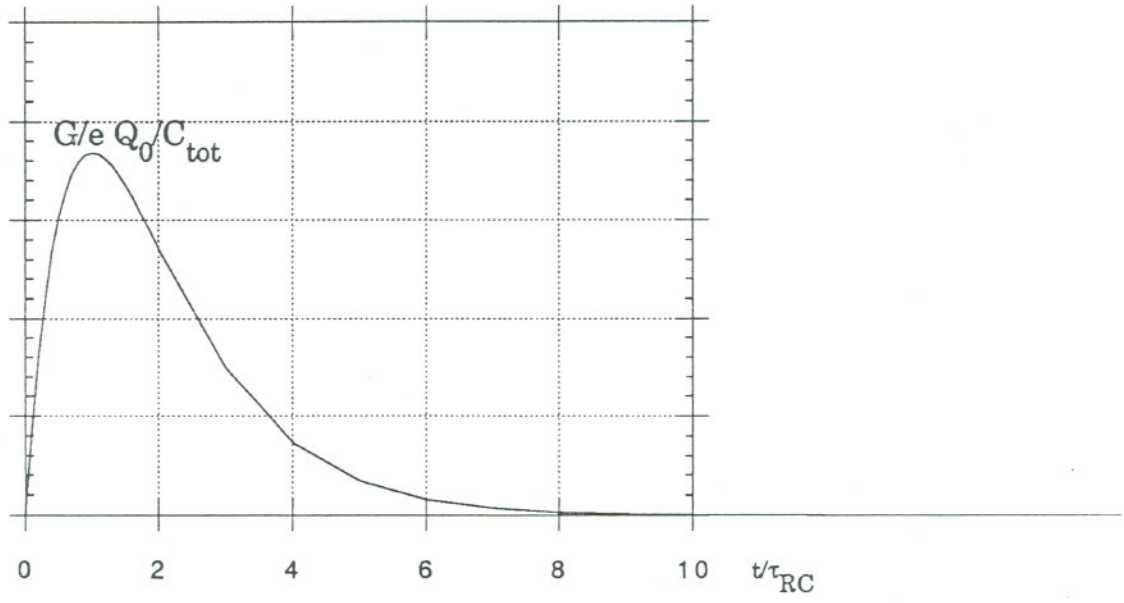


Figure 6.4 : Output Voltage as a function of time.

The peaking time of this signal in Figure 6.4 is approximately $\tau_{RC}$ (also called the shaping time), that is also an approximation value for the pulse width of the output signal fed into the coincidence system, and the coincidence time is the time resolution of the system. In our case $\tau_0$ is less than 1 μs, and we will choose $\tau_{RC}$ larger than $\tau_0$ or of the same order of magnitude as $\tau_0$ , in order to collect almost all the charge while maintaining the time resolution within reasonable values. In the following calculations we will assume that the condition $\tau_0 \leq \tau_{RC}$ is satisfied.

### 6.3. Noise

Detector and amplifiers are both source of electronic noise, and a general presentation of the different sources of noise is showed in Figure 6.5 ; a simple evaluation of the contributions to the $ENC^2$ (equivalent noise charge in electrons in input) is presented.

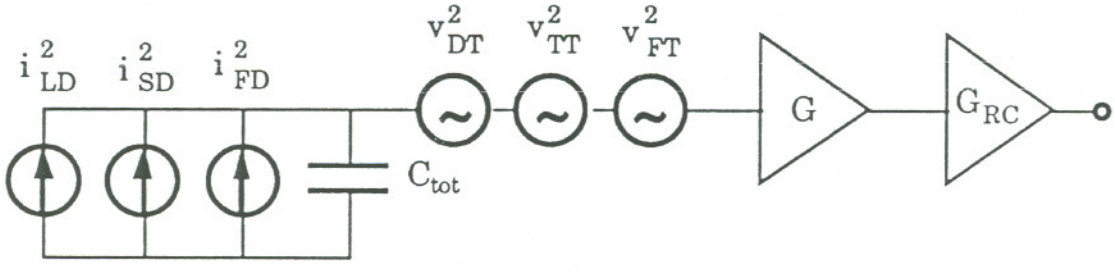


Figure 6.5 : Electronics scheme and noise sources.

The current sources are electron noise sources in the detector, the voltage sources are electron current noise sources in the output of the first stage of amplifier G, transferred in input in the equivalent description presented in Figure 6.5. In detail the noise sources can be expressed [3] in the frequency space as:

$i_{SD}^2 = 2qI_D$ Shot noise in the detector

$i_{FD}^2 = \frac{K_1 I_D^a}{f}$ Flicker noise in the detector

$v_{LT}^2 = \frac{1}{g_m^2}\frac{4kT}{R_L}$ Thermal noise in $R_L$ (output of TFT)

$v_{TT}^2 = \frac{8kT}{3g_m}$ Thermal noise in TFT

$v_{FT}^2 = \frac{K_{TFT}}{C_{in}}\frac{1}{f}$ Flicker noise in TFT

where $I_D$ is the leakage current in the detector, $C_{in}$ is the input capacitance of the first TFT , K are constants.

Since the output noise voltage generated by 1 electron of charge q at the input is $V_o(e) \equiv \frac{q}{C_{tot}} G \frac{1}{e} = \frac{q}{C_{tot}}\frac{G}{e}$ (1/e is the amplification of $G_{RC}$ at the peaking time $\tau_{RC}$), we can define in general the number of equivalent noise electrons at the input N as the ratio $N^2 = \frac{v_{out}^2(noise)}{v_o^2(e)}$, where $v_{out}^2(noise)$ is the average over all the frequencies. In the two different cases, current noise and voltage noise, the corresponding expressions are:

$$N^2 = \frac{v_{out}^2}{v_o^2(e)} = \left(\frac{C_{tot}e}{qG}\right)^2 \int_0^{\infty} v^2 |G|^2 |G_{RC}|^2 df = \left(\frac{C_{tot}e}{q}\right)^2 \int_0^{\infty} v^2 |G_{RC}|^2 df$$

$$N^2 = \frac{v_{out}^2}{v_o^2(e)} = \left(\frac{C_{tot}e}{qG}\right)^2 \int_0^{\infty} \frac{i^2}{|sC_{tot}|^2} |G|^2 |G_{RC}|^2 df = \left(\frac{C_{tot}e}{q}\right)^2 \int_0^{\infty} \frac{i^2}{|sC_{tot}|^2} |G_{RC}|^2 df$$

where $s=i\omega$ and $\omega=2\pi f$ and $|G_{RC}|^2(\omega) = |\hat{G}_{RC}(s)|^2 = \frac{\omega^2\tau_{RC}^2}{1+\omega^2\tau_{RC}^2}$ .

In our case only three of the six noise source are relevant and in Table 6.1 we present the average equivalent noise electrons in input calculated from the integrals above.

Table 6.1 :

| Source of Noise | Spectrum in Frequency Domain | Average Equivalent Noise in Time Domain |
|---|---|---|
| Shot Noise in the Detector | $i_{SD}^2 = 2qI_D$ | $N_{SD}^2 = \frac{e^2}{q}\frac{I_D}{4}\tau_{RC}$ |
| Thermal Noise in the TFT | $v_{TT}^2 = \frac{8kT}{3g_m}$ | $N_{TT}^2 = \frac{e^2}{q^2}\frac{kT}{3g_m}C_{tot}^2\frac{1}{\tau_{RC}}$ |
| Flicker Noise in the TFT | $v_{FT}^2 = \frac{K_{TFT}}{C_{in}}\frac{1}{f}$ | $N_{FT}^2 = \frac{e^2}{q^2}\frac{K_{TFT}}{2}\frac{C_{tot}^2}{C_{in}}$ |

where $I_D \approx 0.5\ 10^{-8} S(mm^2)A$, $S=4\ mm^2$, $g_m \approx 3.1\ 10^{-6}$ A/V, $K_{TFT} \approx 1.3\ 10^{-21}\ C^2/F$, and $C_{tot} \approx C_D + C_{in}$ (for $C_F$ small enough); its easy to see that the noise is minimum when the input capacitance is equal to the detector capacitance, then , choosing $C_{in} = C_D$, $C_{tot} = 2\ C_D$, the final three noise values become:

$$N_{SD}^2 = 0.230 \cdot 10^{-6}\tau_{RC}$$

$$N_{TT}^2 = 0.512 \cdot 10^{-6}\frac{C_D^2}{\tau_{RC}}$$

$$N_{FT}^2 = 1.5 \cdot 10^{-6} C_D$$

where $C_D$ is in pF and $\tau_{RC}$ is in μs. The part of the noise which is linear with shaping time $\tau_{RC}$ is generally called step noise, and the part proportional to $1/\tau_{RC}$ delta noise. The total noise is expressed by

$$N^2 = 0.230 \cdot 10^{-6}\tau_{RC} + 0.512 \cdot 10^{-6}\frac{C_D^2}{\tau_{RC}} + 1.5 \cdot 10^{-6} C_D$$

The minimum of $N^2$ as a function of $\tau_{RC}$ is for $\tau_{RC} = 1.5\ C_D$ μs.

In order to have a reasonable value of noise and a reasonably short shaping time $\tau_{RC}$ the the capacitance of the detector must be keep low, less than 1 pF. If we build a pixel detector of 2 mm size, 25 or 50 μm thick and apply the bias by two parallel plate electrodes the capacitance is too large; a different shapes of electrodes must be used, with less capacitance, such as interdigitated electrodes, in order to reduce by a factor α the capacitance $C_{plate}$ of a parallel plate capacitor $\varepsilon_0\varepsilon\frac{S}{d}$. Collecting electrodes of the same shapes as used in wire chambers [4] could

be chosen, or a plate on one side and wire-like electrodes on the other side; in this case the ratio $\alpha$ ($C_D/C_{plate}$ ) can be expressed as:

$$\alpha = \frac{1}{1+\frac{1}{\pi}\frac{s}{d}\ln\left(\frac{1}{2\pi}\frac{s}{a}\right)}$$

where d is the thickness of the detector, s is the spacing distance between two wire-like metallic strips and a is the radius of the strips. If we use $s/d \approx 10$ and $s/a \approx 50$ we get $\alpha \approx 0.1$ . Assuming this value for $\alpha$ , and a surface of the pixel S = 4 $mm^2$,

$$C_D = \alpha\varepsilon_0\varepsilon\frac{S}{d} = \alpha\frac{424}{d}\,pF$$

where d is in $\mu m$ and $C_D$ in pF.

We can use the formulas above to evaluate noise for our different detector models, for given detector capacitances and shaping times.

## 6.4. Detectors, Noise, Shaping Time: Applications

### 6.4.1. Shaping Time and Efficiency for Ta/a-Si PET

In the case of charged particles (electrons) passing through a thick (50 μm) a-Si detector one half of the signal is due to the electron current in the semiconductor, the other half to the hole current. These two physical phenomena have two different times $\tau_0$ , where $\tau_0$ is the transit time $t_c$ of charges in the detector, that for fully depleted layers can be expressed [5] as $t_c = \frac{0.53d^2}{\mu V}$ s, where d is the thickness of the detector, μ the mobility ($\mu_e$ = 1.2 $cm^2/Vs$, $\mu_h$ = 0.004 $cm^2/Vs$), V the applied bias. For a 50 μm thick layer and applied bias of 1500 V, $t_c(e)$ = 7.4 ns and $t_c(h)$ = 2.2 μs.It turns out that if we choose a shaping time $\tau_{RC}$ large enough to collect all the electrons, but small compared to the transit time for the holes, we would collect half of the signal, but have a discrete time resolution.

A computer calculation was also used to study the collection efficiency $\varepsilon_c$ as a function of applied voltage and shaping time of the 50 μm detector.

We can estimate [6] the voltage $V_c$ that has to be applied to the detector in order to deplete it :

$$V_c = \frac{e \rho d^2}{2 \varepsilon_0 \varepsilon_{Si}}$$

where ρ is the ionized dangling bond density, measured[7] to be 7. $10^{14} cm^{-3}$ , $\varepsilon_{Si}$ is 11.8, d is 50 μm; $V_c$ turns out to be 1340 V. A bias slightly larger than $V_c$ should be enough to fully deplete the detector. The signal due to a minimum ionizing particle passing through the detector (charge uniformly distributed along the track) was computer simulated in order to evaluate the suitable voltage to apply, above this threshold $V_c$.

In Figure 6.6.a the equivalent input current is presented as a function of time for different values of the applied voltage, with a RC shaping time 100 ns. It is shown that the signal height at the peaking time is already saturated at a voltage 1500 V, i.e. 30 V/μm. It can be seen that the height of the signal is half of the step test pulse (equivalent to the total charge collected in a very short while, as if the mobility of both electrons and holes were infinite); in 100 ns just the electrons are collected. In Figure 6.6.b the same graph is shown for a shaping time of 2 μs, with almost the same saturation at 1500 V; now the signal is 2/3 of the total charge, since part of the holes are collected in 2 μs. As a result we can apply a field of 30 V/μm to our detector, reaching a good saturation in pulse height.

In this case (track passing through all the detector, from p-side to n-side) the current contribution is half due to electrons, half to holes; since electrons and holes have very different mobilities, for our bias (30 V/μm) the electrons are all collected in the first 50 ns, while the hole current is much slower as shown in Figure 6.7. The total charge collected is therefore a function of the collection time ( or shaping time of the RC-CR amplifier) as shown in Figure 6.8. Two signals are reconstructed in Figure 6.9.a and 6.9.b, with shaping times 0.1 μs and 1.0 μs; the

pulse heights are 0.5 and 0.6 of the respective original signals. As shown in Figure 6.8, in two decades in the time scale the increase in collection efficiency is very slow; it is reasonable to choose a shaping time of 100 ns (less could be too a short time for the following digital electronics), losing the hole current (half of the signal), but keeping a good time resolution.

In order to evaluate this choice, the loss in efficiency due to the halved signal is to be considered. In Chapter 3. we calculated the efficiency as

$$\varepsilon = \frac{\int_{500}^{\infty} N(n)\, dn}{100000} \approx \frac{\int_{0}^{\infty} N(n)\, dn}{100000}$$

the integral from the noise threshold of 500 electrons of the electron-hole pairs distribution N(n); in this case the scale must change by a factor 2 because the collected charge is half of the electron-hole pairs; using a more reasonable value of the noise (1000 electrons) we obtain:

$$\varepsilon = \frac{\int_{1000}^{\infty} N(\frac{n}{2}) \frac{dn}{2}}{100000} = \frac{\int_{2000}^{\infty} N(m)\, dm}{100000}$$

The N(m) distribution is the same as considered in Chapter 3., with a factor 2 difference of scale, and in the calculation of the integral we just sum in $N_t$ all the bins except the first $N_1$(0÷2000 electrons); from the five runs we obtain different values of $N_1$ and $N_t$ ( $N_1$ = 20, 17, 15, 23, 24; $N_t$ = 475, 498, 481, 481, 445) and the average correction $N_1/N_t$ is 4 % of $\varepsilon$ or $\varepsilon_{tot}$.

The corrected value of $\varepsilon_c$ is then 0.96 $\varepsilon_{tot}$, i.e. $\varepsilon_c$ = 0.96 (7.8 ± 0.2)% = (7.5 ± 0.2)%.

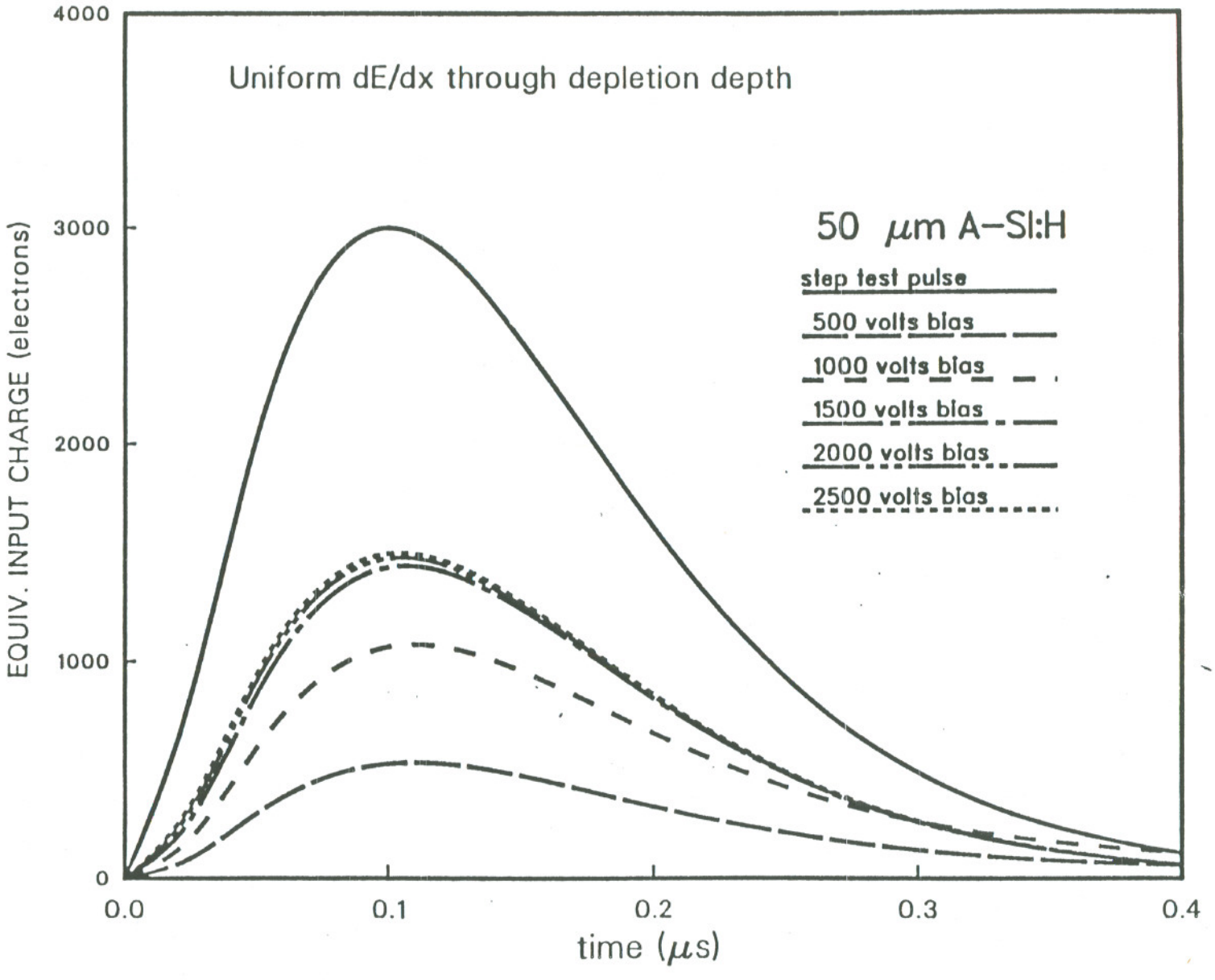


Figure 6.6.a : Output signal (in equivalent input charge units) as a function of time for a shaping time of 100 ns; different biases are applied on a 50 μm detector. The step test pulse corresponds to infinite mobility of charge in the detector, and total collection in zero time.

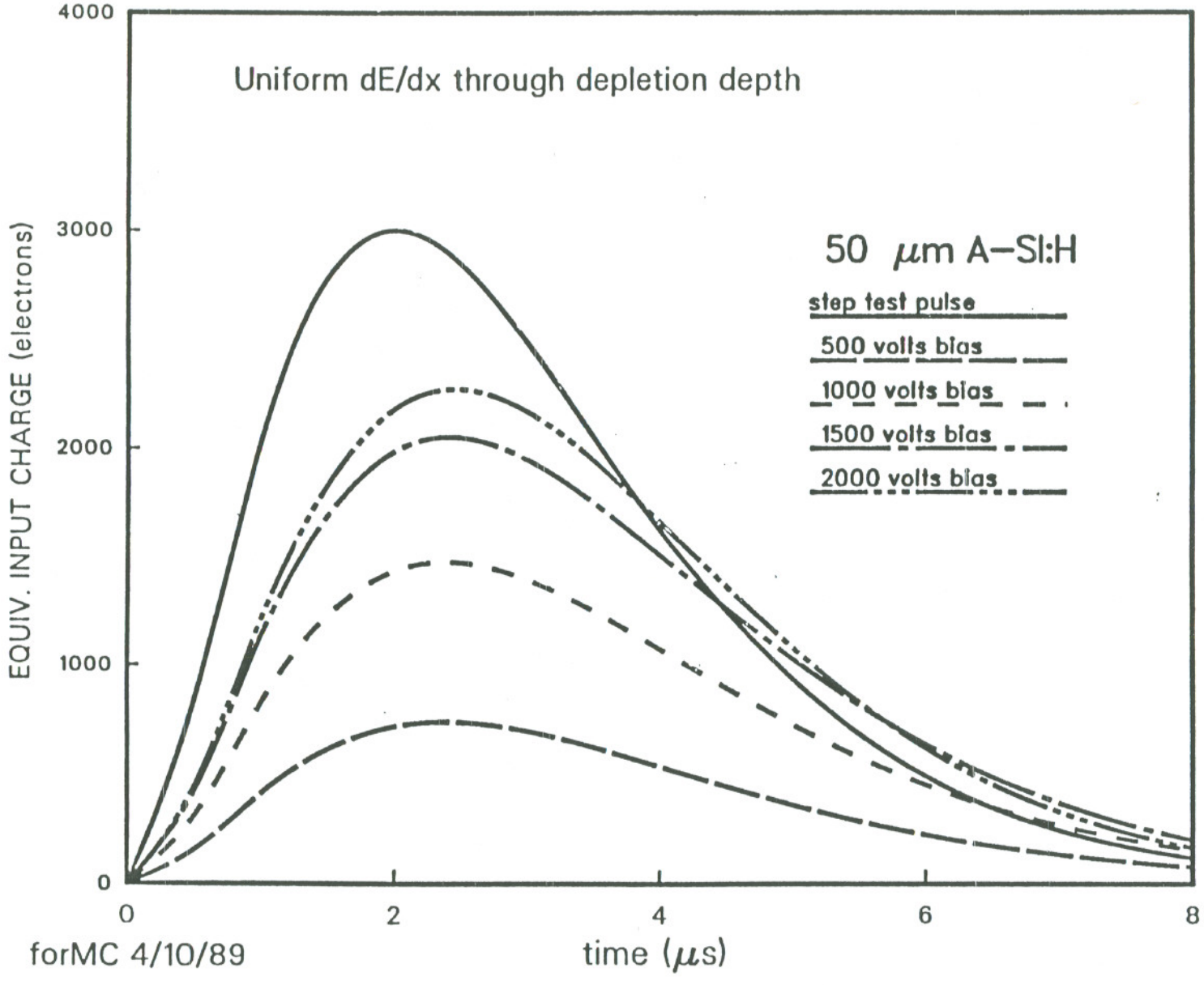


Figure 6.6.b : Output signal (in equivalent input charge units) as a function of time for a shaping time of 2 μs; different biases are applied on a 50 μm detector. The step test pulse corresponds to infinite mobility of charge in the detector, and total collection in zero time.

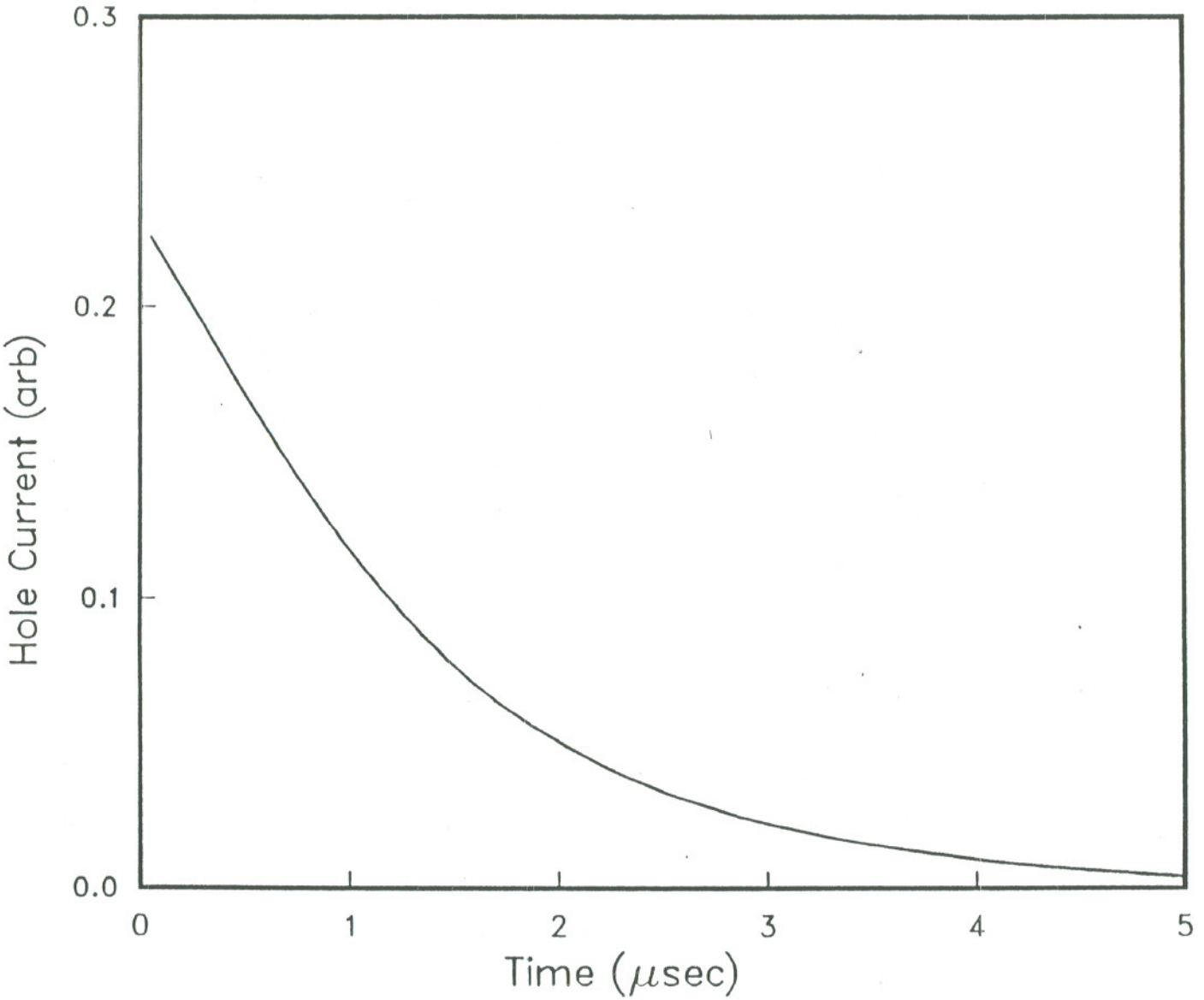


Figure 6.7 : Minimum ionizing particle hole current as a function of time in a 50 μm detector with a 30 V/cm electric field.

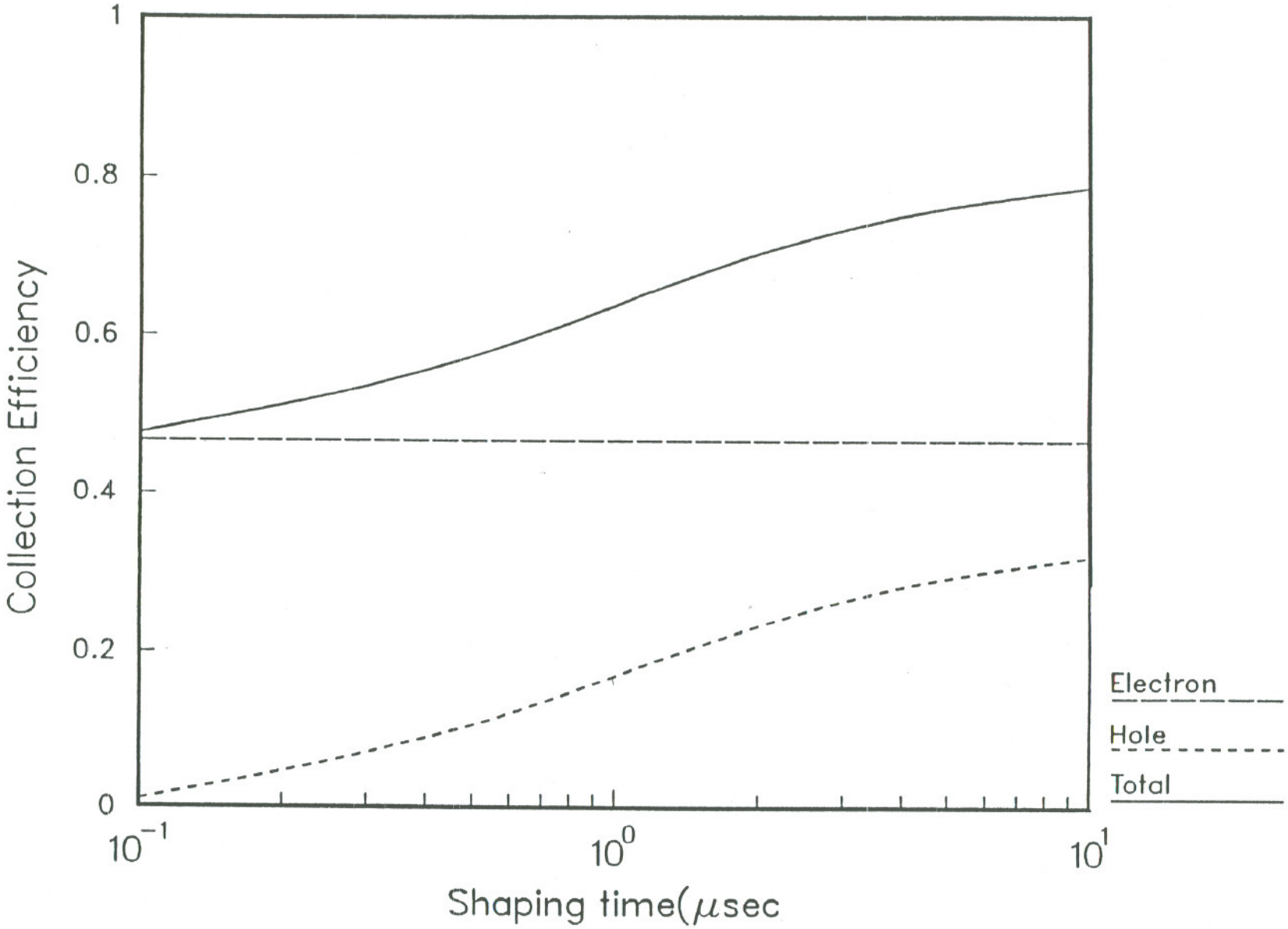


Figure 6.8 : Collection efficiency for the charge released by a minimum ionizing particle through a 50 μm thick detector with a 30 V/cm electric field as function of shaping time.

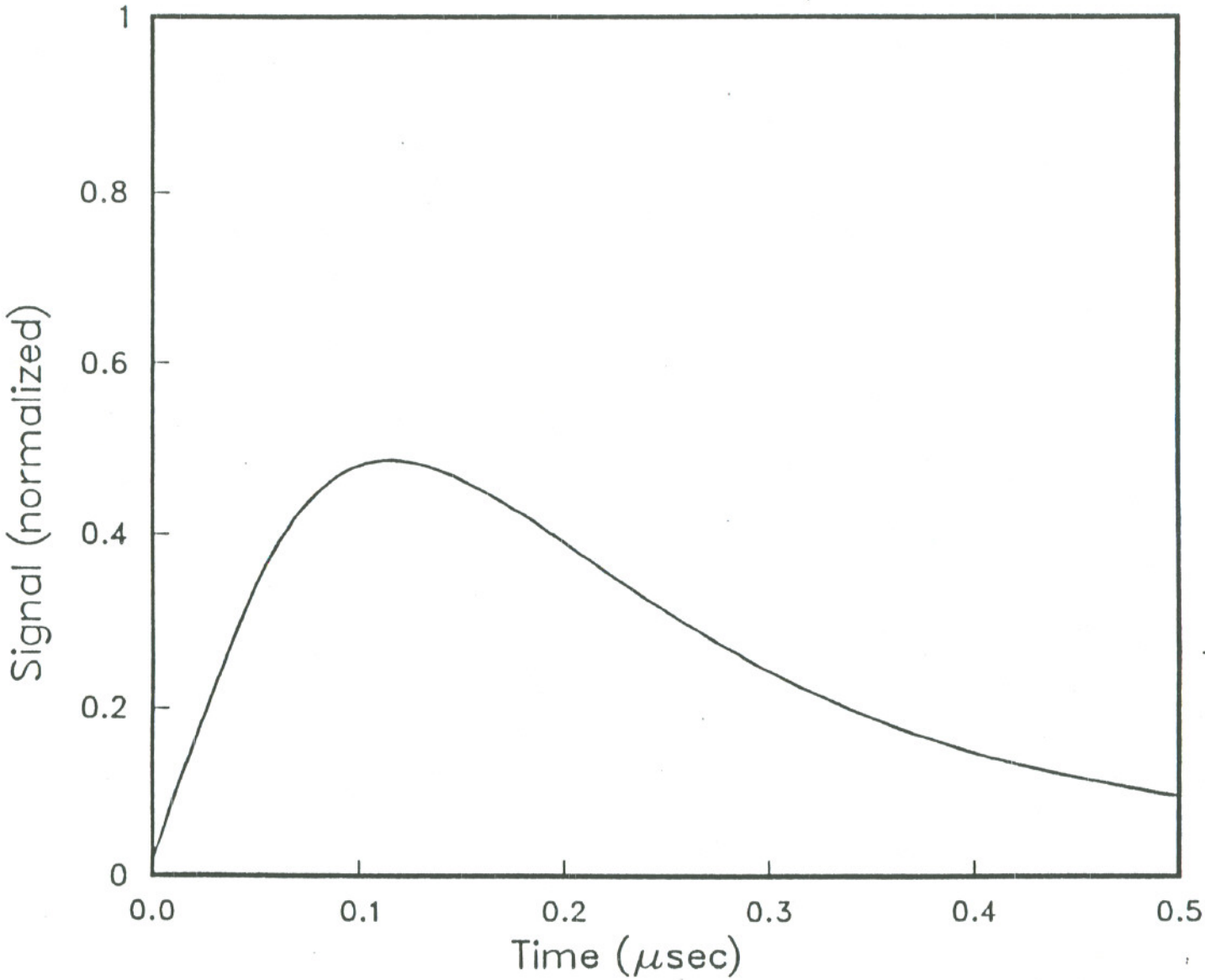


Figure 6.9.a : Output signal as a function of time for a shaping time of 100 ns from a 50 μm detector with a 30 V/cm electric field.

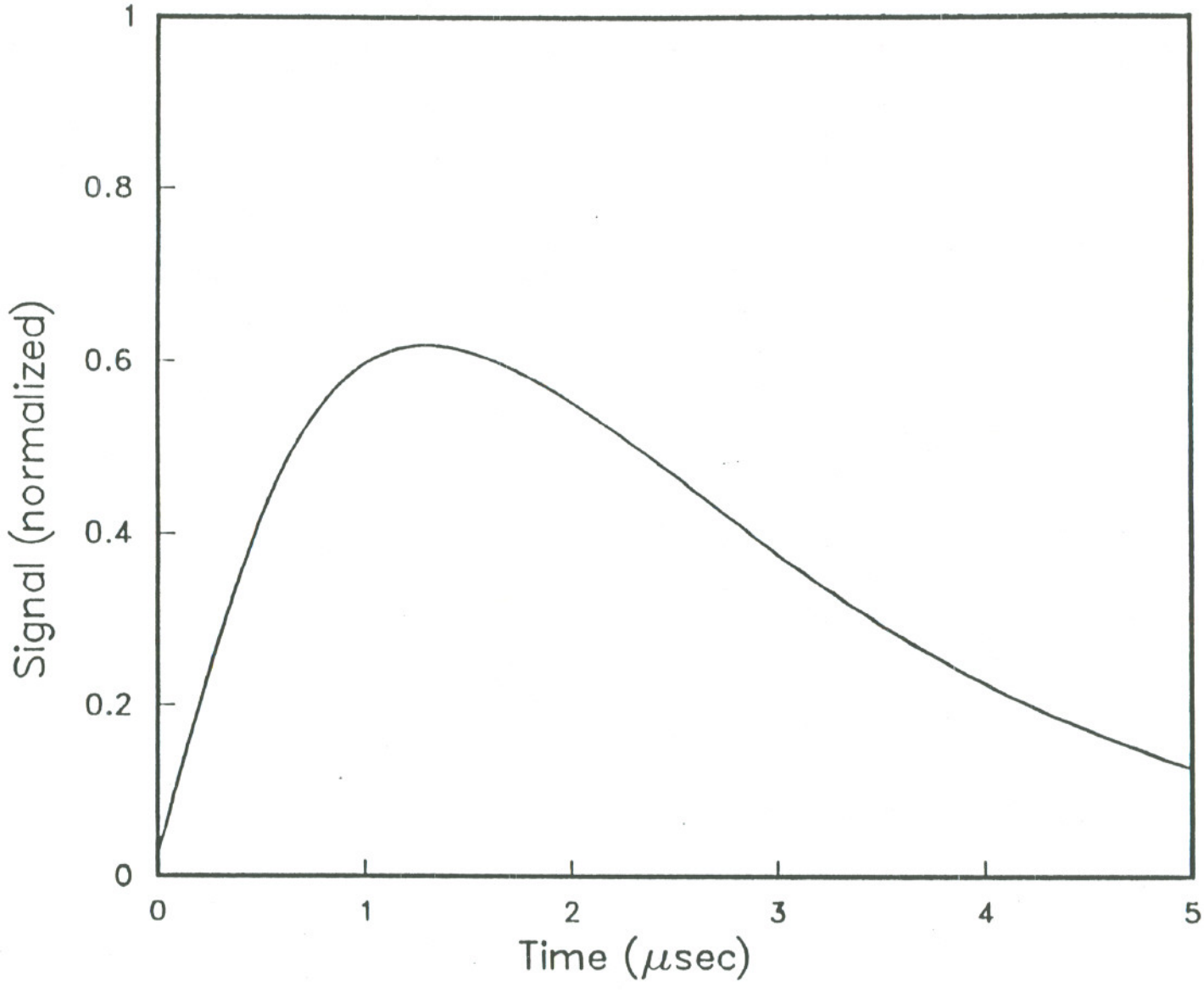


Figure 6.9.b : Output signal as a function of time for a shaping time of 1 μs from a 50 μm detector with a 30 V/cm electric field.

### 6.4.2. Shaping Time for CsI/a-Si and Xe/a-Si PETs

In both Xe/a-Si and CsI/a-Si PET projects a few microns of silicon could be enough to absorb visible (CsI) or UV(Xe) photons, but high capacitance problems make it more reasonable to use a thicker detector, such as 25 μm. The photon creates an electron-hole pair where it interacts with the a-Si; the attenuation length of photons is a function of the wavelength. For short attenuation length the electron-hole pairs are created very close to the p-doped surface layer, then the current is a bare electron current, due to electron moving from the p-layer to the n-layer (reverse bias); since electron mobility is much larger than hole mobility ($\mu_e$ is 1.2 $cm^2/sV$, $\mu_h$ is 4. $10^{-3}$ $cm^2/sV$) [7] , in this case we obtain a much shorter transit time for the total current.

For Xenon UV-photons the attenuation length is much less than a micron, and is of the order of microns for CsI light, as is shown in Table 6.2. In Table 6.2 [8] the attenuation length is shown as a function of the photon wavelength; the emission wavelength is much shorter for CsI(Na), although it has a lower light yield. In both CsI(Na) and CsI(Tl) a fast pure electron current is produced in the amorphous silicon for a 25 μm thick detector. The attenuation length λ is defined from the attenuation coefficient α ($\lambda = \alpha^{-1}$) for a beam $I=I_0\, e^{-\alpha x}$.

Table 6.2 :

| Wavelength (nm) | Energy (eV) | α ($cm^{-1}$) | λ (μm) | Scintillator |
|---|---|---|---|---|
| 350 | 3.54 | $> 10^6$ | $< 10^{-2}$ | |
| 420 | 2.95 | $1.0\ 10^6$ | $10^{-2}$ | CsI(Na) |
| 550 | 2.25 | $1.0\ 10^4$ | 1.0 | CsI(Tl) |
| 700 | 1.77 | $3.5\ 10^3$ | 2.8 | |

Since the only current present is the electron current, the characteristic time $\tau_0$ of the process is the convolution of the transit time of the electrons $t_c$ and the scintillation decay time.

We can estimate (see chapter 1)the voltage $V_c$ that has to be applied to the detector in order to deplete it : $V_c = \frac{e \rho d^2}{2 \varepsilon_0 \varepsilon_{Si}}$ , where ρ is the ionized dangling bond density, measured[7] $7.\ 10^{14} cm^{-3}$ , $\varepsilon_{Si}$ is 11.8, d is 25 μm; $V_c$ turns out to be 335 V. A bias slightly higher than $V_c$ should be enough to fully deplete the detector.

For fully depleted layers the transit time can be expressed [5] as $t_c = \frac{0.53 d^2}{\mu V}$ s, where d is the thickness of the detector, μ the mobility ($\mu_e$ = 1.2 $cm^2/Vs$), V the applied bias. For 25 μm and 500 V (20 V/μm) applied , $t_c(e)$ = 5.5 ns . Since the decay constant for CsI(Na) is much larger, about 500 ns, this can be assumed as $\tau_0$, the same value we should assume for $\tau_{RC}$ .

## 6.5. Conclusions

An amorphous silicon integrated electronics array is presented and amplification, noise and time constants have been discussed. The relatively large pixel size chosen results in a large detector capacitance, which leads to a considerable noise level; a future development of interdigitated electrodes to bias the detector could reduce the capacitance.

In Table 6.3 the noise level for our application is presented, for a 4 $mm^2$ pixel surface and a capacitance reduction factor of 0.1 (using interdigitated electrodes or similar device).

Table 6.3 :

| note on $\tau_{RC}$ | $\tau_{RC}$ ($\mu s$) | d ($\mu m$) | $C_D$ (pF) | $N_{noise}$ (electrons) |
|---|---|---|---|---|
| minimum noise | 2.5 | 25 | 1.7 | 1900 |
| Xe/a-Si applications | 1.0 | 25 | 1.7 | 2000 |
| CsI/a-Si applications | 0.5 | 25 | 1.7 | 2400 |
| minimum noise | 1.2 | 50 | 0.8 | 1300 |
| Ta/a-Si applications | 0.1 | 50 | 0.8 | 2000 |

Shaping time and noise have been shown to be the determining parameters for the efficiency of the system, and its time resolution is assumed to be the shaping time itself; a smaller $\tau_{RC}$ implies a better time resolution, but in general increases the noise and lowers the efficiency directly, cutting out part of the charge, or indirectly, raising the noise level: a compromise solution must be chosen in order to optimize the figure of merit parameter $\varepsilon^2/\tau$.

For Ta/a-Si PET a 50 $\mu m$ thick detector is proposed. Shaping times from 10 ns to 100 ns could be chosen (compatible with the speed of the electronics) collecting only the fast electron charge - half of the total, and a resulting noise of about 2000 electrons is expected; due to the large signal of the electron track in silicon the efficiency is slightly dependent from the noise level and the shaping time (in this situation $\Delta\varepsilon/\varepsilon$ of few percent is obtained).

For CsI/a-Si and Xe/a-Si PETs a 25 $\mu m$ thick detector is proposed; although a few microns are sufficient to detect CsI and Xe scintillation photons, a thick detector is preferred in order to reduce the capacitance and since the photons are stopped in the first micron of material, only the electronic component of the current is expected. A shaping time of 500 ns, approximatively equal to the scintillation decay time of CsI(Na), is chosen, and a noise level of 2400 electrons is calculated in the case of CsI(Na)/a-Si PET. For Xe a shaping time of 1 $\mu s$, which is the average drift time of electrons in 1 cm of Xe, is chosen and 2000 electrons is the noise. Also in this case the efficiency is slightly deteriorated for noise of a few thousand electrons.

## 6.6. References


[1] V. Perez-Mendez et al., *LBL Report 26254* , April 1989.

[2] G. Cho et al., *TFT Amplifiers for Amorphous Silicon Pixel Particle Detector*, to be presented at IEEE Symposium on Nuclear Science, San Francisco, January 1990, to be published in IEEE Trans. Nucl. Sci.

[3] P. R. Gray and R.G. Meyer, *Analysis and Design of Analog Integrated Circuit* , II ed., New York, John Wiley & Sons (1977).

[4] Sauli, *CERN Report 77-09* (1977).

[5] G. F. Knoll, *Radiation Detection and Measurement* , John Wiley & Sons, p.394 (1979).

[6] G. F. Knoll, *Radiation Detection and Measurement* , John Wiley & Sons, p.383 (1979).

[7] S. Qureshi et al., *IEEE Trans. Nucl. Sci. NS-36* , p.194 (1989).

[8] J. D Joannopolous & G. Lucovsky, *Physics of Hydrogenated Amorphous Silicon II* , p.141 (1984).

## 7. Conclusions : Evaluation of Merit Parameter $\varepsilon^2/\tau$

The parameters necessary to evaluate the feasibility and the performance of a PET system are several and strongly interrelated, as shown in Figure 7.1. The key parameters are the detector efficiency $\varepsilon$ , the time resolution $\tau$ and the space resolution $\sigma_R$ , or the combined parameter $\varepsilon^2/\tau$ and $\sigma_R$. In our proposals all the projects have the same spatial resolution of 2 mm determined by the size of the amorphous silicon pixel detectors and we can focus our attention on $\varepsilon^2/\tau$ .

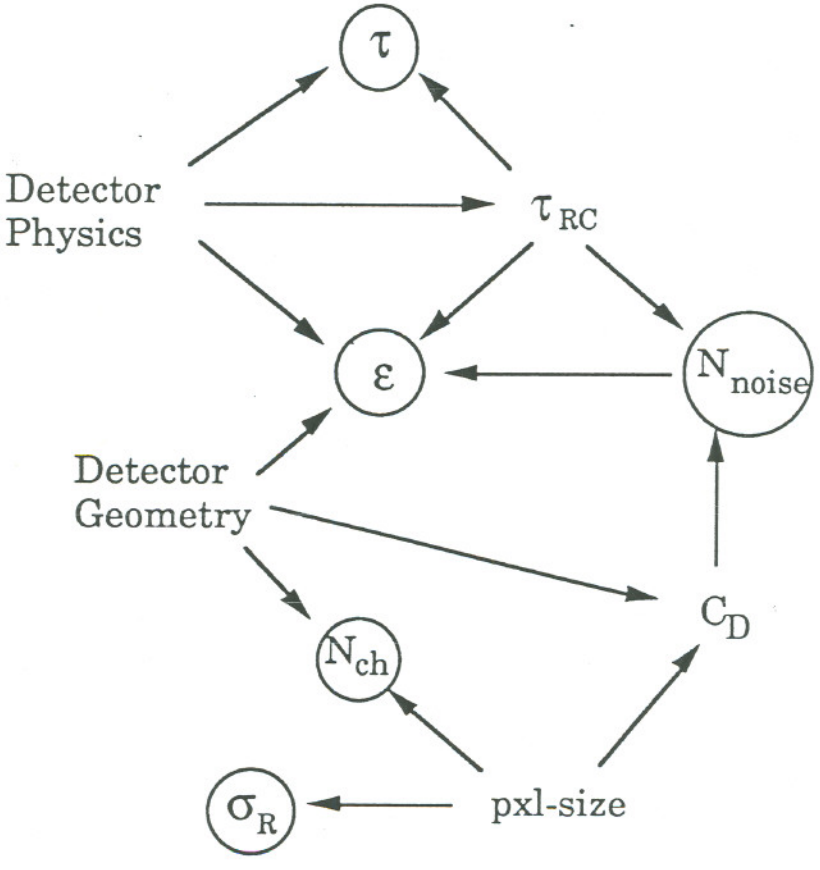


Figure 7.1 : Relationships between PET parameters .

Since in a Positron Emission Tomograph any event is identified by a time coincidence of two $\gamma$-interaction in two opposite detectors, a basic parameter of quality of the system is the true to accidental coincidences ratio. In order to evaluate the T/A ratio let us consider Figure 7.2 : a positron emitter point source of activity S is placed in a phantom and the two 511 keV $\gamma$ emitted back to back can be detected by two identical detectors , both with efficiency $\varepsilon$ and a fraction of solid angle covered G.

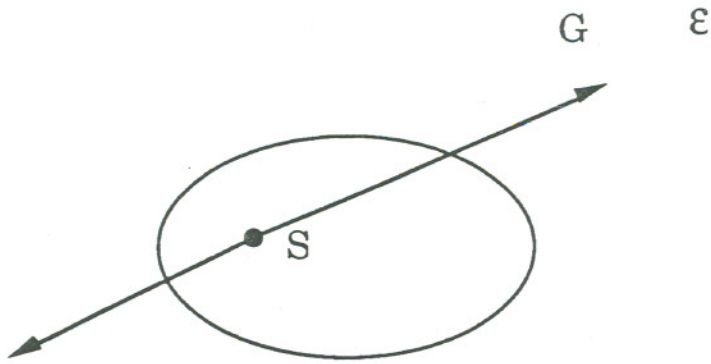


Figure 7.2 : Schematic drawing of a back-to-back 511 keV-γ couple emission in a PET.

Since for each positron 2 γ are produced the γ source will appear to have an activity of 2S if we consider the single rate R in each detector: the single rate on each detector is $R = G\ 2S\ \varepsilon$ and the true coincidence rate is

$T = G\ S\ \varepsilon^2$.

The rate of accidental is proportional to the time window open for the coincidence (or time resolution τ) and to both the single rate in the two detectors

$A = 2\ \tau\ R_1 R_2 = 2\ \tau\ (2G\ S\ \varepsilon)^2$

The ratio T/A turns out to be:

$$\frac{T}{A} = \frac{1}{8T}\frac{\varepsilon^2}{\tau}$$

Since at least a $T/A \geq 1$ is wanted, this relation establishes for each tomograph, characterized by a $\varepsilon^2/\tau$ ratio, a upper limit in acceptable true coincidence counting rate:

$T \leq 1/8\ \varepsilon^2/\tau$ ;

for a $\varepsilon^2/\tau \approx 0.1\ \mu s^{-1}$ a rate $T \leq 10$ kHz is desiderable, while for a better $\varepsilon^2/\tau \approx 1\mu s^{-1}$ a rate $T \leq 100$ kHz is acceptable. In the following pages the $\varepsilon^2/\tau$ parameters for every PET project above presented will be discussed.

## 7.1. A Comparison of $\varepsilon^2/\tau$ of each PET Project

In Table 7.1 the optimum $\varepsilon^2/\tau$s of our projects are compared with other PET systems :

- a PET system [1,2] using lead glass tubes for γ interaction and gas within the tubes for drift of secondary electrons; a wire chamber detects the electrons;
- conventional crystalline scintillator systems (NaI, BGO); in this case, since only the upper limit for the efficiency (interaction efficiency in the crystal) is presented, one should consider the loss of efficiency due to any electronics

threshold that cuts off the events with low light levels, which is not negligible for BGO whose light yield is about 1/5 of the light yield of CsI(Tl), CsI(Na) and NaI(Tl).

Concerning the $\varepsilon^2/\tau$ of our projects:

1. Tantalum(100 μm)/a-Si:H(50 μm) multilayer detectors present a poor efficiency ($\varepsilon \approx 7.8\%$ for 20 double layers) compared to the complexity of the electronics required for such a number of layers; their intrinsic quality is the fast collection (down to 10 ns) of the signal that make this project very attractive in cases in which good time resolution is needed above all. In the best case of a time resolution of 10 ns ($\varepsilon^2/\tau \approx 0.6\ \mu s^{-1}$) a true coincidence rate up to 75 kHz is acceptable.

2. Xenon filled lead glass tubes & a-Si:H detectors present a low efficiency ($\varepsilon \approx 7.5\%$) and because of the low drift velocity of electrons in Xenon a time resolution larger than 1 μs . For $\varepsilon^2/\tau \approx 0.0056\ \mu s^{-1}$ the upper limit for the true coincidence rate is 0.7 kHz.

3. Although a CsI(Na)/a-Si:H multilayer detector is possible with a good efficiency of about 26 % and a reasonable time resolution of 500 ns, a CsI(Na) filled glass tubes array with a-Si:H pixel detectors far exceeds the performances of each of the a-Si:H detectors PET projects studied here.

A 10 mm thick array of CsI(Na) filled glass tubes (2 mm diameter and 0.150 mm wall thickness) with a 2 mm size a-Si:H pixel detectors (25 μm thick) plane presents an efficiency of 33.% and a time resolution of 500 ns, with a $\varepsilon^2/\tau = 0.2178\ \mu s^{-1}$ and an upper limit in true coincidence rate $T < 27$ kHz.

Since the scintillation light signal from CsI is very high above the noise threshold of the a-Si:H detectors, one could collect just half of the light reducing the integration time of the signal from 500 ns to 350 ns with no sensible variation in efficiency but a better time resolution; in this case for a 10 mm thick array $\varepsilon = 32.\%$, $\varepsilon^2/\tau = 0.2926\ \mu s^{-1}$ and $T < 37$ kHz.

A 20 mm thick array yields an efficiency of 56.% , a $\varepsilon^2/\tau = 0.6272\ \mu s^{-1}$ and $T<78$ kHz ; for 350 ns integration time $\varepsilon = 55.\%$, $\varepsilon^2/\tau = 0.8643\ \mu s^{-1}$ and $T < 108$ kHz.

Finally one can consider two 10 mm thick arrays each of them with an a-Si:H detectors plane, to increase efficiency without increasing parallax error. The expected efficiency is 66.%, $\varepsilon^2/\tau = 0.8712\ \mu s^{-1}$ and $T < 109$ kHz; for 350 ns integration time $\varepsilon = 64.\%$, $\varepsilon^2/\tau = 1.1703\ \mu s^{-1}$ and $T < 146$ kHz.

As a result of this study a combination of CsI(Na) filled glass tubes arrays and amorphous silicon pixel detectors offers good efficiency and time resolution, competitive performance, feasibility and cost effectiveness.

In Table 7.1 the different $\varepsilon^2/\tau$s and the main characteristics of the projects studied in this paper are presented and followed by simple graphic represention.

## 7.2. References


[1] A. Del Guerra et al., *IEEE Trans. Nucl. Sci. NS-30* , p.646 (1983).

[2] A. Del Guerra et al., *Proc. VII Intl. Conf. on Positron Annihilation,* New Delhi, World Scientific, p.810 (1985).

Table 7.1 : $\varepsilon^2/\tau$ Parameters for PET Systems

| Detector | γ-converter | Architecture Characteristics | ε (%) | τ (μs) | $\varepsilon^2/\tau$ ($\mu s^{-1}$) | T(max) (kHz)+ | Multi layer |
|---|---|---|---|---|---|---|---|
| wire chamber | lead glass tubes | 10 mm tubes | 7.5 | 0.100 | 0.0563 | 7 | No |
| a-Si:H | lead glass tubes+ Xenon | 10 mm tubes | 7.5 | > 1.0 | 0.0056 | 0.7 | No |
| | NaI(Tl) crystals | 10 mm crystals | ≈ 25*** | 0.230 | 0.2717 | 34 | No |
| | BGO crystals | 10 mm crystals | ≈ 50*** | 0.300 | 0.8300 | 104 | No |
| a-Si:H | Tantalum slab | 20 Ta/a-Si:H layers | 7.8 | 0.1 | 0.0608 | 8 | Yes |
| a-Si:H | Tantalum slab | 20 Ta/a-Si:H layers | 7.8 | 0.01* | 0.6080 | 75 | Yes |
| a-Si:H | CsI(Na) slab | 10 CsI/a-Si:H layers | 26. | 0.500 | 0.1352 | 17 | Yes |
| a-Si:H | CsI(Na) in glass tubes | 5 mm tubes | 17. | 0.500 | 0.0578 | 7 | No |
| a-Si:H | CsI(Na) in glass tubes | 10 mm tubes | 33. | 0.500 | 0.2178 | 27 | No |
| a-Si:H | CsI 50% light collection** | 10 mm tubes | 32. | 0.350 | 0.2926 | 37 | No |
| a-Si:H | CsI(Na) in glass tubes | 20 mm tubes | 56. | 0.500 | 0.6272 | 78 | No |
| a-Si:H | CsI 50% light collection** | 20 mm tubes | 55. | 0.350 | 0.8643 | 108 | No |
| a-Si:H | CsI(Na) in glass tubes | 2 x 10 mm tubes | 66. | 0.500 | 0.8712 | 109 | Yes |
| a-Si:H | CsI 50% light collection** | 2 x 10 mm tubes | 64. | 0.350 | 1.1703 | 146 | Yes |

\+ Maximum True Coincidence Rate for a True/Accidental Coincidence Rate Ratio larger than 1.
* Fast electronics (100 MHz bandwidth).
** CsI(Na) in glass tubes as above, but charge is integrated only for 350 ns, i.e. 50 % of the light collected.
*** Efficiency upper limit considering only interaction probability in crystal.

## Tantalum Slab & a-Si:H Pixel Detectors

(Multilayer)

$\varepsilon \approx 0.5\ \%$

$\tau < 100$ ns

Noise ≈ 2000 electrons

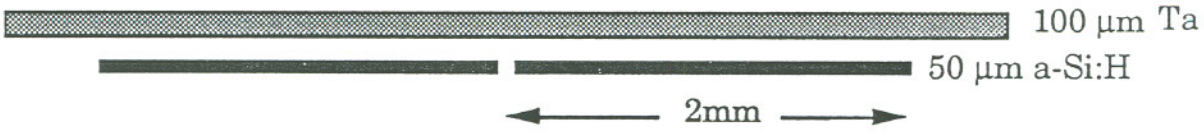


## CsI(Na) Slab & a-Si:H Pixel Detectors

(Multilayer)

$\varepsilon \approx 3.\ \%$

$\tau \approx 500$ ns

Noise ≈ 2000 electrons

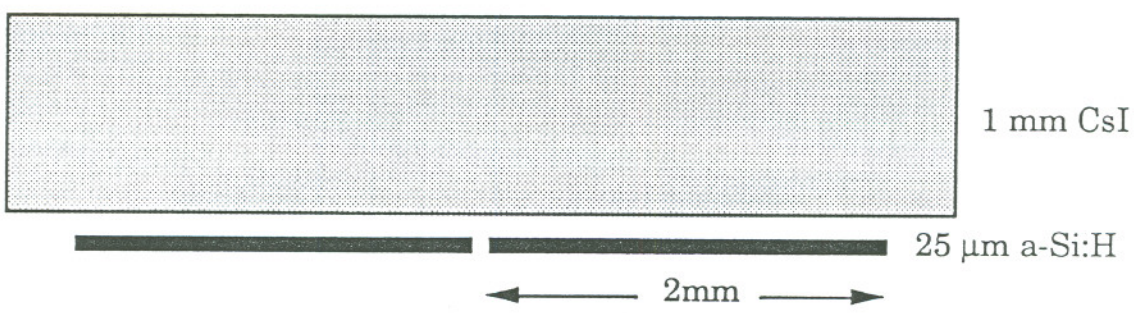

## CsI(Na) Filled Glass Tubes & a-Si:H Pixel Detectors

$\varepsilon \approx 30.\ \%$

$\tau \approx 500$ ns

Noise ≈ 2000 electrons

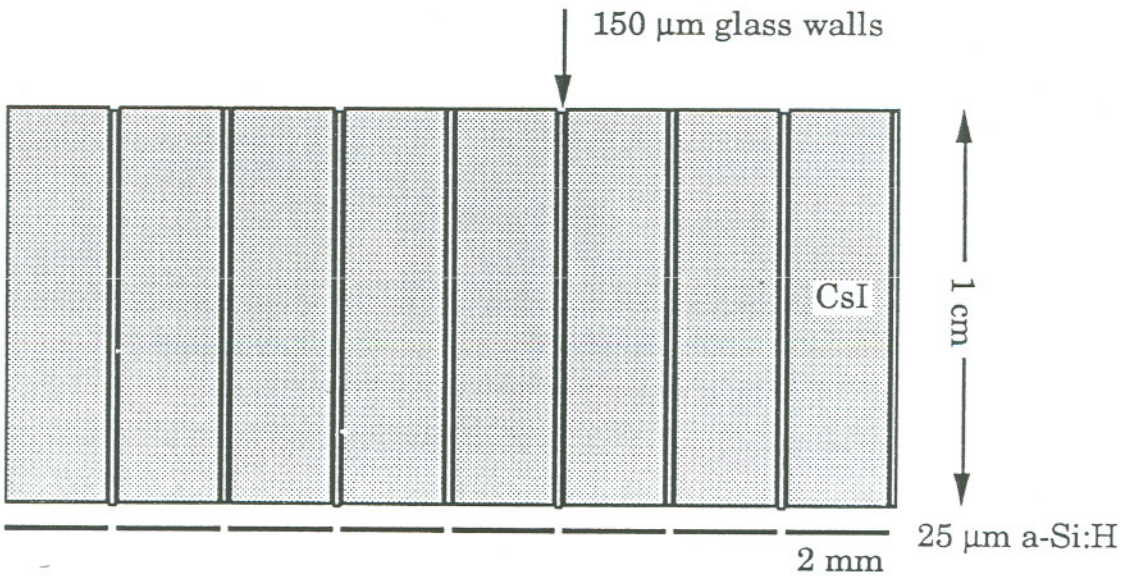


## Xenon Filled Lead Glass Tubes & a-Si:H Pixel Detectors

$\varepsilon \approx 7.5.\ \%$

$\tau > 1$ μs

Noise ≈ 2000 electrons

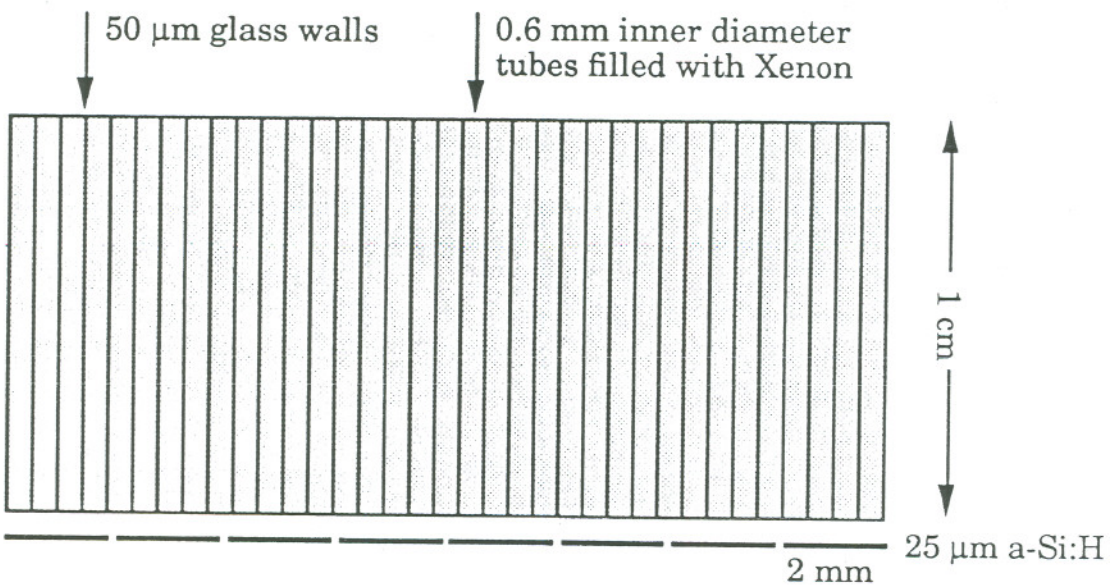

# 8. Appendix

This Appendix presents a references list for Xenon scintillation light , some notes on the Monte Carlo Simulation programs, and the program sources.

## 8.1. A Complete Reference List on Xenon Scintillation Light

### 8.1.1. Electrons in Gases


Birks, *Theory and Practice of Scintillation Counting* .
Brown, *Basic Data of Plasma Physics* .
Herzberg, *Spectra of Diatomic Molecules* .
Lindinger, *Swarms of Ions and Electrons in Gases* .
Loeb, *Basic Processes in Gaseous Detectors* .
Massey, *Electronic and Ionic Impact Phenomena* .
Mc Daniel, *Collision Phenomena in Ionized Gases* .
Meek & Craggs, *Electrical Breakdown in Gases* .
Rice-Evans, *Spark, Streamer, Proportional and Drift Chambers* .


### 8.1.2. Electron Drift Velocity in Rare Gases


Bowe, *Phys.Rev. 117* ,p.1411 (1960).
English, *Canad. J. Phys. 31* , p.768 (1953).
Ibqal et al., *Xe-TPC, Cal. Inst. Tech.* (1986).
Sauli, *CERN 77-09* (1977).
Takahoshi et al., *Nucl. Instr. Meth. 205* , p.591 (1983).


### 8.1.3. Mechanism of Scintillation in Rare Gases


R. Andresen, *Nucl. Instr. Meth. 140* , p.371 (1977).
R. Brodmann et al., *J. Phys. B: Atom. Molec. Phys. 10* , p.3395 (1977).
A. Gedanken et al., *J. Chem. Phys. 57* , p.3456 (1972).
M. Ghenfelstein et al., *Chem. Phys. Letters 49* , p.312 (1977).
D. Haaks et al., *VI Int. Conf. VUV III* , p.3 (1980).
J. Keto, *Phys. Rev. Letters 33* , p.1365 (1974).
H. Koehler et al., *Phys. Rev. 9A* , p.769 (1974).
P. Leichner et al., *Phys. Rev. 13A* , p.1787 (1976).
P. Millet et al., *J. Chem. Phys. 69* , p.92 (1978).
R.S.Mulliken, *J. Chem. Phys. 52* , p.5170 (1970).
A. Policarpo, *Physica Scripta 23* , p.539 (1981).
M. Suzuki et al., *Nucl. Instr. Meth. 164* , p.197 (1979).
Y. Tanaka et al., *J. Opt. Soc. Am. 48* , p.304 (1958).

### 8.1.4. Phenomenology of Scintillation in Rare Gases


Alegra Feio, *Nucl. Instr. Meth. 176* , p.473 (1980).
Breskin, *IEEE Trans. Nucl. Sci.* , (1981).
G. Charpak, *Nucl. Instr. Meth 126* , p.381 (1975).
G. Charpak, *IEEE Trans. Nucl. Sci. NS-23* , p.202 (1976).
C. Conde et al., *IEEE Trans. Nucl. Sci. NS-24* , p.221 (1977).
D. Cumpstey et al., *Nucl. Instr. Meth. 171* , p.473 (1980).
Ibqal et al., *Xe-TPC, Cal. Inst. Tech.* (1986).
H. Nguyen Ngoc, *Nucl. Instr. Meth. 172* , p.603 (1980).
Salete, *Nucl.Instr. Meth. 179* , p.295 (1981).
Takahoshi et al., *Nucl. Instr. Meth. 205* , p.591 (1983).


### 8.1.5. Gas Scintillation Proportional Counters (Reviews)


G. Charpak, *Nucl. Instr. Meth. 176* , p.9 (1980).
G. Charpak, *CERN-EP 83-62* (1983).
A. Policarpo, *Nucl. Instr. Meth 196* , p.53 (1982).
B. Sadoulet, *The Case of GS-Drift Chambers CERN-UCB* (1985).


### 8.1.6. Gas Scintillation Proportional Counters (Applications)


A. Alichanian et al., *Nucl. Instr. Meth.* (1979).
D. Anderson, *Nucl. Instr. Meth. 178* , p.125 (1980).
D. Anderson, *IEEE Trans. Nucl. Sci. NS-27* , p.181 (1980).
D. Anderson, *IEEE Trans. Nucl. Sci. NS-28* , p.842 (1981).
V. Baskakov et al., *Nucl. Instr. Meth. 158* , p.129 (1979).
G. Charpak et al., *IEEE Trans. Nucl. Sci. NS-27* , p.212 (1980).
C. Conde et al., *IEEE Trans. Nucl. Sci. NS-15* , p.84 (1968).
Lyeshenko et al., *Instr. Exp. Tech. (USSR) 14* , p.1328 (1971).
H. Nguyen Ngoc, *Nucl. Instr. Meth. 154*, p.597 (1978).
H. Nguyen Ngoc, *Nucl. Instr. Meth. 172* , p.603 (1980).
A. Policarpo,*Intl. Meet. on Prop. Drift Chambers*, Dubna(USSR), p.302 (1975).
B. Sadoulet et al., *IEEE Trans. Nucl. Sci. NS-34* , p.52 (1987).
B. Sadoulet et al., *IEEE Trans. Nucl. Sci. NS-35* , p.543 (1988).
O. Siegmund et al., *IEEE Trans. Nucl. Sci. NS-30* , p.350 (1983).
Sauli, *Intl. Meet. on Prop. Drift Chambers*, Dubna (USSR), p.11 (1975).
P. Thiess et al., *IEEE Trans. Nucl. Sci. NS-21* , p.125 (1974).

### 8.1.7. Electronic Excitation, Ionization, Elastic Scattering

G. Braglia et al., *Nuovo Cimento 43B* , p.130 (1966).
Druyvensteyn, *Physica 3* , p.65 (1936).
L. Frost & A. Phelps, *Phys. Rev. 136A* , p.1358 (1964).
Kuprianov, *Optics Spectros. 20* , p.85 (1966).
Jesse, *Phys. Rev. 100* , p.1755 (1955).
F. Penning, *Physica 5* , p.286 (1938).
F. Penning et al., *Rev. Mod. Phys. 12* , p.87 (1940).
Platzmann, *Rad. Res. 3* , p.340 (1955).
L. Sin Fai Lam, *J. Phys. B: Atom. Molec. Phys. 15* , p.115 (1982).
Smit, *Physica 3* , p.543 (1937).

### 8.1.8. Fluctuations and Statistics in GSPC

G. Alkhazov et al., *Nucl. Instr. Meth. 48* , p.1 (1967).
Davies, *Statistical Methodes in Research and Production.*
E. De Lima et al., *Nucl. Instr. Meth 192* , p.575 (1982).
F. Fahey et al., *Mod. Phys. 13* , p.25 (1986).

## 8.2. Monte Carlo Simulation: Inputs and Programs

The simulation programs are based on the Electron-Gamma Shower EGS4 code (W.R. Nelson et al., SLAC Report 265, December 1985). Interaction cross section for each material are computed by PEGS4. For low energy electrons limitations in transport length are imposed so that not more then 5 % of the energy of the particle is lost in each step. The simulation programs were run on the LBL VAX Cluster.

### 8.2.1. CsI/Amorphous Silicon Detector

Electrons and photons are transported through a low energy cut off of 10 keV, then are discarded and their energy is considered released in the CsI. In order to compute the interaction cross sections a density of 4.5 g/cm$^3$ is assumed for CsI. The Programs listed are :

CHESBUR.MOR (Mortran Source)
WHOPPER.MOR (Mortran Source)
REFLEX.FOR (Fortran Source)

### 8.2.2. Tantalum/Amorphous Silicon Detector

Electrons are followed in Tantalum and Silicon through a low energy cut-off of 20 keV, photons through 10 keV in Tantalum and 1 keV in Silicon, then they are discarded and their energy is considered released in the material.Interaction cross section are computed by PEGS4 using with $\rho_{Ta}$ = 16.6 g/cm$^3$ and $\rho_{Si}$ = 2.4 g/cm$^3$.

The Program listed is :
BIGMAC.MOR (Mortran Source)

## 8.3. Program Listing

```
MMMMMMMMMM    6666666666666666666666666666666666666666666666666666666666666666666666666666666666666666666666666666666666666666666666    MMMMMMMMMM
MMMMMMMMMM    66666666666666666666  Digital Equipment Corporation - VAX/VMS Version V5.3  66666666666666666666    MMMMMMMMMM
MMMMMMMMMM    6666666666666666666666666666666666666666666666666666666666666666666666666666666666666666666666666666666666666666666666    MMMMMMMMMM

                        M   M   AAA   U   U  RRRR    III   ZZZZZ   III    000
                        MM MM  A   A  U   U  R   R    I       Z     I    0   0
                        M M M  A   A  U   U  R   R    I      Z      I    0   0
                        M   M  A   A  U   U  RRRR     I     Z       I    0   0
                        M   M  AAAAA  U   U  R R      I    Z        I    0   0
                        M   M  A   A  U   U  R  R     I   Z         I    0   0
                        M   M  A   A  UUUUU  R   R   III  ZZZZZ   III    000

  CCCCCCCC  HH      HH  EEEEEEEEEE    SSSSSSSS  BBBBBBBB    UU      UU  RRRRRRRR
  CCCCCCCC  HH      HH  EEEEEEEEEE    SSSSSSSS  BBBBBBBB    UU      UU  RRRRRRRR
CC          HH      HH  EE          SS          BB      BB  UU      UU  RR      RR
CC          HH      HH  EE          SS          BB      BB  UU      UU  RR      RR
CC          HH      HH  EE          SS          BB      BB  UU      UU  RR      RR
CC          HH      HH  EE          SS          BB      BB  UU      UU  RR      RR
CC          HHHHHHHHHH  EEEEEEEE      SSSSSS    BBBBBBBB    UU      UU  RRRRRRRR
CC          HHHHHHHHHH  EEEEEEEE      SSSSSS    BBBBBBBB    UU      UU  RRRRRRRR
CC          HH      HH  EE                  SS  BB      BB  UU      UU  RR  RR
CC          HH      HH  EE                  SS  BB      BB  UU      UU  RR  RR
CC          HH      HH  EE                  SS  BB      BB  UU      UU  RR    RR
CC          HH      HH  EE                  SS  BB      BB  UU      UU  RR    RR
  CCCCCCCC  HH      HH  EEEEEEEEEE  SSSSSSSS    BBBBBBBB    UUUUUUUUUU  RR      RR
  CCCCCCCC  HH      HH  EEEEEEEEEE  SSSSSSSS    BBBBBBBB    UUUUUUUUUU  RR      RR

          MM      MM    000000    RRRRRRRR        ;;;;      333333    77777777
          MM      MM    000000    RRRRRRRR        ;;;;      333333    77777777
          MMMM  MMMM  00      00  RR      RR      ;;;;    33      33          77
          MMMM  MMMM  00      00  RR      RR      ;;;;    33      33          77
          MM  MM  MM  00      00  RR      RR                      33          77
          MM  MM  MM  00      00  RR      RR                      33          77
          MM      MM  00      00  RRRRRRRR        ;;;;          33        77
          MM      MM  00      00  RRRRRRRR        ;;;;          33        77
          MM      MM  00      00  RR  RR          ;;;;            33      77
          MM      MM  00      00  RR  RR          ;;;;            33      77
....      MM      MM  00      00  RR    RR          ;;    33      33    77
....      MM      MM  00      00  RR    RR          ;;    33      33    77
....      MM      MM    000000    RR      RR      ;;        333333    77
....      MM      MM    000000    RR      RR      ;;        333333    77
```

File $1$DUS110:[MAURIZIO.EGS4]CHESBUR.MOR;37 (33586,1,0), last revised on 15-MAY-1989 15:41, is a 39 block sequential file owned by UIC [MAURIZIO]. The records are variable length with implied (CR) carriage control. The longest record is 80 bytes.

Job CHESBUR (924) queued to SYS$PRINT on 25-JAN-1990 15:03 by user MAURIZIO, UIC [MAURIZIO], under account 426105 at priority 100, started on printer LIC0 on 25-JAN-1990 15:03 from queue CSA3$LIC0.

```
MMMMMMMMMM    6666666666666666666666666666666666666666666666666666666666666666666666666666666666666666666666666666666666666666666666    MMMMMMMMMM
MMMMMMMMMM    66666666666666666666  Digital Equipment Corporation - VAX/VMS Version V5.3  66666666666666666666    MMMMMMMMMM
MMMMMMMMMM    6666666666666666666666666666666666666666666666666666666666666666666666666666666666666666666666666666666666666666666666    MMMMMMMMMM
```

```
"*****************************************************************"
"********************** CHEESEBURGER  PROGRAM ********************"
"*****************************************************************"

"*****************************************************************"
"************** STEP 1.  USER-OVER-RIDE-OF-EGS-MACROS *************"
"*****************************************************************"

REPLACE {$MXREG} WITH {4} "MAXIMUM NUMBER OF REGIONS"
REPLACE {$MXMED} WITH {1}   "MAXIMUM NUMBER OF MEDIA"

REPLACE {;COMIN/RANDOM/;} WITH {;COMMON/RANDOM/IXX;}
REPLACE {$RANDOMSET#;} WITH
        {IXX=IXX*663608941;{P1}=0.5+IXX*0.23283064E-09;}

"*****************************************************************"
"****************** ADDITIONAL (NON-EGS) MACROS ******************"
"*****************************************************************"

REPLACE {$MXHCOM} WITH {40000} "MAX SIZE OF HCOM BUFFER"
REPLACE {$MBIN} WITH {52}  "NO. OF BINS FOR THE HIST'S"

"*****************************************************************"
"************************** DECLARATIONS *************************"
"*****************************************************************"

;COMIN/EPCONT,STACK,MEDIA,MISC,THRESH,UPHIOT,USEFUL/;
COMMON//HMEMOR($MXHCOM);
COMMON/LIGHT/XR(25),YR(25),YIL(25);
COMMON/EDATA/SIZEHA,DTH0,N,INP,EDP(20),ENEDEP,
             XL(20),YL(20),ZL(20),XS(20),YS(20),ZS(20);
REAL*8 EDP;
REAL*8 ENEDEP;
CHARACTER*8 ITIME;
CHARACTER*4 MEDARR(24,$MXMED)/$S'CESIUM IODATE           '/;
COMIN/RANDOM/;
DIMENSION ARRAY($MBIN);
"*****************************************************************"
"************** START OF EXECUTABLE CODE *************************"
"*****************************************************************"


"*****************************************************************"
"************** STEP 2.  INITIALIZATION COMES NEXT ***************"
"*****************************************************************"

NMED=$MXMED; "NUMBER OF MEDIA"


DO J=1,NMED [
DO I=1,24 [MEDIA(I,J)=MEDARR(I,J);]]

MED(1)=1; "CsI"
MED(2)=0; "VACUUM IN FRONT OF THE DETECTOR"
MED(3)=0; "VACUUM OUT OF THE SIZE OF THE DETECTOR"
```

```
MED(4)=0; "VACUUM IN THE BACK OF THE DETECTOR"

"SET DETECTOR SIZE"
NL=5;
ND=NL*NL; "NUMBER OF DETECTORS"
DSIZE=.2; "DETECTOR SIZE (CM)"
TOTSIZE=DSIZE*NL ; "CM"
SIZEHA=TOTSIZE/2.;

"LATTICE COORDINATE"

XR(1)=0.              ; YR(1)=0.;
XR(2)=1.*DSIZE        ; YR(2)=0.;
XR(3)=2.*DSIZE        ; YR(3)=0.;
XR(4)=-1.*DSIZE       ; YR(4)=0.;
XR(5)=-2.*DSIZE       ; YR(5)=0.;
XR(6)=-2.*DSIZE       ; YR(6)=1.*DSIZE;
XR(7)=-1.*DSIZE       ; YR(7)=1.*DSIZE;
XR(8)=0.              ; YR(8)=1.*DSIZE;
XR(9)=1.*DSIZE        ; YR(9)=1.*DSIZE;
XR(10)=2.*DSIZE       ; YR(10)=1.*DSIZE;
XR(11)=-2.*DSIZE      ; YR(11)=2.*DSIZE;
XR(12)=-1.*DSIZE      ; YR(12)=2.*DSIZE;
XR(13)=0.             ; YR(13)=2.*DSIZE;
XR(14)=1.*DSIZE       ; YR(14)=2.*DSIZE;
XR(15)=2.*DSIZE       ; YR(15)=2.*DSIZE;
XR(16)=-2.*DSIZE      ; YR(16)=-1.*DSIZE;
XR(17)=-1.*DSIZE      ; YR(17)=-1.*DSIZE;
XR(18)=0.             ; YR(18)=-1.*DSIZE;
XR(19)=1.*DSIZE       ; YR(19)=-1.*DSIZE;
XR(20)=2.*DSIZE       ; YR(20)=-1.*DSIZE;
XR(21)=-2.*DSIZE      ; YR(21)=-2.*DSIZE;
XR(22)=-1.*DSIZE      ; YR(22)=-2.*DSIZE;
XR(23)=0.             ; YR(23)=-2.*DSIZE;
XR(24)=1.*DSIZE       ; YR(24)=-2.*DSIZE;
XR(25)=2.*DSIZE       ; YR(25)=-2.*DSIZE;

RADI=SQRT(DSIZE*DSIZE/3.14);

"SET DETECTOR  THICKNESS"
READ(*,*) DTH;
"DTH=.2; CM"
DTH0=-1.*DTH;

"HISTOGRAMS INIZIALIZATION"


CALL HLIMIT($MXHCOM);

NBIN=$MBIN;

CALL HBOOK1(1,'ENERGY IN 1st PIXEL(MeV)$',
            NBIN,0.,.520);
CALL HBOOK1(2,'ENERGY IN 2nd PIXEL(MeV)$',
            NBIN,0.,.520);
CALL HBOOK1(3,'ENERGY IN 3rd PIXEL(MeV)$',
            NBIN,0.,.520);
CALL HBOOK1(4,'TOTAL ENERGY DEPOSITED IN CsI(MeV)$',
            NBIN,0.,.520);
CALL HBOOK1(5,'FRACTION OF ENERGY OUT OF THE DETECTOR$',
```

```
          50,0.,1.);
CALL HBOOK1(6,'CENTER OF GRAVITY OF THE LIGHT; CYL-COOR (CM)$',
          50,0.,SIZEHA);

CALL HBSTAT(0);

"*********************************************************************"
"*************** STEP 3.  HATCH-CALL COMES NEXT ******************"
"*********************************************************************"

CALL HATCH;

"OUTPUT VARIOUS QUANTITIES ASSOCIATED WITH THE MEDIA"

OUTPUT;  ('1QUANTITIES ASSOCIATED WITH EACH MEDIA:',//);

DO JSEL=1,NMED [
OUTPUT (MEDIA(I,JSEL),I=1,24);  (/,1X,24A1);
OUTPUT RHO(JSEL),RLC(JSEL);
(5X,' RHO=',G15.7,' G/CM**3     RLC=',G15.7,' CM');
OUTPUT AE(JSEL),UE(JSEL);
(5X,' AE=',G15.7,' MEV    UE=',G15.7,' MEV');
OUTPUT AP(JSEL),UP(JSEL);
(5X,' AP=',G15.7,' MEV    UP=',G15.7,' MEV');
"END OF JSEL-LOOP"]


OUTPUT DSIZE; (////,' PIXEL SIZE = ',F5.2,' CM');
OUTPUT TOTSIZE,DTH;(////,' TOTAL DETECTOR SIZE = ',F7.4,' CM',
 /,' DETECTOR THICKNESS = ',F7.4,' CM');

"*********************************************************************"
"***** STEP 4.  DETERMINATION OF INCIDENT PARTICLE PROPERTIES ****"
"*********************************************************************"

IQI=0;   "INCIDENT PARTICLE"

EI=0.511D0;   "TOTAL ENERGY OF PARTICLE (MEV)"
EII=EI;
AVAILE=EI;  "AVAILABLE K.E. (MEV)"
EISING=EI;  "SINGLE PRECISION ENERGY VARIABLE"

XI=0.0; YI=0.0; ZI=-1.*DTH; "STARTING COORDINATES (CM)"
UI=0.0; VI=0.0; WI=1.0;  "INCIDENT DIRECTION COSINES"
IRI=1;  "ENTRANCE REGION DEFINITION"
WTI=1.0;  "WEIGHT FACTOR OF UNITY"


"SELECT THE STARTING RANDOM NUMBER SEED"
" OUTPUT; (/,' INIZIALIZING RANDOM NUMBER ?'); "

READ(*,*) IXXST;
"IXXST=123456789;"

IXX=IXXST;  "INITIALIZED RANDOM NUMBER WITH STARTING SEED"

" OUTPUT; (/,' NUMBER OF EVENTS ?'); "
READ(*,*) NCASES;

"*********************************************************************"
```

```
"****************** STEP 5. SHOWER-CALL---NEXT ******************"
"*****************************************************************"


CALL TIME(ITIME);
OUTPUT ITIME;
(//,' PRIOR TO SHOWER CALL LOOP ===> ITIME=',A8,//);


ESTEPE=0.05;
DO I=1,NMED [ "SET UPPER LIMIT TO USTEP IN ORDER TO HAVE"
              "ENERGY LOSS LESS THAN ESTEPE*ENERGY OF    "
              "THE ELECTRON "
             CALL FIXTMX(ESTEPE,I); ]


DO I=1,NCASES ["START OF SHOWER CALL LOOP"

ENEDEP=0.;
N=0; INP=0;
DO J=1,25 [YIL(J)=0.;]
DO J=1,20 [
           EDP(J)=0.;
           XL(J)=0.; YL(J)=0.; ZL(J)=0.;
           XS(J)=0.; YS(J)=0.; ZS(J)=0.; ]

CALL SHOWER(IQI,EI,XI,YI,ZI,UI,VI,WI,IRI,WTI);

IF(ENEDEP.NE.0.) [

DO K=1,N [
IF(EDP(K).NE.0.) [

BX=XL(K);
BY=YL(K);
BZ=ZL(K);

DO J=1,25 [

CX=XR(J);
CY=YR(J);

OM=OMEGA(RADI,BX,BY,BZ,CX,CY);

YIL(J)=EDP(K)*OM+YIL(J);

] ] ]


SYIL=0.;
DO L=1,25 [
SYIL=SYIL+YIL(L); ]
ENEHA=ENEDEP/2.;
OUTE=(ENEHA-SYIL)/ENEHA;

BARX=0.; BARY=0.; BAR=0.;
DO L=1,25 [
BARX=BARX+YIL(L)*XR(L);
BARY=BARY+YIL(L)*YL(L); ]
BARX=BARX/SYIL;
```

```
BARY=BARY/SYIL;
BAR=SQRT(BARX*BARX+BARY*BARY);

DO ID=1,3 [
VA=YIL(ID);
CALL HFILL(ID,VA); ]

CALL HFILL(4,ENEDEP);
CALL HFILL(5,OUTE);
CALL HFILL(6,BAR);

]

NCOUNT=NCOUNT + 1;
IXXEND=IXX;   "LAST RANDOM NUMBER USED"

"END OF SHOWER CALL LOOP"]


CALL TIME(ITIME);
OUTPUT ITIME;  (//,' END OF SHOWER CALL LOOP ===> ITIME=',A8,//);


"*********************************************************************"
"****************** STEP 6. OUTPUT OF RESULTS ************************"
"*********************************************************************"


OUTPUT NCOUNT,NCASES,IXXST,IXXEND;
('1',I10,' CASES OUT OF ',I10,
     //,' IXXST=',I12,/,' IXXEND=',I12,//);


DO I=1,6 [
          J=I+20;
          CALL HUNPAK(I,ARRAY);
          DO K=1,NBIN [
          KK=K*10;
          WRITE(J,*) KK,ARRAY(K); ]
          ]

CALL HISTDO;              "OUTPUT ALL HISTOGRAMS"

STOP;
END;  "END OF MAIN PROGRAM"

%E
"*********************************************************************"
SUBROUTINE AUSGAB(IARG);
"*********************************************************************"
;COMIN/EPCONT,STACK/;
COMMON//HWEMOR($MXHCOM);
COMMON/LIGHT/XR(25),YR(25),YIL(25);
COMMON/EDATA/SIZEHA,DTH0,N,INP,EDP(20),ENEDEP,
             XL(20),YL(20),ZL(20),XS(20),YS(20),ZS(20);
REAL*8 EDP,ENEDEP;

IF(IQ(NP).EQ.-1.AND.IR(NP).EQ.1) [
IF(INP.NE.NP) [
```

```
N=N+1;
INP=NP;
XS(N)=X(NP);
YS(N)=Y(NP);
ZS(N)=Z(NP); ]

EDP(N)=EDP(N)+EDEP;
ENEDEP=ENEDEP+EDEP;



XL(N)=(XS(N)+2.*X(NP))/3.;
YL(N)=(YS(N)+2.*Y(NP))/3.;
ZL(N)=(ZS(N)+2.*Z(NP))/3.;

]

RETURN;
END;  "END OF SUBROUTINE AUSGAB"

%E
"*********************************************************************"
SUBROUTINE HOWFAR;
"*********************************************************************"
;COMIN/EPCONT,STACK/;
COMMON/EDATA/SIZEHA,DTH0,N,INP,EDP(20),ENEDEP,
             XL(20),YL(20),ZL(20),XS(20),YS(20),ZS(20);
REAL*8 EDP;
REAL*8 ENEDEP;

IRL=IR(NP);
IF(IRL.NE.1) [RETURN;]

XX=X(NP);
YY=Y(NP);
ZZ=Z(NP);
XX1=ABS(XX);
YY1=ABS(YY);
WW=W(NP);

IF(XX1.GE.SIZEHA.OR.YY1.GE.SIZEHA) [ IRNEW=3;
   IDISC=1;   "OUT OF THE SIZE OF THE DETECTOR" ]

   DIS1=-ZZ;
   DIS2=ZZ-DTH0;
   DIS3=SIZEHA-XX1;
   DIS4=SIZEHA-YY1;
   DMI1=AMIN1(DIS1,DIS2);
   DMI2=AMIN1(DIS3,DIS4);
   DNEAR(NP)=AMIN1(DMI1,DMI2);
   IF(WW.GT.0.) [ "FORWARD"
      DIST=DIS1/WW;
      IF(DIST.LE.USTEP) [ USTEP=DIST;
         IRNEW=4; IDISC=1; ] ]
   ELSEIF(WW.LT.0.) [ "BACKWARD"
      DIST=-DIS2/WW;
      IF(DIST.LE.USTEP) [ USTEP=DIST;
         IRNEW=2; IDISC=1;  ] ]

IF(IQ(NP).EQ.-1.AND.IRL.EQ.1) [
```

```
IF(INP.NE.NP) [
N=N+1;
INP=NP;
XS(N)=XX;
YS(N)=YY;
ZS(N)=ZZ; ]

]

RETURN;
END;


%E

"                          *          *                                  "
"                          * FIXTMX  *                                  "
"                          *          *                                  "
"                          ***********                                  "
SUBROUTINE FIXTMX(ESTEPE,MEDIUM);
"                                                                       "
"  THIS ROUTINE CHANGES THE STEP SIZE ALGORITHM USED IN EGS SO THAT     "
"  THE STEP SIZE ARRAYS FOR TMXS CORRESPOND TO AN ARBITRARY,BUT         "
"  FIXED FRACTIONAL ENERGY LOSS ESTEPE.                                 "
"  IT IS ONLY NECESSARY FOR LOW ENERGY ELECTRON PROBLEMS SINCE          "
"  TYPICALLY THE 200*TEFFØ RESTRICTION ON TMXS IS MORE STRINGENT        "
"   FOR ELECTRONS WITH ENERGIES ABOVE A FEW MEV                         "
"                                                                       "
"  NOTE THAT THE $TMXS-OVER-RIDE MACRO IS STILL IN FORCE IN EGS.        "
"                                                                       "
"  THE ROUTINE CHANGES THE VALUES ONLY FOR THE MEDIUM 'MEDIUM'          "
"  AND IT SHOULD PROBABLY BE USED FOR ALL MEDIA IN A PROBLEM.           "
"                                                                       "
"  THE ROUTINE MUST BE CALLED AFTER HATCH HAS BEEN CALLED AND BEFORE    "
"  THE SIMULATION IS BEGUN.                                             "
"                                                                       "
"  THE ROUTINE IS INDEPENDENT OF WHAT UNITS ARE BEING USED, AS LONG     "
"  AS THEY ARE CONSISTENT( E.G. CM, RL OR G/CM**2 )                     "
"                                                                       "
"  IF CALLED WITH ESTEPE=Ø, THE CURRENT ALGORITHM IS USED               "
"                                                                       "
"  FOR A DETAILED DISCUSSION OF THE USE OF THIS ROUTINE, SEE            "
"  'Low Energy Electron Transport with EGS' in Nuclear Instr. and       "
"  Methods A227 (1984)535-548.  D.W.O. Rogers                           "
"                                                                       "
"  VØ1        DEC 1Ø,1981 DAVE ROGERS NRCC                              "
"  VØ2        DEC 1984  EGS4 VERSION                                    "
"***********************************************************************"
;COMIN/MEDIA,ELECIN/;
IF(MEDIUM > $MXMED)["ERROR"  OUTPUT MEDIUM;
(///'Ø********* MEDIUM=',I4,' IN FIXTMX IS TOO LARGE');RETURN;]

IF(ESTEPE = Ø) [RETURN; "I.E. USE THE CURRENT ALGORITHM "]
"SET UP SOME VARIABLES FOR FIRST PASS THROUGH LOOP"
EI =EXP( (1.-EKEØ(MEDIUM))/EKE1(MEDIUM));"ENERGY OF FIRST TABLE ENTRY"
EIL = ALOG(EI);  LEIL=1;
"THIS IS EQUIVALENT TO $SETINTERVAL EIL,EKE; BUT AVOIDS ROUNDOFF"
$EVALUATE EDEDX USING EDEDX(EIL);"GET THE ELECTRON STOPPPING AT EI"
"NOW CALCULATE STEP REQUIRED TO CAUSE AN ESTEPE REDUCTION IN ENERGY"
```

```
SI=ESTEPE*EI/EDEDX;
"TABULATED ENERGIES ARE IN A FIXED RATIO - CALC LOG OF THE RATIO"
ERATIO=-1./EKE1(MEDIUM);

NEKE=MEKE(MEDIUM);"NUMBER OF ELEMENTS IN STORAGE ARRAY"
DO I=1,NEKE-1[
EIP1=EXP((FLOAT(I+1)-EKE0(MEDIUM))/EKE1(MEDIUM));"ENERGY AT I+1"
EIP1L=ALOG(EIP1);LEIP1L=I+1;"DESIGNED THIS WAY=$SETINTERVAL"
$EVALUATE EDEDX USING EDEDX(EIP1L);SIP1=ESTEPE*EIP1/EDEDX;

"NOW SOLVE THESE EQUATIONS                                    "
"  SI   = TMXS1 * EIL   + TMXS0                               "
"  SIP1 = TMXS1 * EIP1L + TMXS0                               "
"                                                             "
TMXS1(I,MEDIUM)=(SI-SIP1)/ERATIO;TMXS0(I,MEDIUM)=SI-TMXS1(I,MEDIUM)*EIL;
"TRANSFER VALUES FOR NEXT LOOP"
EIL=EIP1L;SI=SIP1;]
"NOW PICK UP LAST TABLE ENTRY WHICH APPLIES ONLY TO LAST ENERGY"
TMXS0(NEKE,MEDIUM)=TMXS0(NEKE-1,MEDIUM);
TMXS1(NEKE,MEDIUM)=TMXS1(NEKE-1,MEDIUM);
RETURN;
END; "END OF SUBROUTINE FIXTMX"


FUNCTION OMEGA(RADI,BX,BY,BZ,CX,CY);
RR2=(CX-BX)**2+(CY-BY)**2;
RR=SQRT(RR2);
PSI=ATAN(-BZ/(RR+RADI));
PHI=ATAN(-BZ/(RR-RADI));
IF(PHI.GE.0.) [
THE=.5*(PHI-PSI); ]
ELSE [
THE=.5*(PHI-PSI+3.14); ]
OMEGA=(1.-COS(THE))/2.;
RETURN;
END;
```

```
VVVVVVVVVV    7777777777777777777777777777777777777777777777777777777777777777777777777777777777777777777777777777777777777777777777    VVVVVVVVVV
VVVVVVVVVV    77777777777777777777  Digital Equipment Corporation - VAX/VMS Version V5.3  77777777777777777777    VVVVVVVVVV
VVVVVVVVVV    7777777777777777777777777777777777777777777777777777777777777777777777777777777777777777777777777777777777777777777777    VVVVVVVVVV

                                  M   M   AAA   U   U  RRRR    III   ZZZZZ   III    000
                                  MM MM  A   A  U   U  R   R    I       Z     I    0   0
                                  M M M  A   A  U   U  R   R    I      Z      I    0   0
                                  M   M  A   A  U   U  RRRR     I     Z       I    0   0
                                  M   M  AAAAA  U   U  R R      I    Z        I    0   0
                                  M   M  A   A  U   U  R  R     I   Z         I    0   0
                                  M   M  A   A  UUUUU  R   R  III  ZZZZZ   III    000

                WW       WW  HH       HH    000000    PPPPPPPP    PPPPPPPP    EEEEEEEEEE  RRRRRRRR
                WW       WW  HH       HH    000000    PPPPPPPP    PPPPPPPP    EEEEEEEEEE  RRRRRRRR
                WW       WW  HH       HH  00      00  PP      PP  PP      PP  EE          RR      RR
                WW       WW  HH       HH  00      00  PP      PP  PP      PP  EE          RR      RR
                WW       WW  HH       HH  00      00  PP      PP  PP      PP  EE          RR      RR
                WW       WW  HH       HH  00      00  PP      PP  PP      PP  EE          RR      RR
                WW       WW  HHHHHHHHHHH  00      00  PPPPPPPP    PPPPPPPP    EEEEEEEE    RRRRRRRR
                WW       WW  HHHHHHHHHHH  00      00  PPPPPPPP    PPPPPPPP    EEEEEEEE    RRRRRRRR
                WW  WW   WW  HH       HH  00      00  PP          PP          EE          RR  RR
                WW  WW   WW  HH       HH  00      00  PP          PP          EE          RR  RR
                WWWW  WWWW   HH       HH  00      00  PP          PP          EE          RR    RR
                WWWW  WWWW   HH       HH  00      00  PP          PP          EE          RR    RR
                WW       WW  HH       HH    000000    PP          PP          EEEEEEEEEE  RR      RR
                WW       WW  HH       HH    000000    PP          PP          EEEEEEEEEE  RR      RR

                          MM       MM    000000    RRRRRRRR        ;;;;        11      5555555555
                          MM       MM    000000    RRRRRRRR        ;;;;        11      5555555555
                          MMMM   MMMM  00      00  RR      RR      ;;;;      1111      55
                          MMMM   MMMM  00      00  RR      RR      ;;;;      1111      55
                          MM  MM  MM  00      00  RR      RR                  11      555555
                          MM  MM  MM  00      00  RR      RR                  11      555555
                          MM      MM  00      00  RRRRRRRR        ;;;;        11            55
                          MM      MM  00      00  RRRRRRRR        ;;;;        11            55
                          MM      MM  00      00  RR  RR          ;;;;        11              55
                          MM      MM  00      00  RR  RR          ;;;;        11              55
                    ....  MM      MM  00      00  RR    RR          ;;        11      55      55
                    ....  MM      MM  00      00  RR    RR          ;;        11      55      55
                    ....  MM      MM    000000    RR      RR      ;;        111111    555555
                    ....  MM      MM    000000    RR      RR      ;;        111111    555555

File  $1$DUS110:[MAURIZIO.EGS4]WHOPPER.MOR;15 (33964,1,0), last revised on 24-MAY-1989 11:32, is a 40 block sequential file owned
by UIC [MAURIZIO].  The records are variable length with implied (CR) carriage control.  The longest record is 80 bytes.

Job WHOPPER (922) queued to SYS$PRINT on 25-JAN-1990 15:02 by user MAURIZIO, UIC [MAURIZIO], under account 426105 at priority 100,
started on printer LIC0 on 25-JAN-1990 15:02 from queue CSA2$LIC0.

VVVVVVVVVV    7777777777777777777777777777777777777777777777777777777777777777777777777777777777777777777777777777777777777777777777    VVVVVVVVVV
VVVVVVVVVV    77777777777777777777  Digital Equipment Corporation - VAX/VMS Version V5.3  77777777777777777777    VVVVVVVVVV
VVVVVVVVVV    7777777777777777777777777777777777777777777777777777777777777777777777777777777777777777777777777777777777777777777777    VVVVVVVVVV
```

```
"*********************************************************************"
"**********************  WHOPPER      PROGRAM **********************"
"*********************************************************************"

"*********************************************************************"
"************** STEP 1.  USER-OVER-RIDE-OF-EGS-MACROS **************"
"*********************************************************************"

REPLACE {$MXREG} WITH {3} "MAXIMUM NUMBER OF REGIONS"
REPLACE {$MXMED} WITH {1}   "MAXIMUM NUMBER OF MEDIA"

REPLACE {;COMIN/RANDOM/;} WITH {;COMMON/RANDOM/IXX;}
REPLACE {$RANDOMSET#;} WITH
        {IXX=IXX*663608941;{P1}=0.5+IXX*0.23283064E-09;}

"*********************************************************************"
"******************* ADDITIONAL (NON-EGS) MACROS *********************"
"*********************************************************************"

REPLACE {$MXHCOM} WITH {40000} "MAX SIZE OF HCOM BUFFER"
REPLACE {$MBIN} WITH {52}  "NO. OF BINS FOR THE HIST'S"

"*********************************************************************"
"************************** DECLARATIONS *****************************"
"*********************************************************************"

;COMIN/EPCONT,STACK,MEDIA,MISC,THRESH,UPHIOT,USEFUL/;
COMMON//HMEMOR($MXHCOM);
COMMON/LIGHT/YIELD(3,5,5);
COMMON/EDATA/SIZEHA,DSIZE,DTH0,N,INP,EDP(20),ENEDEP,
             XL(20),YL(20),XS(20),YS(20);
REAL*8 EDP;
REAL*8 ENEDEP;
CHARACTER*8 ITIME;
CHARACTER*4 MEDARR(24,$MXMED)/$S'CESIUM IODATE           '/;
COMIN/RANDOM/;
DIMENSION ARRAY($MBIN);
"*********************************************************************"
"************** START OF EXECUTABLE CODE *****************************"
"*********************************************************************"


"*********************************************************************"
"************** STEP 2.  INITIALIZATION COMES NEXT ***************"
"*********************************************************************"

NMED=$MXMED; "NUMBER OF MEDIA"


DO J=1,NMED [
DO I=1,24 [MEDIA(I,J)=MEDARR(I,J);]]

MED(1)=1; "CsI"
MED(2)=0; "VACUUM IN FRONT OF THE DETECTOR"
MED(3)=0; "VACUUM IN THE BACK OF THE DETECTOR"
```

```
"SET DETECTOR SIZE"
NL=5;
ND=NL*NL; "NUMBER OF DETECTORS"
DSIZE=.2; "DETECTOR SIZE (CM)"
TOTSIZE=DSIZE*NL ; "CM"
SIZEHA=TOTSIZE/2.;

"SET DETECTOR  THICKNESS"
READ(*,*) DTH;
"DTH=.2; CM"
DTH0=-1.*DTH;

"HISTOGRAMS INIZIALIZATION"


CALL HLIMIT($MXHCOM);

NBIN=$MBIN;

CALL HBOOK1(1,'TOTAL ENERGY DEPOSITED IN CsI(MeV)$',
            NBIN,0.,.520);
CALL HBOOK1(2,'ENERGY IN 1st PIXEL(MeV)-100%LIGHT$',
            NBIN,0.,.520);
CALL HBOOK1(3,'ENERGY IN 2nd PIXEL(MeV)-100%LIGHT$',
            NBIN,0.,.520);
CALL HBOOK1(4,'ENERGY IN 3rd PIXEL(MeV)-100%LIGHT$',
            NBIN,0.,.520);
CALL HBOOK1(5,'FRACTION OF ENERGY OUT OF THE DETECTOR-100%$',
            50,0.,1.);
CALL HBOOK1(6,'CENTER OF GRAVITY OF LIGHT;CYLCOOR(CM)-100%$',
            50,0.,DSIZE);
CALL HBOOK1(7,'ENERGY IN 1st PIXEL(MeV)-50%LIGHT$',
            NBIN,0.,.520);
CALL HBOOK1(8,'ENERGY IN 2nd PIXEL(MeV)-50%LIGHT$',
            NBIN,0.,.520);
CALL HBOOK1(9,'ENERGY IN 3rd PIXEL(MeV)-50%LIGHT$',
            NBIN,0.,.520);
CALL HBOOK1(10,'FRACTION OF ENERGY OUT OF THE DETECTOR-50%$',
            50,0.,1.);
CALL HBOOK1(11,'CENTER OF GRAVITY OF LIGHT;CYLCOOR(CM)-TR%$',
            50,0.,DSIZE);
CALL HBOOK1(12,'ENERGY IN 1st PIXEL(MeV)-TR%LIGHT$',
            NBIN,0.,.520);
CALL HBOOK1(13,'ENERGY IN 2nd PIXEL(MeV)-TR%LIGHT$',
            NBIN,0.,.520);
CALL HBOOK1(14,'ENERGY IN 3rd PIXEL(MeV)-TR%LIGHT$',
            NBIN,0.,.520);
CALL HBOOK1(15,'FRACTION OF ENERGY OUT OF THE DETECTOR-TR%$',
            50,0.,1.);
CALL HBOOK1(16,'CENTER OF GRAVITY OF LIGHT;CYLCOOR(CM)-TR%$',
            50,0.,DSIZE);
CALL HBSTAT(0);

"*****************************************************************"
"*************** STEP 3.  HATCH-CALL COMES NEXT ******************"
"*****************************************************************"

CALL HATCH;
```

```
"OUTPUT VARIOUS QUANTITIES ASSOCIATED WITH THE MEDIA"

OUTPUT;  ('1QUANTITIES ASSOCIATED WITH EACH MEDIA:',//);

DO JSEL=1,NMED [
OUTPUT (MEDIA(I,JSEL),I=1,24);  (/,1X,24A1);
OUTPUT RHO(JSEL),RLC(JSEL);
(5X,' RHO=',G15.7,' G/CM**3     RLC=',G15.7,' CM');
OUTPUT AE(JSEL),UE(JSEL);
(5X,' AE=',G15.7,' MEV    UE=',G15.7,' MEV');
OUTPUT AP(JSEL),UP(JSEL);
(5X,' AP=',G15.7,' MEV    UP=',G15.7,' MEV');
"END OF JSEL-LOOP"]


OUTPUT DSIZE; ////,' PIXEL SIZE = ',F5.2,' CM');
OUTPUT TOTSIZE,DTH;////,' TOTAL DETECTOR SIZE = ',F7.4,' CM',
 /,' DETECTOR THICKNESS = ',F7.4,' CM');

"*********************************************************************"
"***** STEP 4.  DETERMINATION OF INCIDENT PARTICLE PROPERTIES ****"
"*********************************************************************"

IQI=0;   "INCIDENT PARTICLE"

EI=0.511D0;   "TOTAL ENERGY OF PARTICLE (MEV)"
EII=EI;
AVAILE=EI;  "AVAILABLE K.E. (MEV)"
EISING=EI;  "SINGLE PRECISION ENERGY VARIABLE"

XI=0.0; YI=0.0; ZI=-1.*DTH; "STARTING COORDINATES (CM)"
UI=0.0; VI=0.0; WI=1.0;  "INCIDENT DIRECTION COSINES"
IRI=1;  "ENTRANCE REGION DEFINITION"
WTI=1.0;  "WEIGHT FACTOR OF UNITY"


"SELECT THE STARTING RANDOM NUMBER SEED"
" OUTPUT; (/,' INIZIALIZING RANDOM NUMBER ?'); "

READ(*,*) IXXST;
"IXXST=123456789;"

IXX=IXXST;  "INITIALIZED RANDOM NUMBER WITH STARTING SEED"

" OUTPUT; (/,' NUMBER OF EVENTS ?'); "
READ(*,*) NCASES;

"*********************************************************************"
"******************* STEP 5. SHOWER-CALL---NEXT ******************"
"*********************************************************************"


CALL TIME(ITIME);
OUTPUT ITIME;
(//,' PRIOR TO SHOWER CALL LOOP ===> ITIME=',A8,//);


ESTEPE=0.05;
DO I=1,NMED [ "SET UPPER LIMIT TO USTEP IN ORDER TO HAVE"
              "ENERGY LOSS LESS THAN ESTEPE*ENERGY OF    "
```

```
              "THE ELECTRON "
             CALL FIXTMX(ESTEPE,I); ]

DO I=1,NCASES ["START OF SHOWER CALL LOOP"

ENEDEP=0.;
N=0; INP=0;

DO L=1,3 [
DO J=1,5 [
   DO K=1,5 [
      YIELD(L,J,K)=0.; ] ] ]

DO J=1,20 [
           EDP(J)=0.;
           XL(J)=0.; YL(J)=0.;
           XS(J)=0.; YS(J)=0.; ]

CALL SHOWER(IQI,EI,XI,YI,ZI,UI,VI,WI,IRI,WTI);

IF(ENEDEP.NE.0.) [

DO K=1,N [
IF(EDP(K).NE.0.) [


CALL COORD(K,NN,FR1,FR2,I1,J1,I2,J2);

IF(NN.NE.0) [
EDP1=EDP(K)*FR1;
CALL ALGPHO(I1,J1,EDP1);

IF(NN.EQ.2) [
EDP1=EDP(K)*FR2;
CALL ALGPHO(I2,J2,EDP1); ] ]


] ]

CALL HFILL(1,ENEDEP);

DO L=1,3   [
   SYIL=0.; BARX=0.; BARY=0.; BAR=0.;

   DO J=1,5  [
   DO K=1,5  [

      COX=(J-3)*DSIZE;
      COY=(K-3)*DSIZE;
      YIL=YIELD(L,J,K);
      SYIL=SYIL+YIL;
      BARX=BARX+YIL*COX;
      BARY=BARY+YIL*COY; ] ]

   BARX=BARX/SYIL;
   BARY=BARY/SYIL;
   BAR=SQRT(BARX*BARX+BARY*BARY);
   OUTE=(ENEDEP-SYIL)/ENEDEP;
```

```
   ID=1+(L-1)*5;

   DO M=1,3  [
      IX=M+2;
      IY=3;
      VA=YIELD(L,IX,IY);
      ID=ID+1;
      CALL HFILL(ID,VA); ]

   ID=ID+1;
   CALL HFILL(ID,OUTE);

   ID=ID+1;
   CALL HFILL(ID,BAR);  ]

] "ENEDEP.NE.0 LOOP"

NCOUNT=NCOUNT + 1;
IXXEND=IXX;   "LAST RANDOM NUMBER USED"

"END OF SHOWER CALL LOOP"]


CALL TIME(ITIME);
OUTPUT ITIME;  (//,' END OF SHOWER CALL LOOP ===> ITIME=',A8,//);


"*********************************************************************"
"******************** STEP 6. OUTPUT OF RESULTS **********************"
"*********************************************************************"


OUTPUT NCOUNT,NCASES,IXXST,IXXEND;
('1',I10,' CASES OUT OF ',I10,
     //,' IXXST=',I12,/,' IXXEND=',I12,//);

DO ID=1,16 [
   CALL HUNPAK(ID,ARRAY);
   J=20+ID;
   DO K=1,NBIN [
      WRITE(J,*) K,ARRAY(K); ] ]

CALL HISTDO;              "OUTPUT ALL HISTOGRAMS"

STOP;
END;  "END OF MAIN PROGRAM"

%E
"*********************************************************************"
SUBROUTINE AUSGAB(IARG);
"*********************************************************************"
;COMIN/EPCONT,STACK/;
COMMON//HMEMOR($MXHCOM);
COMMON/EDATA/SIZEHA,DSIZE,DTH0,N,INP,EDP(20),ENEDEP,
             XL(20),YL(20),XS(20),YS(20);
REAL*8 EDP,ENEDEP;

IF(IQ(NP).EQ.-1.AND.IR(NP).EQ.1) [
IF(INP.NE.NP) [
```

```
NEKE=MEKE(MEDIUM);"NUMBER OF ELEMENTS IN STORAGE ARRAY"
DO I=1,NEKE-1[
EIP1=EXP((FLOAT(I+1)-EKE0(MEDIUM))/EKE1(MEDIUM));"ENERGY AT I+1"
EIP1L=ALOG(EIP1);LEIP1L=I+1;"DESIGNED THIS WAY=$SETINTERVAL"
$EVALUATE EDEDX USING EDEDX(EIP1L);SIP1=ESTEPE*EIP1/EDEDX;

"NOW SOLVE THESE EQUATIONS                                    "
"  SI    = TMXS1 * EIL    + TMXS0                             "
"  SIP1 = TMXS1 * EIP1L + TMXS0                               "
"                                                             "
TMXS1(I,MEDIUM)=(SI-SIP1)/ERATIO;TMXS0(I,MEDIUM)=SI-TMXS1(I,MEDIUM)*EIL;
"TRANSFER VALUES FOR NEXT LOOP"
EIL=EIP1L;SI=SIP1;]
"NOW PICK UP LAST TABLE ENTRY WHICH APPLIES ONLY TO LAST ENERGY"
TMXS0(NEKE,MEDIUM)=TMXS0(NEKE-1,MEDIUM);
TMXS1(NEKE,MEDIUM)=TMXS1(NEKE-1,MEDIUM);
RETURN;
END; "END OF SUBROUTINE FIXTMX"


%E
SUBROUTINE COORD(K,NN,FR1,FR2,I1,J1,I2,J2);
COMMON/EDATA/SIZEHA,DSIZE,DTH0,N,INP,EDP(20),ENEDEP,
             XL(20),YL(20),XS(20),YS(20);
REAL*8 EDP,ENEDEP;
NN=0;
FR1=0.; FR2=0.;
I1=0; J1=0; I2=0; J2=0;
XXL=XL(K); YYL=YL(K);
XXS=XS(K); YYS=YS(K);
AXXL=ABS(XXL); AYYL=ABS(YYL);
AXXS=ABS(XXS); AYYS=ABS(YYS);

IF(AXXL.LT.SIZEHA.AND.AYYL.LT.SIZEHA) [
   XXL=XXL+SIZEHA;
   YYL=YYL+SIZEHA;
   I1=1+INT(XXL/DSIZE);
   J1=1+INT(YYL/DSIZE);    ]
ELSE [ NN=NN+1;FR2=1./3.; ]

IF(AXXS.LT.SIZEHA.AND.AYYS.LT.SIZEHA) [
   XXS=XXS+SIZEHA;
   YYS=YYS+SIZEHA;
   I2=1+INT(XXS/DSIZE);
   J2=1+INT(YYS/DSIZE);    ]
ELSE [ NN=NN+1;FR1=2./3.; ]

IF(NN.EQ.0) [
   IF(I1.EQ.I2.AND.J1.EQ.J2) [ FR1=1.; NN=1; ]
   ELSE [ FR1=2./3.; FR2=1./3.; NN=2; ] ]
ELSEIF(NN.EQ.1) [
   IF(FR2.GT.FR1) [ I1=I2; J1=J2; FR1=FR2; ] ]
ELSE [ NN=0; ]

RETURN;
END;

%E
SUBROUTINE ALGPHO(I1,J1,EDP1);
```

```
COMMON/LIGHT/YIELD(3,5,5);

DIMENSION FE(2);

TR=.20;
FE(1)=.00057/2.; FE(2)=.00015/2.;

II=I1; JJ=J1;

YIELD(1,II,JJ)=EDP1+YIELD(1,II,JJ);

YIELD(2,II,JJ)=EDP1/2.+YIELD(2,II,JJ);

YIELD(3,II,JJ)=EDP1*TR+YIELD(3,II,JJ);

DO H=1,2 [
HH=2*H+1;
DO LL=1,HH [
   DO L=1,HH [
      IM=II-H+L-1;
      JN=JJ-H+LL-1;
      IF(IM.GE.1.AND.IM.LE.5.AND.JN.GE.1.AND.JN.LE.5) [
        JDIS2=(IM-II)*(IM-II)+(JN-JJ)*(JN-JJ);
        H2=H*H;
        IF(JDIS2.GE.H2) [
           YIELD(3,IM,JN)=FE(H)*EDP1+YIELD(3,IM,JN); ] ] ] ] ]
RETURN;
END;
```


File $1$DUS110:[MAURIZIO.REFLE]REFLEX.FOR;30 (33986,1,0), last revised on 7-FEB-1989 11:36, is a 6 block sequential file owned by UIC [MAURIZIO]. The records are variable length with implied (CR) carriage control. The longest record is 80 bytes.

Job REFLEX (928) queued to SYS$PRINT on 25-JAN-1990 15:04 by user MAURIZIO, UIC [MAURIZIO], under account 426105 at priority 100, started on printer LIC0 on 25-JAN-1990 15:04 from queue CSA2$LIC0.

XXXXXXXXXX 9999999999999999999999999999999999999999999999999999999999999999999999999999999999999999999999999999999999999999999999 XXXXXXXXXX
XXXXXXXXXX 99999999999999999999 Digital Equipment Corporation - VAX/VMS Version V5.3 99999999999999999999 XXXXXXXXXX
XXXXXXXXXX 9999999999999999999999999999999999999999999999999999999999999999999999999999999999999999999999999999999999999999999999 XXXXXXXXXX

```
c     This program computes the probability for a
c     photon created in point (b,z) with direction (phi,the)
c     within the tube of radius r0 to reach the end
c     of the tube; ri is the refrection index of the glass.
      program reflex
      integer*4 i1,i2,i3,i4
      real*4 mm,mi
      external refcal,mcal
      dimension m(1000)
      dimension p(1000)
      Common//hmemor(5000)
      call hlimit(5000)
      call hbook1(1,'title$',50,0.01,0.1,1000)
      call hbook1(2,'no. reflex$',50,0.,100,1000)
      call hbstat(0)
      type *,'radius of the tube ? (cm)'
      read(*,*) r0
      type *,'index of refraction ?'
      read(*,*) ri
      type *,'length of the tube (cm) ?'
      read(*,*) z0
      type *,'number of photon to be generated ?'
      read(*,*) n
      type *,'type four integer odd large no.'
      read(*,*)i1,i2,i3,i4
      pihalf=asin(1.)
c
c
c     loop : random generation of photons
c
c
      do i=1,n
      phi=pihalf*ran(i1)
      the=pihalf*(2*ran(i2)-1.)
c      z=z0*ran(i4)
      z=z0
      cphi=cos(phi)
      sthe=abs(sin(the))
      tthe=tan(the)
      cpsi=sthe*cphi
      c=r0*cphi
      b=c*ran(i3)
      ref=refcal(ri,cpsi)
      m(i)=mcal(z,c,b,tthe)
      p(i)=0.5*ref**m(i)
      mi=m(i)
      pi=p(i)
      call hfill(1,pi)
      call hfill(2,mi)
      enddo
      mm=0.
      pm=0.
      do i=1,n
      pm=pm+p(i)
      mm=mm+p(i)*m(i)
      enddo
      mm=mm/pm
      pm=pm/n
      sigt=0.
      do i=1,n
```

```
sig=p(i)-pm
sig=sig*sig
sigt=sigt+sig
enddo
sigt=sigt/n
sigt=sqrt(sigt)
type *,'final random numbers :'
write(*,*)i1,i2,i3,i4
type *,'radius of the tube (cm) =',r0
type *,'index of refraction = ',ri
type *,'length (cm) =',z0
type *,'number of photons =',n
type *,'average no. of reflex =',mm
type *,'mean value of probability =',pm
type *,'standard deviation =',sigt
call histdo
end
function refcal(ri,cpsi)
spsi=sqrt(1.-cpsi*cpsi)
tpsi=spsi/cpsi
spsi1=spsi/ri
cpsi1=sqrt(1.-spsi1*spsi1)
tpsi1=spsi1/cpsi1
r1=(spsi*cpsi1-cpsi*spsi1)/(spsi*cpsi1+cpsi*spsi1)
r2=(tpsi-tpsi1)/(tpsi+tpsi1)
r3=(1.-tpsi*tpsi1)/(1.+tpsi*tpsi1)
r12=r1*r1
r22=r2*r2
r32=r3*r3
refcal=0.5*(r12+r22*r32)
return
end
function mcal(z,c,b,tthe)
tth=abs(tthe)
d=2*c/tth
if(tthe.gt.0) then
a=(2*c-b)/tth
else
a=(c+b)/tth
endif
mcal=1+int((z-a)/d)
return
end
```

```
WWWWWWWWWW    8888888888888888888888888888888888888888888888888888888888888888888888888888888888888888888888888888888888888888888888    WWWWWWWWWW
WWWWWWWWWW    88888888888888888888  Digital Equipment Corporation - VAX/VMS Version V5.3  88888888888888888888    WWWWWWWWWW
WWWWWWWWWW    8888888888888888888888888888888888888888888888888888888888888888888888888888888888888888888888888888888888888888888888    WWWWWWWWWW

                          M   M   AAA   U   U  RRRR    III   ZZZZZ   III    000
                          MM MM  A   A  U   U  R   R    I        Z    I    0   0
                          M M M  A   A  U   U  R   R    I       Z     I    0   0
                          M   M  A   A  U   U  RRRR     I      Z      I    0   0
                          M   M  AAAAA  U   U  R R      I     Z       I    0   0
                          M   M  A   A  U   U  R  R     I    Z        I    0   0
                          M   M  A   A  UUUUU  R   R   III   ZZZZZ   III    000

                     BBBBBBBB      IIIIII      GGGGGGGG  MM      MM    AAAAAA      CCCCCCCC
                     BBBBBBBB      IIIIII      GGGGGGGG  MM      MM    AAAAAA      CCCCCCCC
                     BB      BB      II      GG          MMMM  MMMM  AA      AA  CC
                     BB      BB      II      GG          MMMM  MMMM  AA      AA  CC
                     BB      BB      II      GG          MM  MM  MM  AA      AA  CC
                     BB      BB      II      GG          MM  MM  MM  AA      AA  CC
                     BBBBBBBB        II      GG          MM      MM  AA      AA  CC
                     BBBBBBBB        II      GG          MM      MM  AA      AA  CC
                     BB      BB      II      GG  GGGGGG  MM      MM  AAAAAAAAAA  CC
                     BB      BB      II      GG  GGGGGG  MM      MM  AAAAAAAAAA  CC
                     BB      BB      II      GG      GG  MM      MM  AA      AA  CC
                     BB      BB      II      GG      GG  MM      MM  AA      AA  CC
                     BBBBBBBB      IIIIII      GGGGGG    MM      MM  AA      AA    CCCCCCCC
                     BBBBBBBB      IIIIII      GGGGGG    MM      MM  AA      AA    CCCCCCCC

                          MM      MM    000000    RRRRRRRR        ;;;;        11      5555555555
                          MM      MM    000000    RRRRRRRR        ;;;;        11      5555555555
                          MMMM  MMMM  00      00  RR      RR      ;;;;      1111      55
                          MMMM  MMMM  00      00  RR      RR      ;;;;      1111      55
                          MM  MM  MM  00      00  RR      RR                  11      555555
                          MM  MM  MM  00      00  RR      RR                  11      555555
                          MM      MM  00      00  RRRRRRRR        ;;;;        11            55
                          MM      MM  00      00  RRRRRRRR        ;;;;        11            55
                          MM      MM  00      00  RR  RR          ;;;;        11              55
                          MM      MM  00      00  RR  RR          ;;;;        11              55
                    ....  MM      MM  00      00  RR    RR          ;;        11      55      55
                    ....  MM      MM  00      00  RR    RR          ;;        11      55      55
                    ....  MM      MM    000000    RR      RR      ;;        111111    555555
                    ....  MM      MM    000000    RR      RR      ;;        111111    555555
```

File _$1$DUS110:[MAURIZIO.EGS4.BIGMAK]BIGMAC.MOR;15 (33565,1,0), last revised on 10-MAY-1989 16:32, is a 45 block sequential file owned by UIC [MAURIZIO]. The records are variable length with implied (CR) carriage control. The longest record is 80 bytes.

Job BIGMAC (926) queued to SYS$PRINT on 25-JAN-1990 15:03 by user MAURIZIO, UIC [MAURIZIO], under account 426105 at priority 100, started on printer LIC0 on 25-JAN-1990 15:03 from queue CSA2$LIC0.

```
WWWWWWWWWW    8888888888888888888888888888888888888888888888888888888888888888888888888888888888888888888888888888888888888888888888    WWWWWWWWWW
WWWWWWWWWW    88888888888888888888  Digital Equipment Corporation - VAX/VMS Version V5.3  88888888888888888888    WWWWWWWWWW
WWWWWWWWWW    8888888888888888888888888888888888888888888888888888888888888888888888888888888888888888888888888888888888888888888888    WWWWWWWWWW
```

```
"*********************************************************************"
"********************** BIGMAC  PROGRAM **************************"
"*********************************************************************"

"*********************************************************************"
"************** STEP 1.  USER-OVER-RIDE-OF-EGS-MACROS ****************"
"*********************************************************************"

REPLACE {$MXREG} WITH {7} "MAXIMUM NUMBER OF REGIONS"
REPLACE {$MXMED} WITH {2}   "MAXIMUM NUMBER OF MEDIA"

REPLACE {;COMIN/RANDOM/;} WITH {;COMMON/RANDOM/IXX;}
REPLACE {$RANDOMSET#;} WITH
        {IXX=IXX*663608941;{P1}=0.5+IXX*0.23283064E-09;}

"*********************************************************************"
"****************** ADDITIONAL (NON-EGS) MACROS **********************"
"*********************************************************************"

REPLACE {$MXHCOM} WITH {40000} "MAX SIZE OF HCOM BUFFER"
REPLACE {$MBIN} WITH {62}  "NO. OF BINS FOR THE HIST'S"

"*********************************************************************"
"************************** DECLARATIONS *****************************"
"*********************************************************************"

;COMIN/EPCONT,MEDIA,MISC,THRESH,UPHIOT,USEFUL/;
COMMON//HMEMOR($MXHCOM);
COMMON/GEOM/NSI1,NSI2,NTA1,NTA2,NVA1,NVA2,NVA3,
       TATH,SITH,TOTSIZE;
COMMON/EDATA/EII,SSE,DDE,SSG,DDG,IEMUL,IGMUL,EDSI1,EDSI2,EDP($MXREG);
REAL*4 SSE,DDE,SSG,DDG;
REAL*8 EII,EDSI1,EDSI2,EDP;
REAL*8 ENEDEP;
CHARACTER*8 ITIME;
CHARACTER*4 MEDARR(24,$MXMED)/$S'SILICON                ',
                              $S'TANTALUM               '/;
COMIN/RANDOM/;
DIMENSION ARRAY($MBIN);
"*********************************************************************"
"************** START OF EXECUTABLE CODE *****************************"
"*********************************************************************"


"*********************************************************************"
"************** STEP 2.  INITIALIZATION COMES NEXT *******************"
"*********************************************************************"

NMED=$MXMED; "NUMBER OF MEDIA"


DO J=1,NMED [
DO I=1,24 [MEDIA(I,J)=MEDARR(I,J);]]

NSI1=2; "FIRST SILICON LAYER"
NSI2=4; "SECOND SILICON LAYER"
```

```
NTA1=1; "FIRST TANTALUM LAYER"
NTA2=3; "SECOND TANTALUM LAYER"
NVA1=5; "VACUUM IN FRONT OF THE DETECTOR"
NVA2=6; "VACUUM IN THE BACK OF THE DETECTOR"
NVA3=7; "VACUUM OUT OF THE SIZE OF THE DETECTOR"

MED(NSI2)=1; "SI"
MED(NSI1)=1; "SI"

MED(NTA1)=2; "TA"
MED(NTA2)=2; "TA"

MED(NVA1)=0; "VACUUM"
MED(NVA2)=0;
MED(NVA3)=0;

"SET DETECTOR SIZE"

TOTSIZE=2.; "CM"

"SET TANTALUM AND SILICON THICKNESS"

" OUTPUT; (/,' TANTALUM SLAB THICKNESS ? (MICRON)'); "
READ(*,*) TATHM;
TATH=TATHM*1.E-4; "CM"
" OUTPUT; (/,' SILICON DETECTOR THICKNESS ? (MICRON)');"
READ(*,*) SITHM;
SITH=SITHM*1.E-4; "CM"

"HISTOGRAMS INIZIALIZATION"


CALL HLIMIT($MXHCOM);

NBIN=$MBIN;

CALL HBOOK1(1,'ELECTRON KIN.ENE.SPECTRUM (SINGLE ELE.ENTERS SILICON)$',
            NBIN,0.,.520);
CALL HBOOK1(2,'PHOTON ENE.SPECTRUM (SINGLE PHO.ENTERS SILICON)$',
            NBIN,0.,.520);
CALL HBOOK1(3,'ELECTRON KIN.ENE.SPECTRUM (1PHO/1ELE.ENTERS SILICON)$',
            NBIN,0.,.520);
CALL HBOOK1(4,'PHOTON ENE.SPECTRUM (1PHO/1ELE.ENTERS SILICON)$',
            NBIN,0.,.520);
CALL HBOOK1(5,'ELECTRON KIN.ENE.SPECTRUM (ALL EVENTS-ENTER SILICON)$',
            NBIN,0.,.520);
CALL HBOOK1(6,'PHOTON ENE.SPECTRUM (ALL EVENTS-ENTER SILICON)$',
            NBIN,0.,.520);
CALL HBOOK1(7,'ENERGY DEP. IN FIRST DETECTOR (TRACK ONLY IN SI1)$',
            NBIN,0.,.520);
CALL HBOOK1(8,'ENERGY DEP. IN SECOND DETECTOR (TRACK ONLY IN SI2)$',
            NBIN,0.,.520);
CALL HBOOK1(9,'ENERGY DEP. IN FIRST DETECTOR (TRACK IN BOTH)$',
            NBIN,0.,.520);
CALL HBOOK1(10,'ENERGY DEP. IN SECOND DETECTOR (TRACK IN BOTH)$',
            NBIN,0.,.520);
CALL HBOOK1(11,'TOT.ENERGY DEP. IN BOTH DETECTORS (TRACK IN BOTH)$',
            NBIN,0.,.520);
CALL HBOOK1(12,'ENERGY DEP. IN FIRST TANTALUM SLAB (ALL EVENTS)$',
            NBIN,0.,.520);
```

```
CALL HBOOK1(13,'ENERGY DEP. IN FIRST DETECTOR (ALL EVENTS)$',
            NBIN,0.,.520);
CALL HBOOK1(14,'ENERGY DEP. IN SECOND TANTALUM SLAB (ALL EVENTS)$',
            NBIN,0.,.520);
CALL HBOOK1(15,'ENERGY DEP. IN SECOND DETECTOR (ALL EVENTS)$',
            NBIN,0.,.520);
"*****************************************************************"
"*************** STEP 3.  HATCH-CALL COMES NEXT *****************"
"*****************************************************************"

CALL HATCH;

"OUTPUT VARIOUS QUANTITIES ASSOCIATED WITH THE MEDIA"

OUTPUT;  ('1QUANTITIES ASSOCIATED WITH EACH MEDIA:',//);

DO JSEL=1,2 [
OUTPUT (MEDIA(I,JSEL),I=1,24);  (/,1X,24A1);
OUTPUT RHO(JSEL),RLC(JSEL);
(5X,' RHO=',G15.7,' G/CM**3     RLC=',G15.7,' CM');
OUTPUT AE(JSEL),UE(JSEL);
(5X,' AE=',G15.7,' MEV    UE=',G15.7,' MEV');
OUTPUT AP(JSEL),UP(JSEL);
(5X,' AP=',G15.7,' MEV    UP=',G15.7,' MEV');
"END OF JSEL-LOOP"]


OUTPUT TOTSIZE; (////,' DETECTOR SIZE = ',F5.2,' CM');
OUTPUT TATH,SITH;(////,' THICKNESS OF TANTALUM = ',F7.4,' CM',
 /,' THICKNESS OF SILICON = ',F7.4,' CM');

"*****************************************************************"
"***** STEP 4.  DETERMINATION OF INCIDENT PARTICLE PROPERTIES ****"
"*****************************************************************"

IQI=0;   "INCIDENT PARTICLE"

EI=0.511D0;   "TOTAL ENERGY OF PARTICLE (MEV)"
EII=EI;
AVAILE=EI;  "AVAILABLE K.E. (MEV)"
EISING=EI;  "SINGLE PRECISION ENERGY VARIABLE"

XI=0.0; YI=0.0; ZI=0.0;  "STARTING COORDINATES (CM)"
UI=0.0; VI=0.0; WI=1.0;  "INCIDENT DIRECTION COSINES"
IRI=NTA1;  "ENTRANCE REGION DEFINITION"
WTI=1.0;  "WEIGHT FACTOR OF UNITY"


"SELECT THE STARTING RANDOM NUMBER SEED"
" OUTPUT; (/,' INIZIALIZING RANDOM NUMBER ?'); "

READ(*,*) IXXST;
"IXXST=123456789;"

IXX=IXXST;  "INITIALIZED RANDOM NUMBER WITH STARTING SEED"

" OUTPUT; (/,' NUMBER OF EVENTS ?'); "
READ(*,*) NCASES;

"*****************************************************************"
```

```
"****************** STEP 5. SHOWER-CALL---NEXT ******************"
"*********************************************************************"


CALL TIME(ITIME);
OUTPUT ITIME;
(//,' PRIOR TO SHOWER CALL LOOP ===> ITIME=',A8,//);

ISI1=0; "NUMBER OF EVENTS WITH TRACKS ONLY IN FIRST DETECTOR"
ISI2=0; "NUMBER OF EVENTS WITH TRACKS ONLY IN SECOND DETECTOR"
IAND=0; "NUMBER OF EVENTS WITH TRACKS IN BOTH DETECTORS"

ESTEPE=0.05;
DO I=1,NMED [ "SET UPPER LIMIT TO USTEP IN ORDER TO HAVE"
              "ENERGY LOSS LESS THAN ESTEPE*ENERGY OF    "
              "THE ELECTRON "
             CALL FIXTMX(ESTEPE,I); ]


DO I=1,NCASES ["START OF SHOWER CALL LOOP"

IEMUL=0;
IGMUL=0;
EDSI1=0.;
EDSI2=0.;
NREG=$MXREG;
DO J=1,NREG [ EDP(J)=0.;  ]

CALL SHOWER(IQI,EI,XI,YI,ZI,UI,VI,WI,IRI,WTI);

"FILL HISTOGRAMS OF DEPOSITED ENERGY IN THE DETECTORS"
IF(EDSI1.NE.0..AND.EDSI2.EQ.0.) [
   "TRACK ONLY IN THE FIRST DETECTOR"
   ISI1=ISI1+1;
   CALL HFILL(7,EDSI1); ]
ELSEIF(EDSI1.EQ.0..AND.EDSI2.NE.0.) [
       "TRACK ONLY IN THE SECOND DETECTOR"
       ISI2=ISI2+1;
       CALL HFILL(8,EDSI2); ]
ELSEIF(EDSI1.NE.0..AND.EDSI2.NE.0.) [
       "TRACK IN BOTH OF THE DETECTORS"
       IAND=IAND+1;
       CALL HFILL(9,EDSI1);
       CALL HFILL(10,EDSI2);
       CALL HFILL(11,EDSI1+EDSI2); ]

"FILL HISTOGRAMS OF ENERGY SPECTRA OF THE PARTICLES "
"ENTERING THE FIRST DETECTOR "
IF(IEMUL.EQ.1.AND.IGMUL.EQ.0) [ "ONLY AN ELECTRON ESCAPES TANTALUM"
                                 "LIKELY TO BE A PHOTOELECTRON "
   CALL HFILL(1,SSE); ]
ELSEIF(IEMUL.EQ.0.AND.IGMUL.EQ.1) [ "ONLY A PHOTON ESCAPES TANTALUM"
                                    "LIKELY TO BE A COMPTOM PHOTON"
       CALL HFILL(2,SSG); ]
ELSEIF(IEMUL.EQ.1.AND.IGMUL.EQ.1) [ "an electron and a photon escape"
                  "tantalum, likely to be a compton interaction"
        CALL HFILL(3,DDE);
        CALL HFILL(4,DDG); ]

DO J=1,4 [
```

```
        IF(EDP(J).NE.0.) [
          ENEDEP=EDP(J);
          ID=11+J;
          CALL HFILL(ID,ENEDEP); ] ]

NCOUNT=NCOUNT + 1;
IXXEND=IXX;    "LAST RANDOM NUMBER USED"

"END OF SHOWER CALL LOOP"]



CALL TIME(ITIME);
OUTPUT ITIME;  (//,' END OF SHOWER CALL LOOP ===> ITIME=',A8,//);


"*********************************************************************"
"****************** STEP 6. OUTPUT OF RESULTS ********************"
"*********************************************************************"


OUTPUT NCOUNT,NCASES,IXXST,IXXEND;
('1',I10,' CASES OUT OF ',I10,
     //,' IXXST=',I12,/,' IXXEND=',I12,//);

OUTPUT ISI1,ISI2,IAND;
(/,' NUMBER OF EVENTS WITH TRACKS ONLY IN FIRST DETECTOR',I8,
/,' NUMBER OF EVENTS WITH TRACKS ONLY IN SECOND DETECTOR',I8,
/,' NUMBER OF EVENTS WITH TRACKS IN BOTH DETECTORS',I8);

DO I=1,15 [
          J=I+20;
          CALL HUNPAK(I,ARRAY);
          DO K=1,NBIN [
          KK=K*10;
          WRITE(J,*) KK,ARRAY(K); ]
          ]

CALL HISTDO;              "OUTPUT ALL HISTOGRAMS"

STOP;
END;  "END OF MAIN PROGRAM"

%E
"*********************************************************************"
SUBROUTINE AUSGAB(IARG);
"*********************************************************************"
;COMIN/EPCONT,STACK,RANDOM,USEFUL/;
COMMON//HWEMOR($MXHCOM);
COMMON/EDATA/EII,SSE,DDE,SSG,DDG,IEMUL,IGMUL,EDSI1,EDSI2,EDP($MXREG);
COMMON/GEOM/NSI1,NSI2,NTA1,NTA2,NVA1,NVA2,NVA3,
       TATH,SITH,TOTSIZE;
REAL*4 SSE,DDE,SSG,DDG;
REAL*8 EDP;
REAL*8 EEE,EII,EDSI1,EDSI2;

IRL=IR(NP);    "SET LOCAL VARIABLE"

IF(IRL.EQ.NSI1.AND.IROLD.EQ.NTA1) [
 "PARTICLE ENTERING THE FIRST SILICON LAYER"
```

```
 "KINETIC ENERGY SPECTRUM"
 EEE=E(NP); EEM=E(NP)-RM;
 IF(IQ(NP).EQ.-1) [ IEMUL=IEMUL+1; "ELECTRONS"
   IF(IEMUL.EQ.1.AND.IGMUL.EQ.0) [ SSE=EEM;]
   ELSEIF(IEMUL.EQ.1.AND.IGMUL.EQ.1) [ DDE=EEM;]
   CALL HFILL(5,EEM); ]
 ELSEIF(IQ(NP).EQ.0.AND.EEE.LT.EII) [ "ALL PHOTONS"
                      "BUT NONINTERACTING PHOTONS"
   IF(IEMUL.EQ.0.AND.IGMUL.EQ.1) [ SSG=EEE;]
   ELSEIF(IEMUL.EQ.1.AND.IGMUL.EQ.1) [ DDG=EEE;]
   CALL HFILL(6,EEE); ] ]

"ENERGY DEPOSITION IN EACH REGION"
EDP(IRL)=EDP(IRL)+EDEP;
IF(IRL.EQ.NSI1) [
   EDSI1=EDSI1+EDEP; ]
ELSEIF(IRL.EQ.NSI2) [
       EDSI2=EDSI2+EDEP; ]


RETURN;
END;  "END OF SUBROUTINE AUSGAB"

%E
"*********************************************************************"
SUBROUTINE HOWFAR;
"*********************************************************************"
;COMIN/EPCONT,STACK,BOUNDS,ELECIN/;
COMMON/GEOM/NSI1,NSI2,NTA1,NTA2,NVA1,NVA2,NVA3,
       TATH,SITH,TOTSIZE;

"SET LOCAL VARIABLE"

XX=X(NP); YY=Y(NP); ZZ=Z(NP);
WW=W(NP);
IRL=IR(NP);

SIZEHA=TOTSIZE/2.;
XX1=ABS(XX);
YY1=ABS(YY);
IF(XX1.GE.SIZEHA.OR.YY1.GE.SIZEHA) [
   IDISC=1;  "OUT OF THE SIZE OF THE DETECTOR" ]


ELSEIF(IRL.EQ.NTA1) [  "FIRST TANTALUM LAYER"
       DIS1=TATH-ZZ;
       DIS2=ZZ;
       DNEAR(NP)=AMIN1(DIS1,DIS2);
       IF(WW.GT.0.) [  "FORWARD PARTICLE"
          DIST=DIS1/WW;
          IF(DIST.LE.USTEP)  [USTEP=DIST;
             IRNEW=NSI1; ] ]
       ELSEIF(WW.LT.0.) [ "BACKWARD PARTICLE"
             DIST=-DIS2/WW;
             IF(DIST.LE.USTEP) [USTEP=DIST;
                IRNEW=NVA1;] ]
       ELSE [IDISC=1;] ]

ELSEIF(IRL.EQ.NTA2) [ "SECOND TANTALUM LAYER"
```

```
       DIS1=2.*TATH+SITH-ZZ;
       DIS2=ZZ-TATH-SITH;
       DNEAR(NP)=AMIN1(DIS1,DIS2);
       IF(WW.GT.0.) [ "FORWARD PARTICLE"
          DIST=DIS1/WW;
          IF(DIST.LE.USTEP)  [USTEP=DIST;
             IRNEW=NSI2; ] ]
        ELSEIF(WW.LT.0.) [ "BACKWARD PARTICLE"
               DIST=-DIS2/WW;
               IF(DIST.LE.USTEP)  [USTEP=DIST;
                  IRNEW=NSI1; ] ]
        ELSE [IDISC=1;] ]


ELSEIF(IRL.EQ.NSI1) [ "FIRST SILICON LAYER"
       DIS1=TATH+SITH-ZZ;
       DIS2=ZZ-TATH;
       DNEAR(NP)=AMIN1(DIS1,DIS2);
       IF(WW.GT.0.) [ "FORWARD PARTICLE"
          DIST=DIS1/WW;
          IF(DIST.LE.USTEP)  [USTEP=DIST;
             IRNEW=NTA2; ] ]
        ELSEIF(WW.LT.0.) [ "BACKWARD PARTICLE"
               DIST=-DIS2/WW;
               IF(DIST.LE.USTEP)  [USTEP=DIST;
                  IRNEW=NTA1; ] ]
        ELSE [IDISC=1;] ]

ELSEIF(IRL.EQ.NSI2) [ "SECOND SILICON LAYER"
       DIS1=2.*(TATH+SITH)-ZZ;
       DIS2=ZZ-2.*TATH-SITH;
       DNEAR(NP)=AMIN1(DIS1,DIS2);
       IF(WW.GT.0.) [ "FORWARD PARTICLE"
          DIST=DIS1/WW;
          IF(DIST.LE.USTEP)  [USTEP=DIST;
             IRNEW=NVA2; ] ]
        ELSEIF(WW.LT.0.) [ "BACKWARD PARTICLE"
               DIST=-DIS2/WW;
               IF(DIST.LE.USTEP)  [USTEP=DIST;
                  IRNEW=NTA2; ] ]
        ELSE [IDISC=1;] ]
ELSE [IDISC=1; "VACUUM OR SOMETHING ELSE" ]
RETURN;
END; "END OF SUBROUTINE HOWFAR"

%E
"*************************************************************************"
"                           *         *                                   "
"                           * FIXTMX  *                                   "
"                           *         *                                   "
"                           *********                                     "
SUBROUTINE FIXTMX(ESTEPE,MEDIUM);
"                                                                         "
"  THIS ROUTINE CHANGES THE STEP SIZE ALGORITHM USED IN EGS SO THAT       "
"  THE STEP SIZE ARRAYS FOR TMXS CORRESPOND TO AN ARBITRARY,BUT           "
"  FIXED FRACTIONAL ENERGY LOSS ESTEPE.                                   "
"  IT IS ONLY NECESSARY FOR LOW ENERGY ELECTRON PROBLEMS SINCE            "
"  TYPICALLY THE 200*TEFF0 RESTRICTION ON TMXS IS MORE STRINGENT          "
"   FOR ELECTRONS WITH ENERGIES ABOVE A FEW MEV                           "
"                                                                         "
```

```
"  NOTE THAT THE $TMXS-OVER-RIDE MACRO IS STILL IN FORCE IN EGS.          "
"                                                                         "
"  THE ROUTINE CHANGES THE VALUES ONLY FOR THE MEDIUM 'MEDIUM'            "
"  AND IT SHOULD PROBABLY BE USED FOR ALL MEDIA IN A PROBLEM.             "
"                                                                         "
"  THE ROUTINE MUST BE CALLED AFTER HATCH HAS BEEN CALLED AND BEFORE      "
"  THE SIMULATION IS BEGUN.                                               "
"                                                                         "
"  THE ROUTINE IS INDEPENDENT OF WHAT UNITS ARE BEING USED, AS LONG       "
"  AS THEY ARE CONSISTENT( E.G. CM, RL OR G/CM**2 )                       "
"                                                                         "
"  IF CALLED WITH ESTEPE=0, THE CURRENT ALGORITHM IS USED                 "
"                                                                         "
"  FOR A DETAILED DISCUSSION OF THE USE OF THIS ROUTINE, SEE              "
"  'Low Energy Electron Transport with EGS' in Nuclear Instr. and         "
"  Methods A227 (1984)535-548.  D.W.O. Rogers                             "
"                                                                         "
"  V01        DEC 10,1981 DAVE ROGERS NRCC                                "
"  V02        DEC 1984  EGS4 VERSION                                      "
"*************************************************************************"
;COMIN/MEDIA,ELECIN/;
IF(MEDIUM > $MXMED)["ERROR"  OUTPUT MEDIUM;
(///'0********* MEDIUM=',I4,' IN FIXTMX IS TOO LARGE');RETURN;]

IF(ESTEPE = 0) [RETURN; "I.E. USE THE CURRENT ALGORITHM "]
"SET UP SOME VARIABLES FOR FIRST PASS THROUGH LOOP"
EI =EXP( (1.-EKE0(MEDIUM))/EKE1(MEDIUM));"ENERGY OF FIRST TABLE ENTRY"
EIL = ALOG(EI);  LEIL=1;
"THIS IS EQUIVALENT TO $SETINTERVAL EIL,EKE; BUT AVOIDS ROUNDOFF"
$EVALUATE EDEDX USING EDEDX(EIL);"GET THE ELECTRON STOPPPING AT EI"
"NOW CALCULATE STEP REQUIRED TO CAUSE AN ESTEPE REDUCTION IN ENERGY"
SI=ESTEPE*EI/EDEDX;
"TABULATED ENERGIES ARE IN A FIXED RATIO - CALC LOG OF THE RATIO"
ERATIO=-1./EKE1(MEDIUM);

NEKE=MEKE(MEDIUM);"NUMBER OF ELEMENTS IN STORAGE ARRAY"
DO I=1,NEKE-1[
EIP1=EXP((FLOAT(I+1)-EKE0(MEDIUM))/EKE1(MEDIUM));"ENERGY AT I+1"
EIP1L=ALOG(EIP1);LEIP1L=I+1;"DESIGNED THIS WAY=$SETINTERVAL"
$EVALUATE EDEDX USING EDEDX(EIP1L);SIP1=ESTEPE*EIP1/EDEDX;

"NOW SOLVE THESE EQUATIONS                                               "
"  SI   = TMXS1 * EIL   + TMXS0                                          "
"  SIP1 = TMXS1 * EIP1L + TMXS0                                          "
"                                                                        "
TMXS1(I,MEDIUM)=(SI-SIP1)/ERATIO;TMXS0(I,MEDIUM)=SI-TMXS1(I,MEDIUM)*EIL;
"TRANSFER VALUES FOR NEXT LOOP"
EIL=EIP1L;SI=SIP1;]
"NOW PICK UP LAST TABLE ENTRY WHICH APPLIES ONLY TO LAST ENERGY"
TMXS0(NEKE,MEDIUM)=TMXS0(NEKE-1,MEDIUM);
TMXS1(NEKE,MEDIUM)=TMXS1(NEKE-1,MEDIUM);
RETURN;
END; "END OF SUBROUTINE FIXTMX"
```